UNIVERSITAT POLITÈCNICA DE CATALUNYA BARCELONATECH

Integration of nanofiltration and diffusion dialysis for the sustainable management of acidic liquid wastes

by

Julio López Rodríguez

PhD program in Chemical Process Engineering

Integration of Nanofiltration and Diffusion Dialysis for the sustainable management of acidic liquid wastes

Doctoral thesis by:

Julio López Rodríguez

Thesis advisor:

Oriol Gibert Agulló and José Luis Cortina Pallás

Chemical Enginnering Department

Barcelona, December 2019

Thesis presented to obtain the qualification of Doctor awarded by the Universitat Politècnica de Catalunya

"*I eu cavilo na sombra fresca das carballeiras de Lalín, nos piñeiraes da beiramar de Noia, nos arumes mariñeiros de Bueu, no cume do Montelouro, na frescura do meu mar de Rianxo, na fonte cantareira da Estrada, nos salseiros de Corrubedo, no ar puro de Curtis, na paz vizosa do Lerez… E síntome fortalecido.*"

Castelao, **Sempre en Galiza** (1944)

Acknowledgements

After finishing my BSc in Chemical Engineering in Santiago de Compostela, I moved to Barcelona to start my MSc. Just at the end of the first academic year, my supervisor José Luis Cortina offered me the possibility to do a PhD Thesis in his group. I must admit that I never have in mind the idea to do a doctorate. However, I liked the option of doing the Thesis about separation processes, in this case with membrane technologies, and he just convinced me. Like Vito Corleone, he made me an offer I could not refuse.

One African proverb says that "*If you want to go fast, go alone. If you want to go far, go together*", which I think represents all the work behind this Thesis. I have to give the thanks to a lot of people who have helped and supported me along these four years.

Firstly, I would like to acknowledge my supervisors, José Luis Cortina and Oriol Gibert. Without their guidance and help, I will not be able to have this Thesis. Thank you for all these meetings, paper reviews, advices... I learn a lot from both of you. I would also like to thanks Andriy Yaroshchuk for the knowledge about modelling and nanofiltration membranes that he transferred me.

This thesis was supported by the Waste2Product project (CTM2014-57302-R) and by R2MIT project (CTM2017-85346-R) financed by the Spanish Ministry of Economy and Competitiveness (MINECO) and the Catalan Government (2017-SGR-312). Moreover, my work was supported by the MINECO within the scope of the grant (BES-2015-075051). I also want to thank Dow Chemical and Hydranautics for the supply of membranes.

I want to thank the contribution of Anna de Juan and Rodrigo R. de Oliveira (Universitat de Barcelona), Carlos Ayora and Esther Torres (CSIC), Toni Susín and Rafael Ramírez (UPC) to this Thesis. Moreover, I want to thank these students that helped me with the experimental part: Ariadna Villegas, Tomeu Servera, Kevin Martín, Juan Salinas, Luis Salvador, Daniel León, Ricardo Pirabed, Laia Vilaplana and Bea Casas.

I have to acknowledge Professors Andrea Cipollina and Giorgio Micale (Università degli Studi di Palermo, Italy) for giving me the chance to be part of their research group for a few months and to their work team that made me feel like one more. I would like especially to thank those with whom I worked side by side: Alba Ruiz-Aguirre, Rosa Gueccia and Serena Randazzo. Thanks also to Bartolomé Ortega-Delgado and Serena Lima.

Moreover, I have also to acknowledge the people who have accompanied me in this crossing in the university throughout these four years. I still remember those moments shared in the labs in the

ETSEIB. We were a small but close group. I was sharing my office with Mehrez and Neus, who were almost finishing their Thesis. Furthermore, Mònica, Sandra, Julio Bastos and Edxon were in another office. Mònica and Sandra were also finishing their thesis, while Julio Bastos and Edxon had a position as Post-Doc. In addition, there was Marc, who recently started his Thesis. A couple of months before, Xanel arrived as Post-Doc. Then, we transfer our installations to the EEBE. Edxon, Neus, Julio Bastos and Mehrez left our group, but others came (Mati, Josep, Sina, Brij, Karina, Sonia, Mahdi and Miguel). Mònica and Xanel have helped and advised me along his 4 years in so many topics. I shared with Marc a lot of time in the lab at the beginning of my Thesis and then in our office at the EEBE. Mati was always willing to lend me a hand at the lab. To Edxon for his patience and help with modelling issues at the beginning of my PhD Thesis. I shared a lot of breakfasts and funny moments in the office with Karina and Sonia. I want to thank the "Run Club" formed by Marc, Mehrez and Julio Bastos. We have run a lot of kilometres together, and those breakfasts after running will be hard to forget. Brij and Sina were always smiling and joking. Despite the short time that I spent with Sandra, Neus and Josep, I had fun times with them. Mahdi and Miguel have recently arrived, but they became an important part of the lab soon. I want to give thanks to all the teachers from the group for those moments shared at the coffee time and for being available when I need something from them.

Finally, I want to thank my family, to my parents Julio and Pilar and my sister Marta, who encouraged me to do this PhD Thesis and supported me despite being 1000 km far away. To my girlfriend Alexandra, who was supporting me along this last year of Thesis.

Thank you all. Without all of you, I am entirely sure that this Thesis would not be the same.

Abstract

Nowadays mining and hydrometallurgical industries generate a considerable amount of acidic liquid wastes (ALWs), which are characterised by a low pH and the presence of metals (e.g. Fe, Cu, Zn and Rare Earth Elements (REEs) among others) and non-metals (e.g. As, Se). These effluents are usually treated by the addition of lime to neutralise the acidity and to remove the metals as hydroxides and hydroxyl-sulphates, and the non-metals as calcium-based electrolytes and the resultant effluent is discharged into the natural water bodies. However, the high cost associated with this treatment makes necessary to explore other more sustainable alternatives. Nowadays, the European Union (EU) is promoting circular schemes to valorise effluents for the recovery of valuable elements. Additionally, it is worthy of mention initiatives such as the Critical Raw Material List, which promotes the recovery of valuable compounds from secondary resources. Therefore, ALWs from mining, hydrometallurgical and metallurgical industries can be a source of acid and metal recovery. Among the alternatives to the established neutralisation by lime addition, membrane technologies are being studied. In this thesis, two membrane technologies such as nanofiltration (NF) and diffusion dialysis (DD) will be used for the valorisation of ALWs.

Acid Mine Drainage (AMD), which is a by-product of the mining industry, was the first model system treated with NF for acid recovery and concentrating the metals in solution. AMDs are characterised by a pH<3 and the presence of metals (Al, Fe, Cu and Zn, among others). REEs, which are identified as Critical Raw Materials by the EU, can be found as minor components. Different membranes, including acid-resistant, were tested under different feed composition to evaluate their influence in the membrane performance. NF membranes were able to treat AMD, especially those based on an active layer made of polyamide, with high metal rejections (>98%) and favouring the acid transport. Nevertheless, their low stability in acid media makes these membranes susceptible to use at long-term operation. Changes in the chemical and physical structure of the active layer were evaluated by using FSEM-EDAX, FTIR and XPS. Solution speciation was found to have a significant impact on membrane rejection. Moreover, a numerical approach based on the Solution-Electro-Diffusion model (SEDM) coupled with reactive transport, was developed to characterise the transport of species through membrane permeances. Furthermore, the prediction capability of the developed model was studied and tested to determine its potential application for process design.

Besides, an ALW from a metallurgical industry composed by a mixture of H_2SO_4 and HCl (0.3<pH<0.7) containing non-metallic (As) and metallic (Fe, Cu, Zn) impurities was treated with a polyamide-based membrane (NF270). The membrane was able to reject metals by more than 80%, whereas the transport of arsenic was below 50%. This lower As rejection was related to the presence of As(V) as a non-charged species (i.e. H_3AsO_4), which is not rejected by the electric charge of the membrane.

Finally, a highly acidic (220 g/L H_2SO_4) ALW from a copper smelter containing arsenic as the main impurity (3.4 g/L) was treated with a DD module. The speciation of arsenic as As(III) or As(V) was studied. Acid recovery and ion leakage were studied at different conditions. The speciation of arsenic does not influence the recovery of the acid. Arsenic was not rejected (ion leakage below 50%) by the membrane due to its presence as non-charged species, such as H_3AsO_3 for As(III) and H_3AsO_4 for As(V). However, the membrane can reject more As(III) than As(V) due to the presence of the former as a cation ($H_2AsO_2^+$). DD at the optimum evaluated conditions was able to recover the 69±2% of the acid (146.3 g/L) with arsenic as the main impurity (1.3 g/L and passage of 39±1%), while the total content of metals was below 0.1 g/L.

Resumen

Hoy en día, las industrias mineras e hidrometalúrgicas generan una cantidad considerable de residuos líquidos ácidos (RLAs), caracterizadas por un bajo pH y por la presencia de metales (p. ej. Fe, Cu y Zn y Tierras Raras (TR) entre otros) y no metales (p. ej. As, Be). Estos efluentes se tratan, generalmente, mediante la adición de cal para neutralizar la acidez y eliminar los metales como hidróxidos e hidroxisulfatos, y los no metales como electrolitos en base de calcio. Finalmente, el efluente resultante se descargaría en cuerpos de agua naturales. Sin embargo, el alto coste de este tratamiento hace que sea necesario buscar alternativas más sostenibles. Actualmente, la Unión Europea (UE) promueve la implementación de esquemas circulares recuperar elementos de valor añadido de efluentes. Además, iniciativas como la Lista de Materias Primas Críticas, promueven la recuperación de compuestos valiosos a partir de recursos secundarios. Por lo tanto, los RLAs pueden ser una fuente de ácidos y metales. Entre las alternativas a la neutralización con cal, se están estudiando a día de hoy las tecnologías de membrana. En esta Tesis, se utilizarán dos tecnologías de membrana como la nanofiltracion (NF) y la diálisis de difusión (DD) para la valorización de los RLAs.

El drenaje ácido de minas (DAM), que es un subproducto de la industria minera, fue tratado con NF para la recuperación de ácido y la concentración de los metales en disolución. Los DAMs se caracterizan por un pH ácido (<3) y por la presencia de metales (p. ej. Al, Fe, Cu y Zn, entre otros). Las TRs, identificadas como materias primas críticas por la UE, se encuentran en bajas concentraciones. Se evaluaron distintas membranas de NF, incluyendo resistentes a ácidos, bajo diferentes composiciones de alimentación. Las membranas de NF, sobre todo aquellas con una capa activa hecha de poliamida, permitieron obtener altos rechazos de metales (<98%) y favorecieron el transporte de ácido. Sin embargo, su baja estabilidad en medio ácido hace que sean susceptibles a ser usadas en operaciones a largo plazo. Los cambios en la estructura de la capa activa de la membrana se evaluaron mediante FSEM-EDAX, FTIR y XPS. Se observó que la especiación de la disolución tiene un impacto significativo en el rechazo de la membrana. Además, se desarrolló una aproximación numérica basada en el modelo de Disolución-Electro-Difusión considerando el transporte reactivo, con el fin de caracterizar el transporte de especies mediante permeanzas. Asimismo, se estudió y probó la capacidad de predicción del modelo desarrollado para determinar su aplicación para el diseño de procesos.

Además, un RLA de una industria metalúrgica compuesta por una mezcla de H_2SO_4 y HCl (0.3<pH<0.7) con impurezas no metálicas (As) y metálicas (Fe, Cu, Zn) se trató con una membrana de poliamida (NF270). La membrana fue capaz de rechazar metales en más del 80%, mientras que el transporte de As fue inferior al 50%, que se debe a su presencia como una especie no cargada (es decir, H_3AsO_4) que no es rechazada por la carga de la membrana.

Finalmente, un RLA altamente ácido (220 g/L H_2SO_4) de una fundición de cobre con As como principal impureza (3.4 g/L) se trató en un módulo de DD. La presencia de As(III) y As(V) fue estudiada en la recuperación de ácido y en el transporte de iones bajo distintas condiciones de operación. Se observó que la especiación de As no influye en la recuperación del ácido. El As no fue rechazado (paso de iones por debajo del 50%) por la membrana debido a su presencia como una especie no cargada, como H_3AsO_3 para el As(III) y H_3AsO_4 para el As(V). Sin embargo, la membrana es capaz de rechazar más As(III) que As(V) debido a la presencia del primero como un catión ($H_2AsO_2^+$). Bajo las condiciones de operación óptimas, fue posible recuperar el 69±2% del ácido (146.3 g/L) con As como impureza principal (1.3 g/L y con un paso del 39±1%), mientras que el contenido total de metales estaba por debajo de 0.1 g/L.

Resum

Avui en dia, les industries mineres i hidrometal·lúrgiques generen una quantitat considerable de residus líquids àcids (RLAs), que es caracteritzen per un baix pH i per la presència de metalls (p. ex. Fe, Cu i Zn i Terres Rares (TR) entre d'altres) i no metalls (p. ex. As, Be). Aquests efluents es tracten, generalment, mitjançant l'addició de calç morta per neutralitzar l'acidesa i eliminar els metalls com hidròxids i hidroxisulfats, i els no metalls com electròlits en base de calci. Finalment, l'efluent resultant es descarregaria en cossos d'aigua naturals. No obstant això, l'alt cost associat amb aquest tractament, fa que sigui necessari buscar alternatives més sostenibles. Actualment, la Unió Europea (UE) promou la implementació d'esquemes circulars per recuperar elements de valor afegit de efluents. A més, iniciatives com la Llista de Matèries Primeres Crítiques, promouen la recuperació de compostos valuosos a partir de recursos secundaris. Per tant, els RLAs poden ser una font d'àcids i metalls. Entre les alternatives a la neutralització amb calç, s'estan estudiant a dia d'avui les tecnologies de membrana. En aquesta Tesi, s'han seleccionat dues tecnologies de membrana com la nanofiltració (NF) i la diàlisi de difusió (DD) per a la valorització dels RLAs.

El drenatge àcid de mines (DAM), que és un subproducte de la indústria minera, va ser tractat amb NF per a la recuperació d'àcid i la concentració dels metalls en dissolució. Els DAMs es caracteritzen per un pH àcid (<3) i per la presència de metalls (p. ex. Al, Fe, Cu i Zn, entre d'altres). Les TRs, que s'identifiquen com a matèries primeres crítiques per la UE, es troben en baixes concentracions. S'han avaluat diferents membranes de NF, incloent resistents a àcids, sota diferents composicions d'alimentació. Les membranes de NF, sobretot aquelles amb una capa activa de poliamida, van permetre obtenir alts rebutjos de metalls (<98%) i van afavorir el transport d'àcid. No obstant això, la seva baixa estabilitat en medi àcid fa que siguin susceptibles a ser usades en operacions a llarg termini. Els canvis en l'estructura de la capa activa de la membrana s'han avaluat mitjançant FSEM-EDAX, FTIR i XPS. Es va observar que l'especiació de la dissolució té un impacte significatiu en el rebuig de la membrana. A més, s'ha desenvolupat una aproximació numèrica basada en el model Dissolució-Electro-Difusió considerant el transport reactiu, per tal de caracteritzar el transport d'espècies mitjançant permeances. Així mateix, s'ha estudiat i s'ha provat la capacitat de predicció del model desenvolupat per determinar la seva aplicació per al disseny de processos.

A més, un RLA d'una indústria metal·lúrgica composta per una barreja de H_2SO_4 i HCl (0.3<pH<0.7) amb impureses no metàl·liques (As) i metàl·liques (Fe, Cu, Zn) s'ha tractat amb una membrana de poliamida (NF270). La membrana va ser capaç de rebutjar metalls en més del 80%, mentre que el transport d'As va ser inferior al 50%, degut a la seva presència com una espècie no carregada (és a dir, H_3AsO_4) que no és rebutjada per la càrrega de la membrana.

Finalment, un RLA altament àcid (220 g/L H_2SO_4) d'una fosa de coure amb As com a principal impuresa (3.4 g/L) es va tractar en un mòdul de DD. La presència d'As(III) i As(V) va ser estudiada en la recuperació d'àcid i en el transport de ions sota diferents condicions d'operació. Es va observar que l'especiació d'As no influeix en la recuperació de l'àcid. L'As no va ser rebutjat (pas d'ions per sota del 50%) per la membrana a causa de la seva presència com una espècie no carregada, com H_3AsO_3 per l'As(III) i H_3AsO_4 per l'As(V). No obstant això, la membrana és capaç de rebutjar més As(III) que As(V) a causa de la presència del primer com un catió ($H_2AsO_2^+$). Sota les condicions d'operació òptimes, va ser possible recuperar el 69±2% de l'àcid (146.3 g/L) amb As com a impuresa principal (1.3 g/L i amb un pas de el 39±1%), mentre que el contingut total de metalls estava per sota de 0.1 g/L.

Resumo

Hoxe en día, as industrias mineiras e hidrometalúrxicas xeran unha cantidade considerable de residuos líquidos ácidos (RLAs), que se caracterizan por un baixo pH e pola presencia de metais (p. ex. Fe, Cu, Zn e Terras Raras (TR) entre outros) e non metais (p. ex. As, Be). Estes efluentes trátanse, xeralmente, mediante a adición de cal para neutralizar a acidez e eliminar os metais como hidróxidos e hidroxisulfatos, e os non metais como electrólitos en base de calcio. Finalmente, o efluente resultante descargaríase nos corpos de auga naturais. Nembargantes, o alto custo asociado con este tratamento, fai que sexa necesario buscar alternativas máis sostíbeis. Actualmente, a Unión Europea (UE) promove a implantación de esquemas circulares para valorizar os efluentes para recuperar elementos de valor engadido. Ademais, cabe destacar iniciativas como a Lista de Materias Primas Críticas, que promove a recuperación de compostos valiosos a partir de recursos secundarios. Polo tanto, os RLAs poden ser unha fonte de ácidos e metais. Entre as alternativas á neutralización con cal, están a estudarse a día de hoxe as tecnoloxías de membrana. Nesta Tese, utilizáronse dúas tecnoloxías de membrana como a nanofiltracion (NF) e a diálise de difusión (DD) para a valorización dos RLAs.

A drenaxe ácido de minas (DAM), que é un subproduto da industria mineira, foi tratado con NF para a recuperación de ácido e a concentración dos metais en disolución. Este tipo de disolucións caracterízanse por un pH ácido (<3) e pola presenza de metais (p. ex. Al, Fe, Cu e Zn, entre outros). As TRs, identificadas como materias primas críticas pola UE, atópanse nos RLAs en baixas concentracións. Avaliáronse distintas membranas de NF, incluíndo resistentes a ácidos, baixo diferentes composicións de alimentación. As membranas de NF foron capaces de tratar as DAMs, sobre todo aquelas cunha capa activa feita de poliamida, obtendo altos rexeitamentos de metais (<98%) e favorecendo o transporte de ácido. Nembargantes, a súa baixa estabilidade en medio ácido fainas susceptíbeis a ser usadas en operacións a longo prazo. Os cambios na estrutura da capa activa da membrana avaliáronse mediante FSEM-EDAX, FTIR e XPS. Observouse que a especiación da disolución ten un impacto significativo no rexeitamento da membrana. Ademais, desenvolveuse unha aproximación numérica baseada no modelo de Disolución-Electro-Difusión considerando o transporte reactivo, coa fin de caracterizar o transporte de especies mediante permeanzas. Asemade, estudouse e probouse a capacidade de predición do modelo desenvolto para determinar a súa aplicación no deseño de procesos.

Ademais, un RLA dunha industria metalúrxica composto por unha mestura de H_2SO_4 e HCl (0.3<pH<0.7) con impurezas non metálicas (As) e metálicas (Fe, Cu, Zn) tratouse cunha membrana de poliamida (NF270). A membrana foi capaz de rexeitar metais en máis dun 80%, mentres que o

transporte de As foi inferior ao 50%, debido a súa presenza como unha especie non cargada (é dicir, H_3AsO_4) que non é rexeitada pola carga da membrana.

Finalmente, un RLA altamente ácido (220 g/L H_2SO_4) dunha fundición de cobre con As como a principal impureza (3.4 g/L) tratouse nun módulo de DD. A presenza de As(III) e As(V) estudouse na recuperación de ácido e no transporte de ións baixo distintas condiciones de operación. Observouse que a especiación de As non inflúe na recuperación do ácido. O As non foi rexeitado (paso de ións por baixo ao 50%) pola membrana debido a súa presenza como unha especie no cargada, como H_3AsO_3 para o As(III) e H_3AsO_4 para o As(V). Nembargantes, a membrana foi capaz de rexeitar máis As(III) que As(V) debido á presenza do primeiro como un catión ($H_2AsO_2^+$). Baixo as condicións de operación óptimas, foi posíbel recuperar o 69±2% do ácido (146.3 g/L) con As como impureza principal (1.3 g/L e cun paso do 39±1%), mentres que o contido total de metais estaba por debaixo de 0.1 g/L.

Summary

Abbreviations and symbols

Abbreviations

AEM	Anion Exchange Membrane
AFM	Atomic Force Microscopy
ALW	Acidic Liquid Waste
AMD	Acid Mine Drainage
ATR-FTIR	Attenuated Total Reflectance Fourier Transform Infrared
CEM	Cation Exchange Membrane
DD	Diffusion Dialysis
ED	Electrodialysis
EU	European Union
FO	Forward Osmosis
FS	Flat Sheet
IEP	Iso-Electric Point
MD	Membrane Distillation
MWCO	Molecular Weight Cut-Off
NF	Nanofiltration
REEs	Rare Earth Elements
RO	Reverse Osmosis
SDFM	Solution-Diffusion-Film Model
SEDFM	Solution-Electromigration-Diffusion-Film Model
SEDM	Solution-Electro-Diffusion Model
SEM	Scanning Electron Microscopy
SPIRE	Sustainable Process Industry through Resource and Energy Efficiency
SRB	Sulphate-Reducing Bacteria
SW	Spiral Wound
TFC	Thin-Film Composite
TMP	Trans-Membrane Pressure
UF	Ultrafiltration
XPS	X-ray Photoelectron Spectroscopy

Symbols

$\mathbf{A}$	Debye Hückel parameter (0.5042)
$\mathbf{a_0}, \mathbf{a_1}, \mathbf{a_2}$	Fitting parameters
$\mathbf{c_i}$	Virtual concentration of species i
$\mathbf{IAP}$	Ionic activity product
$\mathbf{j_i}$	Flux of component i through the membrane
$\mathbf{J_v}$	Solvent flux across the membrane
$\mathbf{K_{so}}$	Solubility constant of the mineral
$\mathbf{k_w}$	Hydraulic permeability of the membrane
$\mathbf{P_i}$	Membrane permeance to species i
$\mathbf{Q}$	Flow
$\mathbf{SI}$	Saturation index

V	Tank volume
x	Dimensionless position across the membrane
X	Concentration of the electrolyte
z_i	Charge of species i
ΔP	Difference of pressure across the membrane
$\Delta\pi$	Difference of osmotic pressure across the membrane
α	Equilibrium dissociation constant
γ_i	Activity coefficient of species i
φ	Dimensionless virtual electrostatic potential

Subscripts

f	Feed
i	Species i
p	Permeate
r	Retentate
t	Time

CHAPTER 1

Introduction

1. Introduction

1.1. Towards a circular economy: waste as a resource

Over the past centuries, the industry has implemented a "take-make, consume and dispose of" pattern of growth. This linear model is based on the assumption that raw materials are abundant and available, easy to obtain and cheap to dispose of. Nevertheless, the continuously increasing demand and the scarcity of resources have caused environmental degradation [1].

The European Union (EU) has proposed in 2015 an action plan to move towards a circular economy to improve resource efficiency and to maintain sustainable growth. Circular economy systems maintain the added value in products for as long as possible, while the generation of wastes is avoided or reduced. To diminish the generation of wastes, once the product has reached the end of its life, it must be used to create further value. To achieve that it is necessary to make changes in each step of the value chain, from production to consumption, repair and remanufacturing and waste management (**Figure 1**). It is estimated that circular economy schemes can reduce the need for input materials by 17-24%, which can bring an economic saving of 630 billion € in the industries of the EU [1,2].

The industrial sector, especially the so-called process industries, generates a large amount of wastes that require appropriate disposal. In the EU, the Sustainable Process Industry through Resource and Energy Efficiency (SPIRE) initiative has recently defined the 2050 Roadmap, with a particular focus on resource efficiency. The actions inside the program includes: (1) maximisation of the efficiency in the use of primary resources, by ensuring higher yields for the raw materials, (2) implementation of thefull re-use, recycling or recovery of waste as an alternative resource in all the process streams (e.g. collections, transportation, pre-treatments) to achieve a symbiotic industrial network, and (3) promoting zero discharge, trying to recover the maximum amount of sensible heat from wastewaters [3].

Furthermore, the critical raw materials for the EU that are important for high-tech products and emerging innovations have been identified. These materials are widely used in solar panels, wind turbines and electric vehicles, among others. The first list done by the EU contained 14 critical raw elements and has been enlarged up to 27 in 2017. Nowadays, the list includes phosphate rock, rare earth elements (REEs), natural rubber, silicon metal, coking coal, the platinum group metals and other elements from the periodic table (e.g. Sb, Be, Bi, Co, In and Mg among others). Mostly, these critical raw materials are produced and supplied from non-European countries, mainly by China, USA,

Russia and Mexico. Therefore, the need to obtain alternative routes for the critical raw materials arises [2].

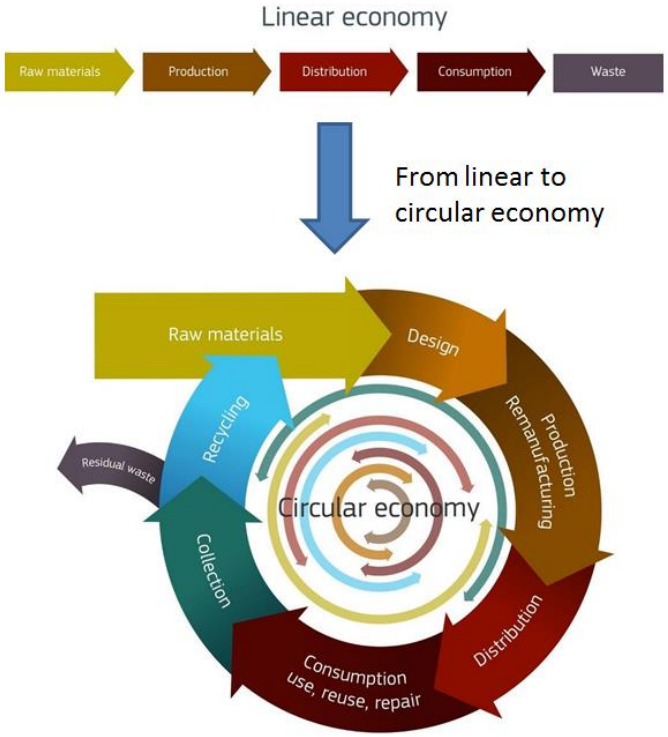

Figure 1. *From linear to circular economy. Source: European Commission [1]*

This thesis is focused on the evaluation of potential routes of revalorization of wastes from the mining, hydrometallurgical and metallurgical industries, especially of the acidic liquid wastes (ALWs). In particular, this PhD thesis is focused on evaluating the potential role of membrane processes as a stage to be integrated into the treatment trains to reach recovery and valorisation routes for ALWs. Then, effort was allocated to study the fundamental processes involved in the separation processes as well as to understand the role of the membrane properties and solutes and the membrane stability in strong acidic media. The scope of the PhD thesis did not include to study and provide the treatment trains.

1.2. Challenges in acidic liquid wastes: from disposal to valorisation of by-products

ALWs from mining, hydrometallurgical or metallurgical industries represent an environmental problem due to their low pH and high content in heavy metals. For this reason, these waters require an appropriate treatment. However, the conventional ones do not contemplate the recovery of

certain valuable elements. In this case, circular approaches to resources recovery schemes can be implemented.

1.2.1. Acidic liquid wastes from the mining industry: Acid Mine Drainage

Acid Mine Drainage (AMD) is a by-product formed when iron sulphide minerals (e.g. pyrite (FeS_2), marcasite, (FeS_2), and pyrrhotite (FeS)) are oxidised in contact with water and oxygen. The generation of AMDs takes place in galleries, mine workings, open pits, waste rock piles and mill tailings in both operating and abandoned poly-sulphide mining sites [4–6]. The oxidation process leads to the generation of H_2SO_4, which has the ability to dissolve soil minerals resulting in the formation of effluents rich in dissolved ferrous and non-ferrous metal sulphates (e.g. Fe, Al, Zn and Cu) and containing non-metallic species (e.g., As, Se) and minor amounts of REEs [7,8]. REEs form part of the critical raw materials of the EU because of their uses in the high-tech industry and for their scarcity since the EU has no primary resources of REEs [2].

One of the most known cases of AMD generation takes place in the Iberian Peninsula, in the so-called Iberian Pyrite Belt. This zone is one of the major sources of pyrite worldwide and has been exploited since 3000 B.C. Mining activity has led to the presence of up to 150 different types of AMDs in the Odiel and Tinto basins. The AMDs generated in the Iberian Pyrite Belt are characterised by low pH (1-3) and concentrations up to 35 g/L Fe, 3.5 g/L Al, 675 mg/L Cu, 798 mg/L Zn and 104 mg/L As, among others [9,10]. Recently, it has been identified that the concentration of REEs is relatively high, achieving values up to 80 mM in comparison with the 0.08 mM found in natural waters [11–13].

Usually, REEs are obtained from different minerals (bastnaesite, monazite and xenotime). To obtain each REE separately it is necessary, first of all, to subject the mineral to acidic leaching (mainly with H_2SO_4), followed by acid neutralisation and different solvent extraction steps [14–17]. However, the exhaustion of these minerals makes necessary to exploit other sources to acquire REEs, especially in Europe, which lacks of primary resources. It has recently been estimated that the total discharge of AMD in the Iberian Pyrite Belt watersheds is around 1 m^3/s in the dry season [18,19] with concentrations of total REEs varying from 0.3 to 11.7 mg/L with an average concentration of 1.0 mg/L [11]. Then, AMDs can be considered as an alternative source for REEs recovery.

The common strategies to mitigate the environmental impact of AMDs rely on remediation techniques based on source and migration control [20]. Source control techniques are applied to avoid the formation of AMDs by restricting the contact of oxygen and/or water with sulphide minerals [21,22]. However, many attempts to prevent AMD generation have proven to be unprofitable with the risk of contaminating surrounding water bodies such as the underground aquifers [23]. Once the AMD is released to the environment, different remediation techniques can be applied, such as [24–28]:

i) AMDs containment to prevent the migration of contaminants, such as geotechnical measures.

ii) Active ex-situ treatments using an energy source, such as pump-and-treat systems. The AMD-contaminated is pumped, treated above ground and, optionally, sent back to the aquifer.

iii) Passive in-situ treatments without any energy source, such as permeable reactive barriers. The AMD-contaminated groundwater is treated in-situ underground in the path of the polluted water flow with a reactive material.

Nowadays, with the new legislation that promotes sustainability and limits the generation of wastes from the mining industry, new approaches are focused on the recovery of valuable components contained in AMDs, such as metals (Zn, Cu and REEs) and un-valuable components such as an acid (mainly H_2SO_4).

The common ex-situ treatment of AMDs is based on the addition of an alkaline agent (e.g. lime, caustic lime or limestone) to neutralise the acidity and to remove the metals as hydroxides [29,30]. The obtained sludge is voluminous, rich in water with a solid content between 2 and 4%, which is mainly composed of a mixture of iron and aluminium hydroxides, oxyhydroxides and hydroxysulphates with minor amounts of other metals. For example, iron, after being totally oxidised to Fe(III), can precipitate as schwertmannite ($Fe_8O_8(OH)_6SO_4$) at pH>4 or as ferrihydrite ($5Fe_2O_3{\cdot}9H_2O$) at pH<4. The precipitation of these minerals is accompanied by the sorption and co-precipitation of heavy metals (Zn, Cu, Mn) and REEs. To dispose the sludge adequately, large and expensive solid-liquid separation units are required [7,29–31]. One advantage of the treatment with alkalis is the potential recovery of metals by selective precipitation through the differences in metal solubilities. Wei et al. [32] were able to precipitate selectively iron and aluminium with different alkalis (NaOH, Na_2CO_3, NH_4OH, CaO and $Ca(OH)_2$). Iron was precipitated (98% of initial content with >93% purity) at pH 3.5–4.0 and, subsequently, aluminium was removed (97% of initial content with >92% purity) at pH 6.0–7.0. However, several disadvantages such as high and continuous consumption of the industrial alkalis, and the water-rich sludge and its further treatment make this process not economically viable [7,33]. Nevertheless, the potential recovery of H_2SO_4, although its value is marginal, is related to a reduction in the alkali consumption and sludge management costs afterwards for its safe disposal and is considered as a relevant sustainability element for the future of hydrometallurgy industry.

The treatment of AMD with biological processes has also been studied. Sulphate-reducing bacteria (SRB) under anaerobic conditions can be employed to remove metals as sulphides [34,35]. SBRs are a group of bacteria (e.g. *Desulfovibrio*, *Desulfotomaculum*) that generates biogenic sulphide from sulphate ions (which can react and precipitate many of the metals as sulphides) and at the same time

leads to the increase in alkalinity and the pH value of water. The media must have several specific conditions to enable SBRs to treat AMDs: i) anaerobic environment (redox potential around –200 mV); ii) pH values higher than 5 and; iii) the presence of an organic substrate to be oxidised as an energy source. The use of SBRs has been studied in permeable reactive barriers [34] or bioreactors [35].

To remove metals from AMDs, the use of low-cost sorbents (e.g. natural zeolites) has also been investigated [36]. A zeolite is a microporous aluminosilicate mineral with a net negative charge, which can be used to remove metallic cations. The use of natural zeolite, clinoptilolite, has been studied to remove heavy metals from waters. The zeolite selectivity has been studied by Blanchard et al. [37] (Pb^{2+}>NH_4^+,Ba^{2+}>Cu^{2+},Zn^{2+}>Cd^{2+},Sr^{2+}>Co^{2+}) and by Zamzow et al. [38] (Pb^{2+}>Cd^{2+}>Cs^+>Cu^{2+}>Co^{2+}>Cr^{3+}> Zn^{2+}>Ni^{2+}>Hg^{2+}). The use of zeolites for AMDs treatment has been reviewed by Wingenfelder et al. [36]. The clinoptilolite, one of the most widely used zeolites, has been found to be stable in moderate acidic solution and suffers from disintegration at pH values below 2.0.

Despite the different techniques used for AMD remediation, any of them have not provided reliable solutions.

1.2.2. Acidic liquid wastes from the metallurgical industry

In the production of primary zinc and copper in metallurgical processes, a gaseous stream is generated during the sintering, roasting and smelting of sulphide minerals. Since this gaseous stream contains dust and sulphur dioxide (SO_2(g)), it is commonly treated with a wet electrostatic precipitator to remove the dust and with a scrubber using cold water to absorb the SO_2(g) [39]. The aqueous stream generated is characterised by a high acidity because of the hydration of SO_2(g) to give H_2SO_4 and by a high content of metallic (e.g. Fe, Zn, Cu…) and non-metallic ions (e.g. As, Se, Sb…) due to the dissolution of remaining soluble dust particles. In some cases, HCl and HF can be released in the flash smelting furnace to the gas that must be treated [40].

The aqueous stream typically contains 1-50 wt. % H_2SO_4, halides such as HCl (0.2-2 g/L) or HF (0.1-1 g/L, including H_2SiF_6) and As (up to 10 g/L). The concentration of metals such as Cu, Zn and Fe can be individually up to 2.5 g/L, whereas Hg and Pb concentration can reach values of 0.05 g/L each one. Moreover, other metals such as Al, Ni, Cr, Cd, Bi and Sb are present at much lower concentrations (below 50 mg/L) [39]. The non-metals behave as weak acids (H_3AsO_4, H_3AsO_3, H_3SbO_3, H_2SeO_4), which makes difficult their separation from the acid. Within this context, the main challenge for smelters is how to deal with the high concentration of As (up to 10 g/L) in these effluents, which requires an appropriate treatment to reduce its concentration.

The conventional treatment relying on neutralisation with lime and sedimentation for solid-liquid separation is effective at low acid (0.5<pH<2) and metal concentrations generating a sludge that is a mixture of gypsum, calcium and iron arsenates and metal hydroxides as well other impurities as Se, Sb and Bi [39]. Nevertheless, this approach is not always effective when applied to H_2SO_4-rich effluents (10-25%).

However, the presence of As or Se requires a pre-treatment, which consists in the oxidation of As(III) and Se(IV) to As(V) and Se(VI) by strong oxidants (ozone, chlorine, hydrogen peroxide) and subsequent coagulation-precipitation with Al or Fe, or through ion exchange or electrochemical treatments to remove arsenic as arsine (AsH_3) [41–43]. Alternative solutions have been applied to separate and recover acid (i.e. H_2SO_4) as a pre-stage for subsequent removal and stabilisation of As as a long term stable mineral form (e.g. scorodite $FeAsO_4 \cdot 2H_2O$). However, the high acidity of metallurgical effluents may limit the removal of As through this way.

Other techniques for acid recovery may be preferred, such as solvent extraction or acid retardation.

Solvent extraction is a separation technique based on the differences of solubilities of one compound between two immiscible liquids, usually an aqueous solution and an organic phase [44–46]. This technique has been employed for the extraction of acids or metals. For instance, Alguacil and López [44] studied the recovery of acids (H_2SO_4, H_3PO_4, HCl, $HClO_4$ and HNO_3) with phosphine oxide Cyanex 923 in toluene. The acid extraction by the organic phase is described by $mH^+_{aq} + X^{m-}_{aq} + L_{org} \rightleftarrows HXL_{org}$. Kerney [45] proposed the use of solvent extraction (tri-octyl-amine or tri-butyl-phosphate extractants) for the treatment of pickling solutions formed by Fe (80-150 g/L), Zn (5-150 g/L) and HCl (10-80 g/L) for the recovery of Zn. At such acidic media, it was possible to extract Zn with solvating extractants, but the presence of Fe and pH affected the extraction capacity. Wisniewski [46] evaluated the extraction of arsenic (As(III) and As(V) from H_2SO_4 solutions (50-200 g/L) with Cyanex 923 diluted a 50% in kerosene. The extractant removed both As(III) and As(V), and its extraction capacity increased at higher acid concentrations, but part of the acid was coextracted.

Acid retardation (i.e. ion exchange) is a process used for acid purification. It is based on the adsorption of the un-dissociated acid on ion-exchange resins and its release during backwashing with water [40,47,48]. Hatch and Dillon [47] evaluated the separation of different acids from electrolytes using anion exchange resins (Dowex 1 X8 and Retardation 550WQ2). Different mixtures (HNO_3 and NH_4NO_3, H_2SO_4 and $NiSO_4$, H_2SO_4 and $FeSO_4$, HCl and NaCl, HCl and $FeCl_2$) were studied. The different elution times for the acid and electrolytes proved to make their separation possible. For example, the separation of 1.8 M H_2SO_4 from 0.25 M $NiSO_4$ yielded a peak acid concentration of 1.4 M, which was almost free of $NiSO_4$. Petkova et al. [48] studied the separation of waste plating H_2SO_4 solutions (250-270 g/L) from metals cations (6-13 g/L Ni, <1 g/L Cu and Fe, <0.5 g/L Zn) by the anion exchange resin

Wofatit SBW. After the adsorption and subsequent elution, it was possible to recover the 80% of the acid, with a low content of metallic impurities (<2 g/L).

Although these technologies can be useful for acid recovery, two drawbacks are associated with them: on the one hand an additional treatment may be needed to purify the acid from residual metallic compounds, and on the other, the need for the regeneration of the organic phase in solvent extraction and the resin in acid retardation can increase the costs of the process.

The presence of both metallic and non-metallic impurities in these kinds of ALWs from metallurgical processes has prevented the reuse of the acid in other stages of the process. The main challenge of smelters industries is to reduce the amount and contaminant load of generated wastes (e.g. lime sludge), as well as to valorise by-products. Taking that into account, the objective would be to recover the maximum amount of a purified H_2SO_4 for further reuse. Additionally, the stringent environmental regulations, especially related to non-metal elements as As and other elements (such as Se, Sb), have made that new solutions promoting circular economy approach be investigated to recover an acid-free of pollutants (i.e. metals and non-metals) and the safe disposal of As.

1.3. Membrane processes for the valorisation of acidic liquid wastes

Over the past years, membrane technologies have been gaining importance in the industry, achieving the same results as conventional methods but saving costs. A membrane can be defined as a semi-permeable barrier or interface that can discriminate particles, molecules or ions depending on their size, charge or diffusivity. Membranes are widely applied in many fields, since they allow to obtain a valuable compound as permeate or remove an undesirable compound from the feed stream, such as removal of CO_2(g) from natural gas, removal of pathogens in wastewater treatment plants and water recovery from desalination of seawater, among others. The advantages of membrane processes comprise low energy consumption, ability to be combined and integrated with other separation processes, possibility of working at mild conditions and no need for additives. Despite these advantages, several disadvantages must be taken into account: membrane fouling, low lifetime, limited selectivity and low flux of permeate produced [49].

The selection of a suitable membrane technology depends strongly on both solution composition and chemical speciation of the components that need to be separated or concentrated, as well as on the membrane properties. As explained above, in the case of the mining, hydrometallurgical and metallurgical industries streams are characterised by a high content of dissolved metallic and non-metallic species and an elevated concentration of strong acids. In such scenario, and under a circular economy perspective, the following challenges are faced for the valorisation of ALWs: (a) the retention of a given valuable metallic or non-metallic species (or family of species) by the membrane

for its further separation and concentration, and (b) the permeance of a valuable compound (e.g. strong acids) through the membrane for its recovery in the permeate. Membrane technologies such as reverse osmosis (RO), membrane distillation (MD), forward osmosis (FO), electrodialysis (ED), nanofiltration (NF) and diffusion dialysis (DD) are the most promising ones to tackle these challenges.

RO is a pressure-driven membrane process used for water desalination that provides a rejection of 99% of dissolved electrolytes and organic molecules of low molar mass [50–52]. Ricci et al. [50] studied the treatment of a gold mining effluent (pH 1.4) by the integration of NF and RO. The RO step was able to reject the metals species by 92% and the acid by 98%. González et al. [52] evaluated the purification of 2 M H_3PO_4 with impurities of 4.9 g/L Fe, 3.4 g/L Mg and 3.0 g/L Al, among others with the SXO1 RO membrane. The membrane was able to reject the metals by more than 98%, while 46% of the acid was recuperated.

MD is a thermal-driven membrane process that uses a micro-porous hydrophobic membrane that separates a warm solution from a cold solution. Vapours and volatile compounds are transported across the membrane from the warm to the cold side, and then they condensate at the surface [53,54]. Kesieme et al. [53] employed MD for the recovery of water from sulphuric leaching solutions, containing 1.08 M H^+, 15.7 g/L Fe and 4.4 g/L Al, among others. Water recovery higher than 80% was achieved with a content of acid lower than 1mM. From the initial solution, the acid and the metals were concentrated up to a factor of 4, except for Ca, which precipitated onto the membrane surface. Zhang et al. [54] studied the transport of H_2SO_4 across a MD membrane, achieving a sulphate rejection of 98%. The authors found that the flux of the acid increased with temperature but decreased at higher concentrations.

FO is attracting the attention of researchers for its remarkable potential in desalination and wastewater treatment. Unlike RO, FO does not require an external pressure, and high osmotic pressure is needed to drive the water transport from the feed to the draw solution. However, there are only a few studies on the application of FO to the removal of metals. You et al. [55] fabricated an inorganic membrane to remove heavy metals (Cd, Pb, Cu and Zn with total concentration of 200 mg/L) at pH 4.5, using 2 M NaCl as draw solution. The membrane was able to achieve metal removals of 94% and high water fluxes (69 L/m^2 h).

ED is a membrane process that relies on the use of ion-exchange membranes to drive the transport of ions under an electric field. These membranes have charged groups attached to the polymer backbone and have the ability to exclude partially or fully ions with the same charge of the membrane. The membrane stack contains intercalated Anion and Cation Exchange membranes (AEM and CEM, respectively) between which feed water is allowed to flow. Under the application of an electric field, cations in feed solution migrate towards the cathode and anions towards the anode. Each set of anion and cation membranes forms a cell pair. Cations pass through CEM (negatively

charged) and are retained by AEM (positively charged). Anions in solution experience the opposite trend. At the end, two stream products are obtained, one enriched in ions and another one depleted of them. This technique has proven to be useful for the purification and concentration of industrial spent acids [56–58]. Boucher et al. [56] studied the recovery of acids from effluents from the zinc industry (200 g/L H_2SO_4, 10 g/L Zn, 10 g/L Mg and 1 g/L Mn). In the ion rich-stream, it was possible to recover 67% of the acid, while the transport of metals to the stream was below 8%. Buzzi et al. [57] applied ED for the treatment of an AMD (pH 2.4) containing Na, Mg, Ca and Fe(III) as main impurities. ED allowed the recovery of water, which was characterized by a pH 3, and the removal of metals by 97% (most of the metals concentration remained below the detection limit.

These mentioned membrane processes have proven to be effective for treating ALWs. However, they are more focused on the recovery of water instead of a valuable component present in water. Moreover, they present several disadvantages: RO requires a high hydraulic pressure (60-80 bar) for operating; MD needs an external thermal energy to heat the solution to more than 60 °C; FO is highly dependent on the selected draw solution, and ED requires a high external voltage for the ion separation, which can increase if concentration polarization or precipitation occurs. Therefore, other techniques such as NF and DD can be more appropriate for the recovery of valuable components.

NF is a pressure-driven membrane process that exhibits high rejections for multi charged ions (>90%) while allowing single-charged ions to permeate through the membrane (**Figure 2**).

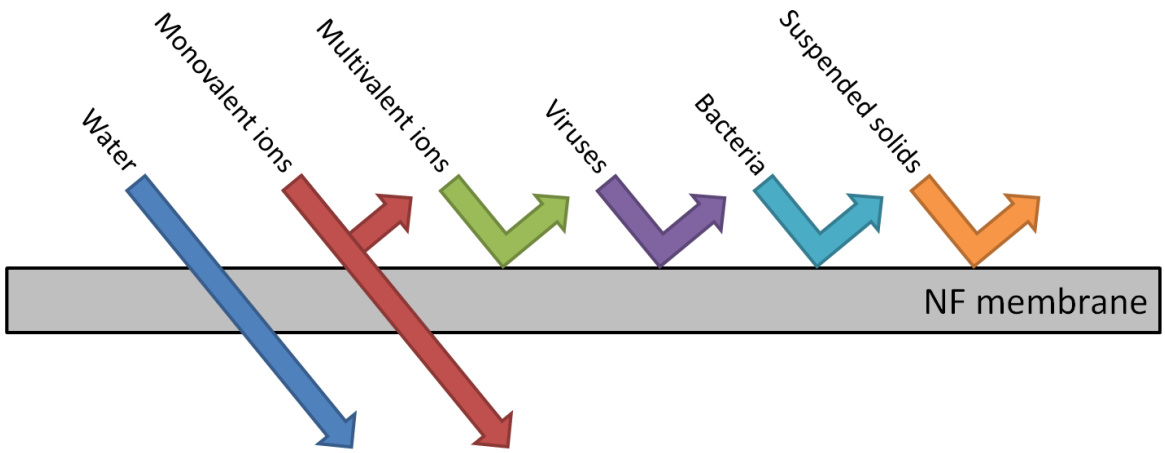

Figure 2. *Scheme describing the average rejection performance of NF membranes (arrows indicate the observed rejection trends)*

NF membranes were initially described as “loose ultrafiltration (UF)” or “open RO” membranes because of their properties. They exhibited higher fluxes than RO membranes and higher rejections than UF membranes. The first generation of NF membranes was made of cellulose, but due to their low stability, polymeric membranes are being employed. In the case of Dow Chemical Company, the development of the NF membranes was devoted to removing sulphate from the water streams

generated in the extraction wells from the oil-extraction industry. A new generation of Thin-Film Composite (TFC) membranes was created by using the know-how from the production of polyamide RO membranes, by modifying the nature of the active layer and its morphology [59,60].

Nowadays, there is still an open discussion about the membrane structure, since several researchers consider that the NF membranes have fixed pores and that their main exclusion mechanism is due to the difference sizes of species and membrane pores, similarly to UF membranes (i.e. size exclusion or steric hindrance), whereas other researchers defend that NF membranes do not have pores, but instead they present a free-volume originated due to the movement of polymeric chains (i.e. dense membranes), and the main exclusion mechanism is due to the differences in the diffusivities of solutes (i.e. solution-diffusion) [59,60].

Nowadays, TFC commercial NF membranes have three differentiate layers: (1) a thin active layer, which has the selectivity to species and is usually made of polyamide; (2) an intermediate layer made of polysulphone and, (3) a polyester layer which gives mechanical strength to the structure.

When placed in contact with aqueous solutions, NF membranes present a superficial charge due to the dissociation of the free functional groups of the active layer. For example, polyamide-based membranes present carboxylic (R-COOH) and amine ($R\text{-}NH_2$) ionisable groups, which are responsible for the membrane charge. At acidic pH, the membrane presents a positively charged surface due to the fully and partial protonation of carboxylic (R-COOH) and amine ($R\text{-}NH_3^+$) groups, respectively. Under this condition, the transport of anions is favoured, while the one of cations is hindered. Instead, at basic pH, carboxylic groups are dissociated ($R\text{-}COO^-$) and are responsible for the negative membrane charge, which results in a better passage of cations [59–61]. Therefore, under the appropriate conditions, NF membranes can be suitable for handling ALWs since they can allow the transport of acids (e.g. $H^+ X^-$), while multi-charged metal ions could be better rejected.

DD is a membrane-based process used for acid recovery from solutions containing metals. The process is driven by a concentration gradient and uses typically polymeric AEMs, whose positive charge, provided by the quaternary ammonium groups, allows the acid (HX) in solution to permeate while the other positively charged metal ions are effectively rejected by the membranes (**Figure 3**). The acid anion (X^-) is transported across the AEM with the co-transport of the fastest cation in solution (H^+) to hold the electroneutrality condition [62]. It is a fact that the H^+ properties, in terms of being co-transported with the acid anion are much higher than any other positively charged cation (single or multi-charged). One parameter of importance is the electrolyte-effect. The addition of electrolytes with the same anion as the one of the acid promotes the transport of H^+ across the membrane [63]. Moreover, water transport across an AEM may occur and it could be due to: (1) osmotic pressure differences due to the composition of both solutions (i.e. osmotic flux), which

results on water transport from the water to the acid side and, (2) water transport associated with the solvation of ions (i.e. "drag flux") from the acid to water side [64].

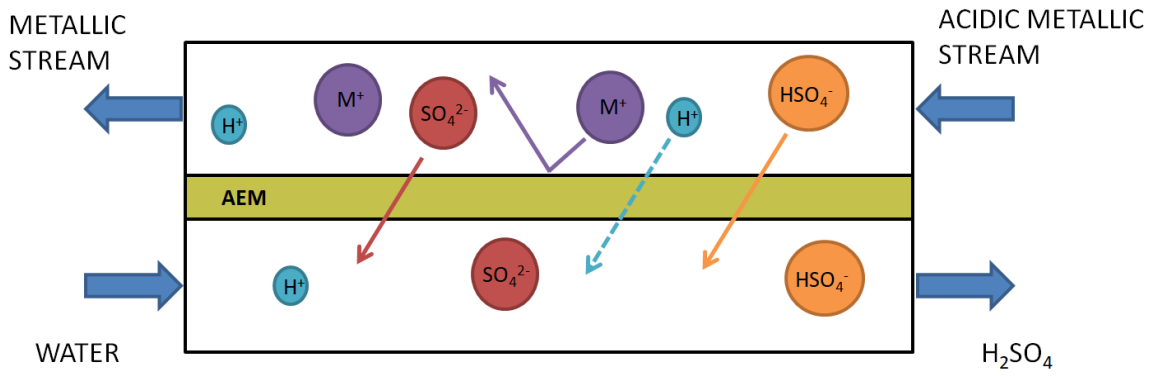

Figure 3. *Scheme of a DD cell containing AEM treating acidic waters (arrows indicate the observed rejection trends)*

NF and DD can be suitable for the treatment of acidic waters and the recovery and purification of acids. Nevertheless, the stability of these membranes at the long-term operation must be studied (**Figure 4**). Since polymeric NF membranes are stable from pH 2 to higher values and ALW, often present a lower pH, ceramic NF membranes able to resist such low pH values are emerging as a promising alternative. Concerning DD, membrane degradation at low pH is not a problematic issue because the AEMs used in DD can resist pH values as low as –0.5.

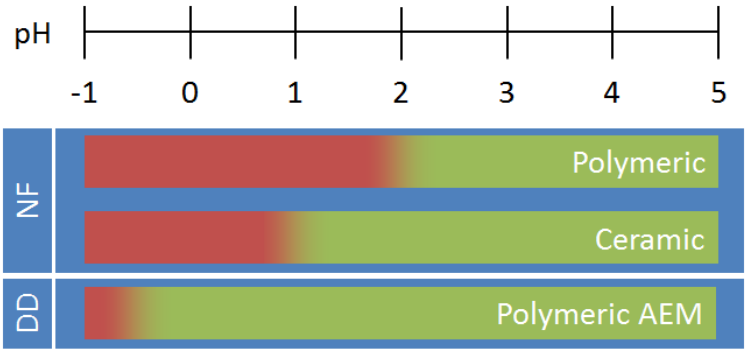

Figure 4. *Stability of NF membranes and AEMs at acidic pHs*

The applicability of both techniques will be discussed in more detail in sections 1.3.1 and 1.3.2. However, before this, the membrane transport phenomena for both NF and DD will be addressed.

Concentration polarisation

Concentration polarisation is a phenomenon related to the accumulation of solutes in the membrane boundary layer, with a higher concentration than in the bulk solution. Solute moves from the bulk solution into the boundary layer by a convective flow, and it goes back to the bulk solution by slow back diffusion. The retained ions in the concentration polarisation layer cause an increase in the osmotic pressure and then, lower permeate fluxes. Moreover, a decrease in rejections can be observed due to the higher concentration in the membrane-solution interface. This phenomenon can be reduced by introducing turbulence promoters on the feed side as spacers in the membrane module or operating the membrane stack in cross-flow mode [60].

Donnan exclusion

In 1911 Donnan developed a mathematical basis of the ability of a membrane to discriminate between oppositely charged ions in solution. When the membrane carries fixed charges, the co-ions (same charge as the membrane) tend to be excluded from the membrane resulting in a high rejection of the ions. This property makes the membrane selective for ions of the opposite charge [65].

The Iso-Electric Point (IEP) of a membrane must be taken into account as it determines its charge, which in turn strongly influences, as described above, the separation mechanism. The IEP represents the pH at which the charge of the membrane is zero. When the pH of the bulk solution is below the IEP, the membrane is positively charged and, conversely, at pH above the IEP the membrane is negatively charged [66]. This paramount has a significant relevance in the treatment of waters in NF and DD since membrane charge is defined by the pH of solution. However, most of the commercial NF membranes will exhibit a positive charge at acidic pH, and then will reject cations, whereas commercial DD membranes will present a positive charge, which will favour the transport of anions.

Dielectric exclusion

The Donnan equilibrium is not sufficient to explain the high rejection observed for multi-charged counter-ions, which makes the model to underestimate rejection of double-charged ions. The concept of Dielectric exclusion was postulated to explain this phenomenon [67].

The mechanism of dielectric exclusion was firstly considered by Glueckauf (1962) [68]. This phenomenon is associated with the difference in dielectric constant between the aqueous media (i.e. solution) and the polymeric matrix (i.e. membrane). Electrostatic interactions arise between the ions in solution and the membrane polarisation charges, which are induced by the ions themselves on the discontinuity surface located in the boundary between the two dielectric media. Polarisation charges have the same sign as the ions in solution. Due to the fact that dielectric constant of solution is remarkably higher than the corresponding to the polymeric matrix, the interaction between them causes and additional rejection mechanism for each ion, independent of its sign [67]. It must be

noticed that in the case that the membrane presents fixed charges, they will make a screening of interactions with polarisation charges stronger, making dielectric exclusion weaker [67,69].

It is remarkable that dielectric exclusion mechanism is more universal than Donnan exclusion because membrane can have or not fixed charge, but the matrix of the membrane exhibits a low dielectric constant. Dielectric exclusion is equivalent to a decrease in the bulk electrolyte concentration, which causes an increase at Donnan exclusion [67,69]. Donnan equilibrium is, thus, favourable to counter-ions, while dielectric exclusion does not discriminate ions according to their charge [67,69]

1.3.1. Nanofiltration

Impact of speciation on the performance of nanofiltration membranes in acidic solutions

The speciation of the solution has been found to have a significant impact on the NF membrane performance. For instance, Visser et al. [70] investigated the transport of H_2SO_4 across aromatic and semi-aromatic polyamide-based NF membranes and found that at pH>pK_a=1.92, (i.e. when the dominant (>90%) anion in solution is SO_4^{2-}) H_2SO_4 rejection was higher than 99.9%. Contrary, at low pH (pH<pK_a=1.92) (when the dominant (>90%) form of H_2SO_4 is HSO_4^-) the rejection decreased to values below 20%. This change in tendency can be related to (1) the change in membrane charge from a negative to a positive charge and, (2) the presence of HSO_4^- at high acid concentrations, which is less affected by dielectric exclusion than SO_4^{2-}.

The effect of speciation on metals behaviour and rejection extents has also been studied. Shang et al. [71] evaluated how pH affects vanadium speciation and its effect on the performance of Desal DL and DK membranes. V(V) rejection was 98% for DK and 96% for DL membrane from pH 2.5 to 6.5. Further increase of pH resulted on lower rejections (84% for DK and 85% for DL) because high molecular species ($V_{10}O_{28}^{6-}$) transform into species of lower molecular weight ($V_4O_{12}^{4-}$ and $V_3O_9^{3-}$).

The transport of inorganic non-charged species has also been studied in the literature [72–77]. One case of study is the phosphoric acid [72–74], whose non-charged species (H_3PO_4) predominates over the mono-charged ($H_2PO_4^-$) at pH lower than 2. Guastalli et al. [73] recovered 56% and 77% of phosphoric acid from industrial rinsing water containing dissolved aluminium by using MPF-34 and Desal-DL membranes, respectively. The transport of phosphoric acid across the membrane as a non-charged species was explained by the authors with steric hindrance (i.e. those molecules with molecular weight than the membrane MWCO are rejected). Diallo et al. [74] filtered phosphoric acid solutions at different concentrations (0.12, 1.2 and 5.9 mol/L) with MPF-34. Rejections decreased from 40% at 0.12 mol/L to almost zero values at 5.9 mol/L due to the increase in H_3PO_4 fraction. By determining the pore size at these acidic conditions revealed that it decreased at higher acid

concentrations. Moreover, the fact that concentration polarisation does not occur suggested that there is no steric hindrance. This suggested that the electric effects, which resulted from the interactions between $H_2PO_4^-$ and the membrane, controlled the global rejection of phosphoric acid. Another case of study is the Mo and Ge containing acid solutions [75,76]. The Mo(VI) as a neutral species (H_2MoO_4) exhibited a rejection near zero, while the deprotonation of the molecule at pH 6, increased its rejection. In the case of Ge(IV), present in solution as $Ge(OH)_4$, rejections were independent of pH and lower than 20%. Meschke et al. [75,76]concluded that the transport of both non-charged species was controlled by diffuse and convective flow, and the higher rejections for Mo were related to the larger molecular size. Werner et al. [77] evaluated the transport of In(III) and Ge(IV) through NF membranes. They obtained rejection values below 15% in acidic media for Ge(IV) due to its presence as $Ge(OH)_4$, while In(III) was fully rejected over a wide range of pH, even at neutral pH where In(III) is mainly present as $In(OH)_3$. These differences in rejections between $Ge(OH)_4$ and $In(OH)_3$ were explained by their different molecular size. In(III) is coordinated with three OH^- groups, surrounded by another three water molecules, while $Ge(OH)_4$ is coordinated in a tetrahedral structure smaller than that of $In(OH)_3$. Despite these studies, there is not still a consensus about the rejection mechanisms of non-charged inorganic compounds.

Application of nanofiltration membranes for the treatment of acidic liquid wastes

Several researchers have worked on the recovery of metal and acid from industrial or natural acid waters. NF is one of the most suitable options for the treatment of acidic waters due to its ability to reject multi-charged ions, allowing free acid permeation.

The application of NF membranes to treat AMD has been studied in the literature [66,70,78–81]. For example, Mullet et al. [66] applied to AMD with two polyamide NF membranes (NF270 and TriSep TS80) working at recovery ratios of 70% and observed that at pH values lower than the IEP, cation rejection was maximised. Zhong et al. [78] treated AMD from a copper mine with a polymeric NF membrane (DK4040F) achieving high metal rejections (>93%) at pH 3. Data about the transport of acid was not provided. Al-Zoubi et al. [79] performed an optimisation study with polymeric NF membranes (Alfalaval NF99 and Osmonics DK) for the treatment of AMD (pH 2.6). Large-scale operation showed metal (Cu, Fe, Mn, Ca, Mg and Al) rejection higher than 98% and sulphate rejection higher than 80%. In a later work [80], they tested the polymeric NF99, DK and GE membranes and observed high rejection of heavy metal (>98%) for the two first membranes. In this case, sulphate rejections were around 98%, obtaining a permeate richer in acid than the feed stream. The pH of the permeate pH was 2.5, while the feed had a pH of 2.7. Mullet et al. [66] studied the behaviour of the polymeric membrane NF270, obtaining rejections higher than 88% for Ca, Cu, Mg, Mn and sulphate. No data about the transport of H^+ was provided. Fornarelli et al. [81] tested NF270 to study the effects of pH on AMD filtration. High metal rejection was obtained (>95% for Ca, Cu, Mg and Mn(III))

at pH lower than 3, which was attributed to a positively charged membrane surface, while at higher pH values (above membrane IEP, and then a negatively charged membrane) lower rejections were obtained (between 89 and 94%). Sulphate rejections decreased from 97 to 89% due to the existence of single charged sulphate specie (HSO_4^-), as explained in the previous section. No data about the transport of H^+ was provided. Visser et al. [70] tested several membranes to treat AMD from a gold mine (pH 4.1). Low H_2SO_4 rejections were obtained with at high acid concentrations, demonstrating the large impact of H_2SO_4 dissociation on membrane performance. NF70 and NF90 showed the best performance to treat AMD (rejections >90% for sulphate, chloride, Na and Ca). No data about the transport of H^+ was provided.

Some attempts to remove metallic impurities from acidic industrial streams have been reported [52,82–87]. For example, Nÿstrom et al. [82] separated metal sulphates and nitrates from acid media achieving high rejections (around 99%) with the membrane NF-45. Erikson et al. [83] studied how to purify 33% H_2SO_4 by NF. Rejections for metals such as Fe, Zn, Cd and Cu were higher than 99%, achieving a recovery of the 50% of the acid. González et al. [52] performed a similar study, but, instead of purifying H_2SO_4, they purified H_3PO_4 solutions. By comparing NF and RO membranes, NF achieved metal rejections similar to RO (>95% for Fe, Mg and Al, among others) and higher fluxes (almost 4 times) than RO membranes. Moreover, with NF membranes the acid permeated more than 80%. Skidmore and Hutter [84] patented a method for purifying H_3PO_4 by NF, working at temperatures below 35 °C in order to increase the life of the membrane from 300 to 2000 hours. Rejections higher than 90% of multi-charged ions (Al, Fe and Mg, among others) were obtained. Galiana-Aleixandre et al. [85,86] proposed a NF process to remove sulphate and reuse water. They also obtained high rejections of Cr (no specified) and sulphate (>97%). Gherasim and Mikulášek [87] achieved high rejections of Pb (>98%) with commercial polyamide membrane (AFC80) when they evaluated how operating variables influence the removal of heavy metal ions from aqueous solutions. No data about the transport of H^+ was provided.

Therefore, as reported by these previous studies, H_2SO_4 can be, under appropriate pH, recovered in the permeate stream, while metal species are retained in the concentrated side.

Membrane stability at acidic media

NF membranes, especially those based on an active layer made of polyamide, are widely used for the treatment of ALWs. However, one of the most significant concerns of polyamide-based NF membranes is their low chemical resistance in very high acidic conditions, because long-term exposure to acid can cause the hydrolysis of polymeric chains as described elsewhere [88–91]. Platt et al. [88] concluded that the instability of membranes depends on time exposure, temperature, type of acid and concentration. For example, NF45 and Desal DK membranes exhibited worse chemical stability in HNO_3 (5% w/w) than in H_2SO_4 (20% w/w) after ageing for one to three months.

Additionally, the membranes became more unstable at a higher temperature. After one month of immersion in both acids at 80 °C, both membranes exhibited zero sucrose and glucose retention. Manis et al. [89] also studied the stability of Desal DK in H_2SO_4 solutions. After ageing the membrane in 2 M for two months, the Desal DK showed an increase of permeate flux and copper transport. Navarro et al. [90] aged Desal 5DL in phosphoric acid and concluded that the membrane properties, such as volume charge density, membrane charge, rejections and water fluxes, changed after immersion. This ageing affected the membrane selectivity and changed the membrane charge. Tanninen et al. [91] performed stability tests for NF270, Desal KH and Desal-5 DK in 2% H_2SO_4 at 60°C. The Desal-5DK was the first one to suffer from hydrolysis, exhibiting the double of water flux and a decrease in Cu retention (from 96 to 77%) after 3 days of immersion.

To solve this problem, research has been focused on the development of acid-resistant NF membranes, such as the Duracid (proprietary, GE Osmonics), MPF-34 (proprietary, Koch Membrane Systems) and Hydracore 70pHT (proprietary, Hydranautics) ones, which offer as good rejections as the polyamide ones do [50,73,92]. Mostly, the composition of these acid-resistant membranes is proprietary, but it is expected that the active layer is made of sulphamide or a sulphonated polyethersulphone. Manis et al. [89] also performed stability tests with the MPF-34 in 2 M H_2SO_4 and, after ageing the membrane for 8 weeks, it was able to keep its properties in terms of permeate flux and copper rejection.

NF ceramic membranes are attracting the attention of researchers as an alternative to polymeric membranes due to their higher chemical, mechanical and thermal stability, which can result in a longer lifetime. However, due to their higher fabrication cost and low selectivity, ceramic NF membranes are still not applied at a large scale [93,94]. Usually, the active layer of ceramic membranes is made of zirconia (ZrO_2) or titania (TiO_2) and is supported on a layer of alumina (Al_2O_3). Only a few works are found in the literature on the use of NF ceramic membranes [95–98]. Benfer et al. [95] synthesised ZrO_2 and TiO_2 NF membranes by the sol-gel method and evaluated their performance filtering sodium electrolytes. The ZrO_2 membrane exhibited higher salt rejections (27% for NaCl and 66% Na_2SO_4, while these were 6% and 11% for the TiO_2 membrane), whereas the TiO_2 membrane had better solvent fluxes (three times higher). Both membranes were characterised by pore size measurements and revealed that the ZrO_2 membrane had smaller pore size and narrower pore size distribution (0.75-1.75 nm) than TiO_2 membrane (0.5-2.5 nm). Voigt et al. [96] fabricated TiO_2 membranes with a pore size of 0.9 nm (Molecular Weight Cut-Off (MWCO) of 450 Da) to decolour textile wastewater, and achieved an efficiency of 70-100%. In a latter work, by using a two-step coating process, they developed TiO_2 NF membranes with a MWCO of 250 Da and water flux of 10 L/(m^2·h·bar). Wadekar and Vidic [98] compared the performance of a polymeric (NF270) and a polymeric membrane (TiO_2, MWCO of 500 Da) to treat the drainage of an abandoned coal mine at pH 7.8. NF270 was able to reject multi-charged ions (>96%), while the ceramic membranes exhibited

much lower rejections (50-70%). No studies are found about the performance of ceramic NF membranes in acidic media.

Describing the transport of species across nanofiltration membranes

Modelling of ion rejection in NF is useful for the process optimisation and scale-up. Nevertheless, and contrarily to RO processes, there is still a lack of mathematical models to scale and predict the behaviour of NF membranes. The transport of species (both charged and non-charged) across a NF membrane depends on many factors, such as the active layer properties (e.g. its composition, the content and properties of ionisable acid-base groups and free volume distribution size), the aqueous composition (pH and species concentration) and the interaction between these two factors.

Two kinds of models can be found to describe the transport of species across a NF membrane: (1) those based on the assumption that the NF membrane has nanopores, and (2) the phenomenological models based on irreversible thermodynamics.

Models based on nanopores require membrane parameters such as pore size distributions and geometries, surface charge densities and dielectric constants to be measured experimentally. Overall, the nanopore models suffer from questionable applications of macroscopic principles to nanopores and challenges in verifying the membrane properties used as inputs of the model [99].

Although nanopore models provide qualitative but useful insights into NF, the phenomenological descriptions based on irreversible thermodynamics have proven to be more practical in describing NF for engineering purposes. The latter ones present several advantages over the previous ones, such as the fact that they do not require data about pore size and geometries, surface charge densities nor dielectric constants, which are hard to be measured experimentally. Thus, until a more precise characterisation of the complex chemical and pore structure of NF membrane active layer is possible, phenomenological models are preferable for describing NF with a few thermodynamic coefficients that can be determined experimentally [99].

Phenomenological models based on the Solution-Diffusion model are widely used to describe the transport of species across a NF membrane [99–103]. This model is based on the following assumptions: i) the membrane does not present fixed pores but instead contains a free volume, and ii) the separation of different solutes is achieved due to the differences of diffusivities inside the membrane.

Yaroshchuk et al. [100] coupled the Solution-Diffusion model to film model theory for single electrolytes, giving rise to the so-called Solution-Diffusion-Film model (SDFM) for single electrolytes. The SDFM was later extended to electrolyte mixtures by including coupling between the electro-diffusion fluxes of different ions via the electric field of the membrane potential [101–103]. This

extended model, named Solution-Electromigration-Diffusion-Film model (SEDFM), provides a good description of the dependence of solute rejections on trans-membrane flux for electrolyte mixtures formed by one dominant electrolyte and trace ions [101–104]. The SEDFM also takes into account the concentration polarisation phenomena, whereby the ion transfer occurs by electro-diffusion and convection. The objective of these models (SDFM and SEDFM) is to determine the membrane permeances to single ions (P_i) from experimental data. P_i is defined as the easiness of one species to permeate and depends upon both the membrane and ion properties, as well as the interaction between them. Different properties such as species diffusivities, membrane thickness and partition coefficients are included within membrane permeances.

Generally, most of the efforts have been made to describe the transport of strong electrolytes in single solutions where interactions between the different species present in the solution are not expected. Nevertheless, such scenario does not take place in ALWs from mining and hydrometallurgical and metallurgical industries, where each element may give rise to multiple species in equilibrium with each other. One such an example is H_2SO_4, which at pH values close to the pK_a (1.92) is dissociated in the species HSO_4^- and SO_4^{2-} in commeasurable concentrations. Despite this, to date, only limited works have been reported to describe the transport of species being in chemical equilibrium with other species (i.e. considering “reactive transport”). One of these was carried out by Nir et al. [105,106], who modelled the transport of proton and hydroxyl through RO membranes by considering the chemical equilibrium between them. Niewersch et al. [72,107] modelled the trans-membrane ion fluxes numerically under high-acidity conditions in NF by considering chemical equilibrium between the different species in solutions from acidic hydrolysis of sewage sludge or leaching of sewage sludge ash. The obtained solutions were a mixture of phosphate, sulphate, Mg, K, Fe and Al at acidic pH (from 1.5 to 3.0). Based on the SEDM, they were able to characterise the transport of species for the recovery of H_3PO_4 from sulphuric solutions.

The SEDM relies on a minimum set of membrane parameters, namely membrane permeances to species, and assumes a Solution-Diffusion-Electromigration ion-transport mechanism in the membrane. An apparent weakness of this engineering model is that its application requires, in principle, separate experimentation for each given feed composition. On the other side, the model uses the concentrations of a virtual solution, which is defined as a solution that is in thermodynamic equilibrium with an infinitely small fluid volume inside the membrane. By introducing this concept, no more membrane properties other than phenomenological coefficients need to be specified. In order to determine the ion concentration and electrostatic potential inside the membrane, more detailed information about the membrane properties may be needed [99].

1.3.2. Diffusion dialysis

DD has proven to be an effective technique for purification and recovery of acids such as H_2SO_4, HCl or H_3PO_4. Li et al. [108] investigated the recovery of H_2SO_4 from vanadium leaching solutions (2.4 mol/L H^+, 4.2 g/L V(V), 13.8 g/L Al) with the AEM DF120. An acid recovery of 84% was achieved while metals were rejected (>90%) at feed/dialysate flow rates ratios between 1.0 and 1.3. Wei et al. [63] evaluated the recovery of H_2SO_4 from an acid leach solution with two types of AEM (DF120-I and DF120-III). The addition of electrolytes such as $FeSO_4$ and $VOSO_4$, which contained the same anion as the one of the acid (i.e.SO_4) promoted the diffusion of H^+ through the membrane (electrolyte-effect). At a flow rate ratio of 1, H_2SO_4 was recovered on an 83%, with metal rejections >93%. Working at a higher flow rate ratio (1.6) the H_2SO_4 recovery increased (87%), but also the transport of iron and vanadium (90%). Jeong et al. [109] treated an industrial ALW containing 4.5 M H_2SO_4, Fe (5.2%w/w) and Ni (1.8%w/w) with an AEM (Selemion DSV). Acid recovery depended on its initial concentration, water and acid flow rates, their ratio and temperature. Metal rejection barely varied when flow rate increased from $0.25{\cdot}10^{-3}$ to $1.25{\cdot}10^{-3}$ $m^3/(m^2{\cdot}h)$ (96 and 99% for Ni and Fe, respectively) and almost 80% of H_2SO_4 was recovered with impurities of 2.0 g/L. Gueccia et al. [64] studied the recovery of HCl from pickling solutions with AEMs (Fumasep) at different HCl (up to 105 g/L) and Fe(II) (up to 150 g/L) concentrations. They found that osmotic flux prevailed at low HCl concentrations, while at high HCl concentrations the “drag flux” predominated. Moreover, they developed a mathematical model to determine the membrane permeabilities to the acid and electrolyte. Wang et al. [110] treated a stone coal acid leaching containing a mixture of H_3PO_4, HF and H_2SO_4 with an AEM (DF120-III). Rejection of S was the lowest (68%), while the ones for P and F were higher (90% and 98%, respectively). The high rejections of F were related to its presence as AlF^{2+} and AlF_2^+, which are expected to be repelled by the positively charged AEM.

Palatý and Žáková have carried out studies on the application of DD for acid recovery under different acid feed compositions [111–117]. In their works, they characterised the transport of species across an AEM (Neosepta-AFN) and studied how speciation affected the transport of acids and metals. They have worked with different kinds of acids and electrolytes, such as H_2SO_4 and its mixture with $CuSO_4$ or $ZnSO_4$, HCl with $FeCl_3$ or $NiCl_2$, HNO_3, H_3PO_4 and HF. These works are explained in the paragraphs below.

Regarding the transport of H_2SO_4, they found that the membrane mass transfer coefficients (i.e. permeability to the acid) are dependent on H_2SO_4 concentration, while the major resistance is found in the membrane (>50%) instead of the liquid films [111]. Moreover, when they treated mixtures of H_2SO_4 and $CuSO_4$ or $ZnSO_4$ [112,113], they concluded that the electrolyte flux was the sum of the contribution of species flux. The concentration of metals in the diffusate increased with the

concentration of metal electrolyte and decreased at higher acid concentrations. The effect of acid on metal rejection was related to changes in speciation towards the free metallic ion.

They have studied other kind of systems containing HCl [114,115]. For the system HCl-$FeCl_3$ [114] the addition of chloride (as $FeCl_3$) promoted the transport of HCl across the AEM, reaching higher concentrations in the water compartment than in the feed side. The values for overall diffusion dialysis coefficient (i.e. the transport in the liquid films of the acid and water side, as well as the one across the AEM), which depended on HCl and $FeCl_3$ concentration, were higher than those for H_2SO_4. For the system HCl-$NiCl_2$ [115], the acid permeated easily across the AEM, while the electrolyte was effectively rejected. The increase in acidity led to a higher passage of $NiCl_2$ across the AEM, which was related to the higher fraction of Ni^{2+} than $NiCl^+$. The transport of Ni was due to the smaller size of Ni^{2+} than of $NiCl^+$ despite the repulsive forces between Ni^{2+} and the fixed charges in the AEM. Calculated permeability coefficient for $NiCl_2$ was two orders of magnitude lower than the one for HCl.

The transport of inorganic acids has been also studied [116,117]. The apparent diffusivity of acids (H_2SO_4, HCl, HNO_3, H_3PO_4 and HF) was determined based on Fick's first and second laws [116]. Highest diffusivity values were for HCl (at concentrations below 0.76 M) and for HNO_3 (at concentrations below 0.195 M), while the lowest values were for H_3PO_4. HNO_3 and H_3PO_4 exhibited a decrease in apparent diffusivity with increasing their concentration, while H_2SO_4 and HF showed the opposite trend. In a further work [117], the transport of strong (e.g. HNO_3) and incompletely dissociated acids (e.g. H_2SO_4) was studied based on the Nernst-Planck equation. The transport for acids was described by the sum of the dissociated forms (i.e. NO_3^- and HNO_3(aq) for HNO_3 and HSO_4^- and SO_4^{2-} for H_2SO_4). H_3O^+ showed higher mobility than the other species; thus, the AEM exhibited a high proton leakage, which could be beneficial in the separation of inorganic acids and their electrolytes. NO_3^- and SO_4^{2-} showed similar mobilities for the more diluted acid concentrations, but the former showed higher mobility at higher concentrations (>0.5 M).

AEMs are widely used for the purification of highly concentrated acids, and most of the commercial manufacturers provide acid-stable AEMS that can work up to pH below 0. As result, no studies were found about the stability of AEMs in acidic media.

Describing the transport of solutes across anion exchange membranes: ions and non-charged species

Different models can be found to describe the transport of ions across an AEM: the ones based on the extended Nernst-Planck equation and those based on the Fick's law.

The model developed by Palatý and Žáková is one of the first models based on the extended Nernst-Planck equation for describing the transport of species across an AEM for DD [117]. As above-

mentioned, these authors considered the different forms of the acid to describe the transport of the acid across AEMs. Koter and Kultys have also carried out different works related to describe the transport of species across AEMs [118,119]. The transport of weak acids, such as H_2SO_4, requires a very detailed description. The model is based on the extended Nernst-Planck equation coupled with Donnan equilibrium. Moreover, the ion transport across both liquid films at both sides of the membrane was considered within the mathematical model. They focused on the transport of two acids (H_3PO_4 and H_2SO_4). The concept of "reactive transport" was also applied, and the transport of the acid across the AEM considers the total passage of its different deprotonated species (i.e. HSO_4^- and SO_4^{2-} for H_2SO_4). Their model contained only two fitting parameters such as the concentration of AEM fixed charges and the pore factor, which contained the porosity, tortuosity of the AEM and the ratio of ion diffusivities. However, no efforts have been carried with more complex solutions, such as those coming from metallurgical industries. The mathematical complexity of these systems of equations has made that alternative models for engineering purposes are preferred, such as the ones based on Fick's law.

In fact, mathematical models based on Fick's law have been able to describe and to characterise properly the behaviour of an AEM in DD applications. Different approaches can be found in this category. The simplest approach has as objective to determine an overall diffusion dialysis coefficient, which includes the liquid resistances in both films and the AEM [110,120,121]. However, these models do not consider either water transport across the AEM or speciation in solution, and its applicability is limited to the characterisation of transport of elements across the AEM regardless its speciation. Other models, such as the one developed by Luo et al. [122] allows to determine the membrane permeability in mixtures of acids and sodium electrolytes. The contribution of the dissociated acid forms was considered within the mathematical model. Membrane permeabilities were determined for H_2SO_4 (2.5 μm/s), HCl (1.6 μm/s) and H_3PO_4 (0.1 μm/s). The obtained values were influenced by ionic diffusivity and initial concentrations. A recent model based on Fick's law was developed by Gueccia et al. [64], to describe the transport of HCl and $FeCl_2$ across a Fumasep Fad AEM. Both liquid films were considered within the model, and it was possible to characterise the transport of species using permeabilities. Moreover, a dependence on permeabilities with acid and electrolyte concentration was observed. This model considered the water transport across the AEM by considering the osmotic flux (from water to acid side) and the "drag" flux (from acid to water side).

DD has proved to be a membrane technology able to recover and purify acids from industrial effluents. However, the studies in the literature are focused on strong (e.g. HCl, HNO_3) and weak (e.g. H_2SO_4) electrolytes, whereas only few studies are found in the literature about the behaviour of fully protonated acids, such as H_3AsO_3 for As(III) and H_3AsO_4 for As(V). Scarce information is found about the transport mechanisms in AEMs for those species.

1.4. References

[1] European Commission, Communication from the Commission - Towards a circular economy: A zero waste programme for Europe, 2014.

[2] European Commission, Report on Critical Raw Materials and the Circular Economy PART 3/3, 2018. doi:10.1097/PPO.0b013e3181b9c5d5.

[3] Spire, SPIRE 2050 Vision. Towards the Next Generation of European Process Industries, (2019). https://www.spire2030.eu/what/walking-the-spire-roadmap/spire-2050-vision.

[4] A.S. Sheoran, V. Sheoran, Heavy metal removal mechanism of acid mine drainage in wetlands: A critical review, Miner. Eng. 19 (2006) 105–116. doi:10.1016/j.mineng.2005.08.006.

[5] D.B. Johnson, K.B. Hallberg, Acid mine drainage remediation options: A review, Sci. Total Environ. 338 (2005) 3–14. doi:10.1016/j.scitotenv.2004.09.002.

[6] D.W. Blowes, C.J. Ptacek, J.L. Jambor, C.G. Weisener, D. Paktunc, W.D. Gould, D.B. Johnson, The Geochemistry of Acid Mine Drainage, in: Treatise on Geochemistry, Elsevier, 2014: pp. 131–190. doi:10.1016/B978-0-08-095975-7.00905-0.

[7] G.S. Simate, S. Ndlovu, Acid mine drainage: Challenges and opportunities, J. Environ. Chem. Eng. 2 (2014) 1785–1803. doi:10.1016/j.jece.2014.07.021.

[8] E. Macingova, A. Luptakova, Recovery of metals from acid mine drainage, Chem. Eng. Trans. 28 (2012) 109–114. doi:10.3303/CET1228019.

[9] C.R. Cánovas, S. Peiffer, F. Macías, M. Olías, J.M. Nieto, Geochemical processes in a highly acidic pit lake of the Iberian Pyrite Belt (SW Spain), Chem. Geol. 395 (2015) 144–153. doi:10.1016/j.chemgeo.2014.12.007.

[10] M. Olías, J.M. Nieto, R. Pérez-López, C.R. Cánovas, F. Macías, A.M. Sarmiento, L. Galván, Controls on acid mine water composition from the Iberian Pyrite Belt (SW Spain), Catena. 137 (2016) 12–23. doi:10.1016/j.catena.2015.08.018.

[11] C. Ayora, F. Macías, E. Torres, A. Lozano, S. Carrero, J.M. Nieto, R. Pérez-López, A. Fernández-Martínez, H. Castillo-Michel, Recovery of Rare Earth Elements and Yttrium from Passive-Remediation Systems of Acid Mine Drainage, Environ. Sci. Technol. 50 (2016) 8255–8262. doi:10.1021/acs.est.6b02084.

[12] S.A. Welch, A.G. Christy, L. Isaacson, D. Kirste, Mineralogical control of rare earth elements in acid sulfate soils, Geochim. Cosmochim. Acta. 73 (2009) 44–64. doi:10.1016/j.gca.2008.10.017.

[13] D. Merten, J. Geletneky, H. Bergmann, G. Haferburg, E. Kothe, G. Büchel, Rare earth element patterns: A tool for understanding processes in remediation of acid mine drainage, Chemie Der Erde - Geochemistry. 65 (2005) 97–114. doi:10.1016/j.chemer.2005.06.002.

[14] F. Xie, T. An, D. Dreisinger, F. Doyle, A critical review on solvent extraction of rare earths from

aqueous solutions, Miner. Eng. 56 (2014) 10–28. doi:10.1016/j.mineng.2013.10.021.

[15] R.D. Abreu, C.A. Morais, Study on Separation of Heavy Rare Earth Elements by Solvent Extraction with Organophosphorus Acids and Amine Reagents, Miner. Eng. 61 (2014) 82–87. doi:10.1016/j.mineng.2014.03.015.

[16] J. Kulczycka, Z. Kowalski, M. Smol, H. Wirth, Evaluation of the recovery of Rare Earth Elements (REE) from phosphogypsum waste - Case study of the WIZÓW Chemical Plant (Poland), J. Clean. Prod. 113 (2016) 345–354. doi:10.1016/j.jclepro.2015.11.039.

[17] L. Wang, Y. Yu, X. Huang, Z. Long, D. Cui, Toward greener comprehensive utilization of bastnaesite: Simultaneous recovery of cerium, fluorine, and thorium from bastnaesite leach liquor using HEH(EHP), Chem. Eng. J. 215–216 (2013) 162–167. doi:10.1016/j.cej.2012.09.126.

[18] J. Sánchez España, E. López Pamo, E. Santofimia, O. Aduvire, J. Reyes, D. Barettino, Acid mine drainage in the Iberian Pyrite Belt (Odiel river watershed, Huelva, SW Spain): Geochemistry, mineralogy and environmental implications, Appl. Geochemistry. 20 (2005) 1320–1356. doi:10.1016/j.apgeochem.2005.01.011.

[19] M. Olías, C.R. Cánovas, J.M. Nieto, A.M. Sarmiento, Evaluation of the dissolved contaminant load transported by the Tinto and Odiel rivers (South West Spain), Appl. Geochemistry. 21 (2006) 1733–1749. doi:10.1016/j.apgeochem.2006.05.009.

[20] A. Akcil, S. Koldas, Acid Mine Drainage (AMD): causes, treatment and case studies, J. Clean. Prod. 14 (2006) 1139–1145. doi:10.1016/j.jclepro.2004.09.006.

[21] N. Kuyucak, Acid mine drainage prevention and control options, Mine, Water Environ. 95 (1999) 96–102.

[22] N.O. Egiebor, B. Oni, Acid rock drainage formation and treatment: a review, Asia-Pacific J. Chem. Eng. 2 (2007) 47–62. doi:10.1002/apj.57.

[23] O. Dianrdo, P.D. Kondos, D.J. Mackinnon, R.G.L. McGready, P.A. Riveros, M. Skaff, Study on metals recovery/recycling from acid mine drainage, MEND Treat. Comm. (1991). doi:10.1017/CBO9781107415324.004.

[24] M.A. Caraballo, F. Macías, T.S. Rötting, J.M. Nieto, C. Ayora, Long term remediation of highly polluted acid mine drainage: A sustainable approach to restore the environmental quality of the Odiel river basin, Environ. Pollut. 159 (2011) 3613–3619. doi:10.1016/j.envpol.2011.08.003.

[25] M. Kalin, A. Fyson, W.N. Wheeler, The chemistry of conventional and alternative treatment systems for the neutralization of acid mine drainage, Sci. Total Environ. 366 (2006) 395–408. doi:10.1016/j.scitotenv.2005.11.015.

[26] C. Costello, Acid Mine Drainage : Innovative Treatment Technologies Prepared by Technology Innovation Office, U.S. Environ. Prot. Agency, Off. Solid Waste Emerg. Response. (2003). https://clu-in.org/download/studentpapers/costello_amd.pdf.

[27] J. Fripp, P.F. Ziemkiewicz, H. Charkavorki, Acid Mine Drainage Treatment, in: EMRRP-SR-14,

2000. https://sav.el.erdc.dren.mil/elpubs/pdf/sr14.pdf (accessed June 8, 2017).

[28] PIRAMID Consortium, Engineering guidelines for the passive remediation of acidid and/or metalliferous mine drainage and similar wastewaters, 2003. doi:10.1016/j.ecoleng.2008.08.016.

[29] D.B. Johnson, K.B. Hallberg, Acid mine drainage remediation options: a review, Sci. Total Environ. 338 (2005) 3–14. doi:10.1016/j.scitotenv.2004.09.002.

[30] S. Santos, R. Machado, M.J.N. Correia, J.R. Carvalho, Treatment of acid mining waters, Miner. Eng. 17 (2004) 225–232. doi:10.1016/j.mineng.2003.09.015.

[31] G. Lee, J.M. Bigham, G. Faure, Removal of trace metals by coprecipitation with Fe, Al and Mn from natural waters contaminated with acid mine drainage in the Ducktown Mining District, Tennessee, Appl. Geochemistry. 17 (2002) 569–581. doi:10.1016/S0883-2927(01)00125-1.

[32] X. Wei, R.C. Viadero, K.M. Buzby, Recovery of iron and aluminum from acid mine drainage by selective precipitation, Environ. Eng. Sci. 22 (2005) 745–755. doi:10.1089/ees.2005.22.745.

[33] F. Fu, Q. Wang, Removal of heavy metal ions from wastewaters: A review, J. Environ. Manage. 92 (2011) 407–418. doi:10.1016/j.jenvman.2010.11.011.

[34] O. Gibert, J. de Pablo, J.L.L. Cortina, C. Ayora, Treatment of acid mine drainage by sulphate-reducing bacteria using permeable reactive barriers: A review from laboratory to full-scale experiments, Rev. Environ. Sci. Biotechnol. 1 (2002) 327–333. doi:10.1023/A:1023227616422.

[35] C.-M. Neculita, G.J. Zagury, B. Bussière, Passive Treatment of Acid Mine Drainage in Bioreactors using Sulfate-Reducing Bacteria: Critical review and research needs, J. Environ. Qual. 36 (2007) 1–16. doi:10.2134/jeq2006.0066.

[36] U. Wingenfelder, C. Hansen, G. Furrer, R. Schulin, Removal of heavy metals from mine waters by natural zeolites, Environ. Sci. Technol. 39 (2005) 4606–4613. doi:10.1021/es048482s.

[37] G. Blanchard, M. Maunaye, G. Martin, Removal of heavy metals from waters by means of natural zeolites, Water Res. 18 (1984) 1501–1507. doi:10.1016/0043-1354(84)90124-6.

[38] M.J. Zamzow, B.R. Eichbaum, K.R. Sandgren, D.E. Shanks, Removal of Heavy Metals and Other Cations from Wastewater Using Zeolites, Sep. Sci. Technol. 25 (1990) 13–15. doi:10.1080/01496399008050409.

[39] European IPPC Bureau, Reference Document on Best Available Techniques for the Non-Ferrous Metals Industries, 2017. doi:10.2760/8224.

[40] A. Agrawal, K.K. Sahu, An overview of the recovery of acid from spent acidic solutions from steel and electroplating industries, J. Hazard. Mater. 171 (2009) 61–75. doi:10.1016/j.jhazmat.2009.06.099.

[41] M. Bissen, F.H. Frimmel, Arsenic - A review. Part II: Oxidation of arsenic and its removal in water treatment, Acta Hydrochim. Hydrobiol. 31 (2003) 97–107. doi:10.1002/aheh.200300485.

[42] T.S.Y. Choong, T.G. Chuah, Y. Robiah, F.L. Gregory Koay, I. Azni, Arsenic toxicity, health hazards and removal techniques from water: an overview, Desalination. 217 (2007) 139–166. doi:10.1016/j.desal.2007.01.015.

[43] V.K. Sharma, M. Sohn, Aquatic arsenic: Toxicity, speciation, transformations, and remediation, Environ. Int. 35 (2009) 743–759. doi:10.1016/j.envint.2009.01.005.

[44] F.J. Alguacil, F.A. López, The extraction of mineral acids by the phosphine oxide Cyanex 923, Hydrometallurgy. 42 (1996) 245–255. doi:10.1016/0304-386X(95)00101-L.

[45] U. Kerney, Treatment of spent pickling acids from hot dip galvanizing, Resour. Conserv. Recycl. 10 (1994) 145–151. doi:10.1016/0921-3449(94)90047-7.

[46] M. Wisniewski, Extraction of arsenic from sulphuric acid solutions by Cyanex 923, Hydrometallurgy. 46 (2003) 235–241. doi:10.1016/s0304-386x(97)90003-7.

[47] M.J. Hatch, J.A. Dillon, ACID RETARDATION A Simple Physical Method for Separation of Strong Acids from Their Salts, I&EC Process Des. Dev. 2 (1963) 253–263.

[48] E. Petkova, H. Vassilev, V. Shkodrova, Separation of waste plating solution sulphuric acid from metal cations by anion exchange, Hydrometallurgy. 6 (1981) 291–297.

[49] M. Mulder, Basic Principles of Membrane Technology, Springer Netherlands, 1996. doi:10.1007/978-94-009-1766-8.

[50] B.C. Ricci, C.D. Ferreira, A.O. Aguiar, M.C.S. Amaral, Integration of nanofiltration and reverse osmosis for metal separation and sulfuric acid recovery from gold mining effluent, Sep. Purif. Technol. 154 (2015) 11–21. doi:10.1016/j.seppur.2015.08.040.

[51] B.C. Ricci, C.D. Ferreira, L.S. Marques, S.S. Martins, B.G. Reis, M.C.S. Amaral, Assessment of the chemical stability of nanofiltration and reverse osmosis membranes employed in treatment of acid gold mining effluent, Sep. Purif. Technol. 174 (2017) 301–311. doi:10.1016/j.seppur.2016.11.007.

[52] M.P. González, R. Navarro, I. Saucedo, M. Avila, J. Revilla, C. Bouchard, Purification of phosphoric acid solutions by reverse osmosis and nanofiltration, Desalination. 147 (2002) 315–320. doi:10.1016/S0011-9164(02)00558-1.

[53] U.K. Kesieme, N. Milne, C.Y. Cheng, H. Aral, M. Duke, Recovery of water and acid from leach solutions using direct contact membrane distillation, Water Sci. Technol. 69 (2014) 868–875. doi:10.2166/wst.2013.788.

[54] G. Zhang, Q. Zhang, K. Zhou, Study on concentrating sulfuric acid solution by vacuum membrane distillation, J. Cent. South Univ. Technol. 6 (1999) 99–102. doi:10.1007/s11771-999-0007-5.

[55] S. You, J. Lu, C.Y. Tang, X. Wang, Rejection of heavy metals in acidic wastewater by a novel thin-film inorganic forward osmosis membrane, Chem. Eng. J. 320 (2017) 532–538. doi:10.1016/j.cej.2017.03.064.

[56] M. Boucher, N. Turcotte, V. Guillemette, G. Lantagne, A. Chapotot, G. Pourcelly, R. Sandeaux, C. Gavach, Recovery of spent acid by electrodialysis in the zinc hydrometallurgy industry : performance study of different cation-exchange membranes, Hydrometallurgy. 45 (1997) 137–160.

[57] D.C. Buzzi, L.S. Viegas, M.A.S. Rodrigues, A.M. Bernardes, J.A.S. Tenório, Water recovery from acid mine drainage by electrodialysis, Miner. Eng. 40 (2013) 82–89. doi:10.1016/j.mineng.2012.08.005.

[58] M.C. Martí-Calatayud, D.C. Buzzi, M. García-Gabaldón, E. Ortega, A.M. Bernardes, J.A.S. Tenório, V. Pérez-Herranz, Sulfuric acid recovery from acid mine drainage by means of electrodialysis, Desalination. 343 (2014) 120–127. doi:10.1016/j.desal.2013.11.031.

[59] A.W. Mohammad, Y.H. Teow, W.L. Ang, Y.T. Chung, D.L. Oatley-Radcliffe, N. Hilal, Nanofiltration membranes review : Recent advances and future prospects, Desalination. 356 (2015) 226–254. doi:10.1016/j.desal.2014.10.043.

[60] A.I. Schäfer, A.G. Fane, T.D. Waite, Nanofiltration - Principles and Applications, Elsevier L, 2005.

[61] D.L. Oatley-Radcliffe, M. Walters, T.J. Ainscough, P.M. Williams, A.W. Mohammad, N. Hilal, Nanofiltration membranes and processes: A review of research trends over the past decade, J. Water Process Eng. 19 (2017) 164–171. doi:10.1016/j.jwpe.2017.07.026.

[62] J. Luo, C. Wu, T. Xu, Y. Wu, Diffusion dialysis-concept, principle and applications, J. Memb. Sci. 366 (2011) 1–16. doi:10.1016/j.memsci.2010.10.028.

[63] C. Wei, X. Li, Z. Deng, G. Fan, M. Li, C. Li, Recovery of H2SO4 from an acid leach solution by diffusion dialysis, J. Hazard. Mater. 176 (2010) 226–230. doi:10.1016/j.jhazmat.2009.11.017.

[64] R. Gueccia, S. Randazzo, D. Chillura Martino, A. Cipollina, G. Micale, Experimental investigation and modeling of diffusion dialysis for HCl recovery from waste pickling solution, J. Environ. Manage. 235 (2019) 202–212. doi:10.1016/j.jenvman.2019.01.028.

[65] R.W. Baker, Membrane Technology and Applications, 2nd ed., John Wiley & Sons, 2004.

[66] M. Mullett, R. Fornarelli, D. Ralph, Nanofiltration of mine water: impact of feed pH and membrane charge on resource recovery and water discharge, Membranes (Basel). 4 (2014) 163–180. doi:10.3390/membranes4020163.

[67] S. Bandini, D. Vezzani, Nanofiltration modeling: The role of dielectric exclusion in membrane characterization, Chem. Eng. Sci. 58 (2003) 3303–3326. doi:10.1016/S0009-2509(03)00212-4.

[68] E. Glueckauf, A new approach to ion-exchange polymers, in: Proc. R. Soc. A Math. Phys. Eng. Sci., Washington DC, 1962: p. 1334.

[69] A.A.E. Yaroshchuk, Dielectric exclusion of ions from membranes, Adv. Colloid Interface Sci. 85 (2000) 193–230. doi:10.1016/S0001-8686(99)00021-4.

[70] T.J.K. Visser, S.J. Modise, H.M. Krieg, K. Keizer, The removal of acid sulphate pollution by

nanofiltration, Desalination. 140 (2001) 79–86.

[71] G. Shang, G. Zhang, C. Gao, W. Fu, L. Zeng, A novel nanofiltration process for the recovery of vanadium from acid leach solution, Hydrometallurgy. 142 (2014) 94–97. doi:10.1016/j.hydromet.2013.11.007.

[72] C. Niewersch, A.L.B. Bloch, S. Yüce, T. Melin, M. Wessling, Nanofiltration for the recovery of phosphorus — Development of a mass transport model, Desalination. 346 (2014) 70–78. doi:10.1016/j.desal.2014.05.011.

[73] A.R. Guastalli, J. Labanda, J. Llorens, Separation of phosphoric acid from an industrial rinsing water by means of nanofiltration, Desalination. 243 (2009) 218–228. doi:10.1016/j.desal.2008.04.024.

[74] H. Diallo, M. Rabiller-Baudry, K. Khaless, B. Chaufer, On the electrostatic interactions in the transfer mechanisms of iron during nanofiltration in high concentrated phosphoric acid, J. Memb. Sci. 427 (2013) 37–47. doi:10.1016/j.memsci.2012.08.047.

[75] K. Meschke, B. Daus, R. Haseneder, J.U. Repke, Strategic elements from leaching solutions by nanofiltration – Influence of pH on separation performance, Sep. Purif. Technol. 184 (2017) 264–274. doi:10.1016/j.seppur.2017.04.048.

[76] K. Meschke, N. Hansen, R. Hofmann, R. Haseneder, J.U. Repke, Characterization and performance evaluation of polymeric nanofiltration membranes for the separation of strategic elements from aqueous solutions, J. Memb. Sci. 546 (2018) 246–257. doi:10.1016/j.memsci.2017.09.067.

[77] A. Werner, A. Rieger, M. Mosch, R. Haseneder, J.U. Repke, Nanofiltration of indium and germanium ions in aqueous solutions: Influence of pH and charge on retention and membrane flux, Sep. Purif. Technol. 194 (2018) 319–328. doi:10.1016/j.seppur.2017.11.006.

[78] C.-M. Zhong, Z.-L. Xu, X.-H. Fang, L. Cheng, Treatment of Acid Mine Drainage (AMD) by Ultra-Low-Pressure Reverse Osmosis and Nanofiltration, Environ. Eng. Sci. 24 (2007) 1297–1306. doi:10.1089/ees.2006.0245.

[79] H. Al-Zoubi, A. Rieger, P. Steinberger, W. Pelz, R. Haseneder, G. Härtel, Optimization Study for Treatment of Acid Mine Drainage Using Membrane Technology, Sep. Sci. Technol. 45 (2010) 2004–2016. doi:10.1080/01496395.2010.480963.

[80] H. Al-Zoubi, A. Rieger, P. Steinberger, W. Pelz, R. Haseneder, G. Härtel, Nanofiltration of Acid Mine Drainage, Desalin. Water Treat. 21 (2010) 148–161. doi:10.5004/dwt.2010.1316.

[81] R. Fornarelli, M. Mullett, D. Ralph, Factors influencing nanofiltration of acid mine drainage, Reliab. Mine Water Technol. (2013) 563–568.

[82] M. Nyström, J. Tanninen, M. Mänttäri, Separation of metal sulfates and nitrates from their acids using nanofiltration, Membr. Technol. 2000 (2000) 5–9. doi:10.1016/S0958-2118(00)86633-1.

[83] P.K. Eriksson, L.A. Lien, D.H. Green, Membrane technology for treatment of wastes containing

dissolved metals, in: V. Ramachandram, C.C. Nesbitt (Eds.), Second Int. Symp. Extr. Process. Treat. Minimization Wastes, 1996: pp. 649–658.

[84] H.J. Skidmore, K.J. Hutter, Methods of purifying phosphoric acid, US 5945000 A, 1999. https://www.google.es/patents/US5945000?dq=purification+of+aqueous+phosphoric+acid+by+hot+filtration+using+a+polyamide+nanofilter&hl=es&sa=X&ved=0ahUKEwiA8Z2CxKfLAhWDVRQKHYXxCm4Q6AEIHDAA (accessed March 4, 2016).

[85] M. V. Galiana-Aleixandre, A. Iborra-Clar, A. Bes-Piá, J.A. Mendoza-Roca, B. Cuartas-Uribe, M.I. Iborra-Clar, Nanofiltration for sulfate removal and water reuse of the pickling and tanning processes in a tannery, Desalination. 179 (2005) 307–313. doi:10.1016/j.desal.2004.11.076.

[86] M. V. Galiana-Aleixandre, J.A. Mendoza-Roca, A. Bes-Piá, Reducing sulfates concentration in the tannery effluent by applying pollution prevention techniques and nanofiltration, J. Clean. Prod. 19 (2011) 91–98. doi:10.1016/j.jclepro.2010.09.006.

[87] C.-V. Gherasim, P. Mikulášek, Influence of operating variables on the removal of heavy metal ions from aqueous solutions by nanofiltration, Desalination. 343 (2014) 67–74. doi:10.1016/j.desal.2013.11.012.

[88] S. Platt, M. Nyström, A. Bottino, G. Capannelli, Stability of NF membranes under extreme acidic conditions, J. Memb. Sci. 239 (2004) 91–103. doi:10.1016/j.memsci.2003.09.030.

[89] A. Manis, K. Soldenhoff, E. Jusuf, F. Lucien, Separation of copper from sulfuric acid by nanofiltration, in: Fifth Int. Membr. Sci. Technol. Conf., 2003.

[90] R. Navarro, M.P. González, I. Saucedo, M. Avila, P. Prádanos, F. Martínez, A. Martín, A. Hernández, Effect of an acidic treatment on the chemical and charge properties of a nanofiltration membrane, J. Memb. Sci. 307 (2008) 136–148. doi:10.1016/j.memsci.2007.09.015.

[91] J. Tanninen, S. Platt, M. Nyström, Nanofiltration of sulphuric acid from metal sulphate solutions, Proc. Imstec 2003, Sydney. (2003) 1–6.

[92] T. Schütte, C. Niewersch, T. Wintgens, S. Yüce, Phosphorus recovery from sewage sludge by nanofiltration in diafiltration mode, J. Memb. Sci. 480 (2015) 74–82. doi:10.1016/j.memsci.2015.01.013.

[93] S.M. Samaei, S. Gato-Trinidad, A. Altaee, The application of pressure-driven ceramic membrane technology for the treatment of industrial wastewaters – A review, Sep. Purif. Technol. 200 (2018) 198–220. doi:10.1016/j.seppur.2018.02.041.

[94] V. Gitis, G. Rothenberg, Ceramic Membranes. New opportunities and Practical Applications, 1st ed., Wiley-VCH Verlag GmbH & Co. KGaA, Weinheim, Germany, 2016. doi:10.1002/9783527696550.

[95] S. Benfer, U. Popp, H. Richter, C. Siewert, G. Tomandl, Development and characterization of ceramic nanofiltration membranes, Sep. Purif. Technol. 22–23 (2001) 231–237. doi:10.1016/S1383-5866(00)00133-7.

[96] I. Voigt, G. Fischer, P. Puhlfürß, M. Schleifenheimer, M. Stahn, TiO2-NF-membranes on capillary supports, Sep. Purif. Technol. 32 (2003) 87–91. doi:10.1016/S1383-5866(03)00064-9.

[97] I. Voigt, M. Stahn, S. Wöhner, A. Junghans, J. Rost, W. Voigt, Integrated cleaning of coloured waste water by ceramic NF membranes, Sep. Purif. Technol. 25 (2001) 509–512. doi:10.1007/978-3-642-54734-2.

[98] S.S. Wadekar, R.D. Vidic, Comparison of ceramic and polymeric nanofiltration membranes for treatment of abandoned coal mine drainage, Desalination. 440 (2018) 135–145. doi:10.1016/j.desal.2018.01.008.

[99] A. Yaroshchuk, M.L. Bruening, E. Zholkovskiy, Modelling nanofiltration of electrolyte solutions, Adv. Colloid Interface Sci. 268 (2019) 39–63. doi:10.1016/j.cis.2019.03.004.

[100] A. Yaroshchuk, X. Martínez-Lladó, L. Llenas, M. Rovira, J. de Pablo, J. Flores, P. Rubio, Mechanisms of transfer of ionic solutes through composite polymer nano-filtration membranes in view of their high sulfate/chloride selectivities, Desalin. Water Treat. 6 (2009) 48–53.

[101] A. Yaroshchuk, M.L. Bruening, E.E. Licón Bernal, Solution-Diffusion-Electro-Migration model and its uses for analysis of nanofiltration, pressure-retarded osmosis and forward osmosis in multi-ionic solutions, J. Memb. Sci. 447 (2013) 463–476. doi:10.1016/j.memsci.2013.07.047.

[102] A. Yaroshchuk, X. Martínez-Lladó, L. Llenas, M. Rovira, J. de Pablo, Solution-diffusion-film model for the description of pressure-driven trans-membrane transfer of electrolyte mixtures: One dominant salt and trace ions, J. Memb. Sci. 368 (2011) 192–201. doi:10.1016/j.memsci.2010.11.037.

[103] N. Pages, A. Yaroshchuk, O. Gibert, J.L. Cortina, Rejection of trace ionic solutes in nanofiltration : Influence of aqueous phase composition, Chem. Eng. Sci. 104 (2013) 1107–1115. doi:10.1016/j.ces.2013.09.042.

[104] A. Yaroshchuk, M.L. Bruening, An analytical solution of the solution-diffusion-electromigration equations reproduces trends in ion rejections during nanofiltration of mixed electrolytes, J. Memb. Sci. 523 (2017) 361–372. doi:10.1016/j.memsci.2016.09.046.

[105] O. Nir, L. Ophek, O. Lahav, Acid-base dynamics in seawater reverse osmosis: experimental evaluation of a reactive-transport algorithm, Environ. Sci. Water Res. Technol. 2 (2015) 107–116. doi:10.1039/C5EW00228A.

[106] O. Nir, N.F. Bishop, O. Lahav, V. Freger, Modeling pH variation in reverse osmosis, Water Res. 87 (2015) 328–335. doi:10.1016/j.watres.2015.09.038.

[107] C. Niewersch, Nanofiltration for phosphorus recycling from sewage sludge, Verlagshaus Mainz GmbH, 2013.

[108] W. Li, Y. Zhang, H. Jing, X. Zhu, Y. Wang, Separation and recovery of sulfuric acid from acidic vanadium leaching solution by diffusion dialysis, J. Environ. Chem. Eng. 4 (2016) 1399–1405. doi:10.1016/j.jece.2015.11.038.

[109] J. Jeong, M.S. Kim, B.S. Kim, S.K. Kim, W.B. Kim, J.C. Lee, Recovery of H2SO4 from waste acid solution by a diffusion dialysis method, J. Hazard. Mater. 124 (2005) 230–235. doi:10.1016/j.jhazmat.2005.05.005.

[110] K. Wang, Y. Zhang, J. Huang, T. Liu, J. Wang, Recovery of sulfuric acid from a stone coal acid leaching solution by diffusion dialysis, Hydrometallurgy. 173 (2017) 9–14. doi:10.1016/j.hydromet.2017.07.005.

[111] Z. Palatý, A. Žáková, Transport of sulfuric acid through anion-exchange membrane NEOSEPTA-AFN, J. Memb. Sci. 119 (1996) 183–190.

[112] Z. Palatý, A. Žáková, Separation of H2SO4 + CuSO4 mixture by diffusion dialysis, J. Hazard. Mater. 114 (2004) 69–74. doi:10.1016/j.jhazmat.2004.06.023.

[113] Z. Palatý, A. Žáková, Separation of H2SO4 + ZnSO4 mixture by diffusion dialysis, Desalination. 169 (2004) 277–285. doi:10.1016/j.desal.2004.01.001.

[114] Z. Palatý, A. Žáková, P. Doleček, Modelling the transport of Cl- ions through the anion-exchange membrane NEOSEPTA-AFN systems HCl/membrane/H2O and HCl-FeCl3/membrane/H2O, J. Memb. Sci. 165 (2000) 237–249. doi:10.1016/S0376-7388(99)00239-2.

[115] Z. Palatý, A. Žková, Separation of HCl+NiCl2 mixture by diffusion dialysis, Sep. Sci. Technol. 42 (2007) 1965–1983. doi:10.1080/15363830701313362.

[116] Z. Palatý, A. Žáková, Apparent diffusivity of some inorganic acids in anion-exchange membrane, J. Memb. Sci. 173 (2000) 211–223. doi:10.1016/S0376-7388(00)00363-X.

[117] Z. Palatý, A. Žáková, Transport of some strong incompletely dissociated acids through anion-exchange membrane, J. Colloid Interface Sci. 268 (2003) 188–199. doi:10.1016/j.jcis.2003.07.034.

[118] S. Koter, M. Kultys, Electric transport of sulfuric acid through anion-exchange membranes in aqueous solutions, J. Memb. Sci. 318 (2008) 467–476. doi:10.1016/j.memsci.2008.03.010.

[119] S. Koter, M. Kultys, Modeling the electric transport of sulfuric and phosphoric acids through anion-exchange membranes, Sep. Purif. Technol. 73 (2010) 219–229. doi:10.1016/j.seppur.2010.04.005.

[120] J.J. Tang, K.G. Zhou, Q.X. Zhang, Sulfuric acid recovery from rare earth sulphate solutions by diffusion dialysis, Trans. Nonferrous Met. Soc. China (English Ed. 16 (2006) 951–955. doi:10.1016/S1003-6326(06)60358-0.

[121] J. Xu, D. Fu, S. Lu, The recovery of sulphuric acid from the waste anodic aluminum oxidation solution by diffusion dialysis, Sep. Purif. Technol. 69 (2009) 168–173. doi:10.1016/j.seppur.2009.07.015.

[122] J. Luo, C. Wu, Y. Wu, T. Xu, Diffusion dialysis processes of inorganic acids and their salts : The permeability of different acidic anions, Sep. Purif. Technol. 78 (2011) 97–102. doi:10.1016/j.seppur.2011.01.028.

CHAPTER 2

Objectives

2. Objectives

The main objective of the current PhD Thesis is to develop new processes that integrate membrane technologies (NF and DD) to provide new valorisation schemes for mining and metallurgical streams where added value metals (e.g. critical elements, precious metals or rare earth elements) and acids can be recovered and, if needed, reused internally or externally in other sectors. The integration of membrane technologies for the valorisation of ALWs are directed to promote circular material flows aligned with the Circular Economy paradigm under implementation by the EU.

Other main objectives of the Thesis are to identify the mass transport processes involved in the membrane technologies implemented and to develop and apply a model that satisfactorily describes the transport process through the membranes, not only in the filtration of single solutions but also of complex solutions mimicking real ALWs where speciation plays a crucial role in the removal of species, and therefore reactive transport needs to be considered. This represents a novelty of this Thesis, since the current modelling efforts done so far do not consider reactive transport.

- Specific objectives for Nanofiltration studies include:
    - To evaluate the influence of chemical speciation in strongly acidic solutions (sulphuric acid-based) containing alkaline, transition, non-metals (e.g. As) and REEs on the membrane performance.
    - To develop a reactive mass transfer model to describe and predict ion flux across the membrane and its validation with experimental results.
    - To characterise the relevant properties of the membranes evaluated and to describe the main transport mechanism and the influence of the acidity on the chemistry of the active layer.
- Specific objectives for Diffusion dialysis studies include:
    - To evaluate the acid recovery potential and the limitations of the presence of weak acids (H_3AsO_3 and H_3AsO_4).
    - To evaluate the influence of chemical speciation of acid and non-metals (i.e. As) on the membrane performance from the gas cleaning of metallurgical industries.

CHAPTER 3

Thesis Overview

3. Thesis overview

In this PhD thesis, NF and DD membrane technologies have been employed for the valorisation of ALWs. The main effort has been devoted to NF by studying different solutions which mimicked ALWs from mining and hydrometallurgical industries (1<pH<3) containing metals (e.g. REEs, Fe, Al, Cu) and to describe the transport of species across the membrane by mathematical models. Within this context, NF membranes can be useful for metal removal and its concentration in solution from ALWs and at the same time, to obtain an acid-rich permeate free of metals. DD was employed for the treatment of the effluent of the gas cleaning of a copper smelter, which was composed by H_2SO_4 (pH<0), containing As as the main impurity As. In this case, the transport of species across the AEM was not described with mathematical models. In this case, the goal of DD is to recover a high acidic stream free of impurities. **Table 1** collects the objectives stablished in Section 2, and how they were achieved.

First of all, the transport of H_2SO_4 at pHs from 1 to 3 across a flat sheet (FS) commercial polymeric NF membrane (NF270) was characterised, and a mathematical model on the basis of SEDM including reactive transport was developed for weak electrolytes (HSO_4^- / H^+ SO_4^{2-}) (**Publication 1**). This study was followed on by a second one where a synthetic solution mimicking AMD instead of a single H_2SO_4 solution was filtered under the same membrane and FS configuration. This synthetic AMD was characterised by an acidic pH (1<pH<3), and contained dissolved metals, mainly Al(III) and others such as Cu, Ca, Zn, and in a minor extent REEs. The SEDM was applied by considering reactive transport to determine the membrane permeances to the different species present in the AMD (**Publication 2**). Furthermore, the stability of the employed polymeric NF membrane under acidic conditions was studied by assessing its degradation after exposing it under different acidic conditions. Additionally, the performance of the same membrane to filtrate other kind of AMD was tested under a spiral-wound (SW) configuration, and the SEDFM was applied (**Publication 3**). In this case, the solution mimicked an AMD from a poly-sulphide mine containing Na, Fe, Zn and Cu at pH values between 2 and 3. On a step forward, the effect of the main components in AMDs such as Fe(III) (**Publication 4**) and Al(III) (**Publication 5**) on the performance of FS NF membranes (NF270, HydraCoRe 70pHT and Desal DL) and, more particularly, on the membrane permeances towards the different solutes was studied.

ALWs (0.5<pH<1) coming from the metallurgical industry containing As as main impurity were treated with the same polymeric NF membrane (NF270), placing the focus on the transport of non-charged inorganic species (e.g. H_3AsO_4) (**Publication 6**).

Table 1. *Tasks performed to reach the stablished objectives*

	Objectives	Tasks done		Publ.
Nanofiltration	To evaluate the influence of chemical speciation in strongly acidic solutions (sulphuric acid-based) containing alkaline, transition, non-metals (e.g. As) and REEs on the membrane performance	H_2SO_4 solutions	Effect of pH	1
		AMDs	Effect of pH, Al and Fe concentration	2, 3, 4, 5
		Industrial effluents	Effect of As speciation	6
	To develop a reactive mass transfer model to describe and predict ion flux across the membrane and its validation with experimental results	Model for weak electrolytes (based on SEDM)		1
		SEDM coupled with reactive transport for complex solutions		2, 4, 5, 6
		Predictive model		8
	To characterise the relevant properties of the membranes evaluated and to describe the main transport mechanism and the influence of the acidity on the chemistry of the active layer	Stability tests		2
		Membrane characterization		7
Diffusion dialysis	To evaluate the acid recovery potential and the limitations of the presence of weak acids (H_3AsO_3 and H_3AsO_4)	H_2SO_4 recovery from copper smelter		9
		Influence of As speciation (As(III) or As(V))		
	To evaluate the influence of chemical speciation of acid and non-metals (i.e. As) on the membrane performance from the gas cleaning of metallurgical industries	Effect of flow rates on acid recovery and its purification		

In views of the limited stability of the employed polymeric membrane (NF270) at acidic media, additional efforts were oriented towards the assessment and characterisation of acid-resistant polymeric (MPF-34) and ceramic membranes (TiO_2) in treating AMDs (**Publication 7**).

Results from Publications 5 and 6 allowed to study the dependence of membrane permeances to species on concentration of H+ and Fe as major species. A mathematical model was developed to predict the behaviour of NF membranes in AMD (**Publication 8**).

Finally, the application of DD for acid recovery was studied for effluents (220 g/L H_2SO_4 and 3.4 g/L As) from the gas cleaning of a copper smelter (**Publication 9**). The effluent contained other impurities such as Zn (0.5 g/L) and other metals as traces at concentrations of mg/L (e.g. Fe, Pb, Cd, Ni, Cu and Hg). The performance of the AEM Neosepta AFX was studied, and the effect of the main operating variables was studied on the acid recovery and metal leakage. The presence of As as a neutral species may limit the applicability of DD. Then, the limitations and the influence of As in the acid recovery were evaluated.

Figure 5 shows a scheme of the thesis overview.

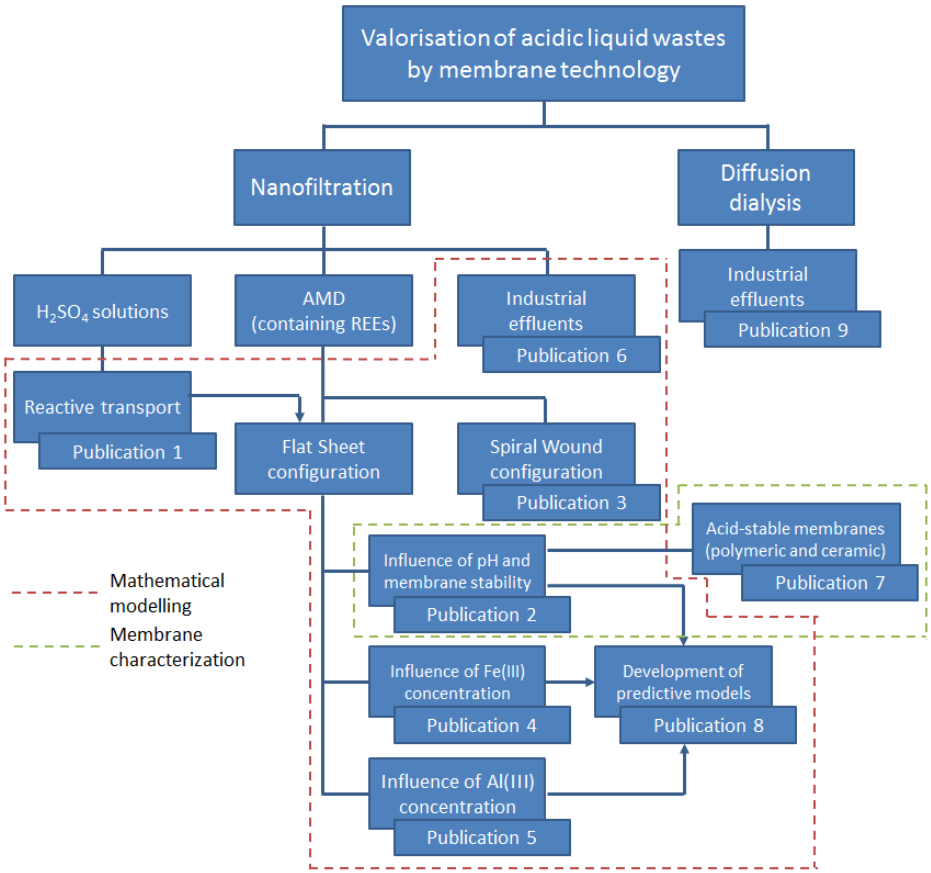

Figure 5. *Thesis overview*

Publication 1: López, J., Reig, M., Yaroshchuk, A., Licon, E., Gibert, O., Cortina, J.L. "*Experimental and theoretical study of nanofiltration of weak electrolytes: $SO_4^{2-}/HSO_4^-/H^+$ system*" Journal of Membrane Science 550 (2018) 389 - 398

Publication 2: López, J., Reig, M., Gibert, O., Torres, E., Ayora, C., Cortina, J.L. "*Application of nanofiltration for acidic waters containing rare earth elements: Influence of transition elements, acidity and membrane stability*" Desalination 430 (2018) 33 - 44

Publication 3: López, J., Reig, M., Gibert, O., Valderrama, C., Cortina, J.L. "*Evaluation of NF membranes as treatment technology of acid mine drainage: metals and sulfate removal*" Desalination 440 (2018) 122 - 134

Publication 4: López, J., Reig, M., Gibert, O., Cortina, J.L. "*Integration of nanofiltration membranes in recovery options of rare earth elements from acidic mine waters*" Journal of Cleaner Production 210 (2019) 1249 - 1260

Publication 5: López, J., Reig, M., Gibert, O., Cortina, J.L. "*Recovery of sulphuric acid and added value metals (Zn, Cu and rare earths) from acidic mine waters using nanofiltration membranes*" Separation and Purification Technology 212 (2019) 180 - 190

Publication 6: López, J., Reig, M., Gibert, O., Cortina, J.L. "*Increasing sustainability on the metallurgical industry by integration of membrane nanofiltration processes: Acid recovery*" Separation and Purification Technology 226 (2019) 267 - 277

Publication 7: López, J., Reig, M., Vecino, X., Gibert, O., Cortina, J.L. "*Comparison of acid-resistant ceramic and polymeric nanofiltration membranes for acid mine waters treatment: Limitations on acid purification and its recovery*" Chemical Engineering Journal 382 (2020) 122786

Publication 8: López, J., Reig, M., Vecino, X., Gibert, O., Cortina, J.L. "*From Membrane Permeances to the Prediction of Membrane Nanofiltration Performance in acidic solutions: application to the Recovery of Rare Earths Elements from Acid Mine Waters*" Under review in Separation and Purification Technology

Publication 9: López, J., de Oliveira, R. R., Reig, M., Vecino, X., Gibert, O., de Juan, A., Cortina, J.L. "*Integration of diffusion dialysis for sulphuric acid recovery from copper metallurgical process streams: the arsenic challenge*" Under review in Separation and Purification Technology

CHAPTER 4

Publication 1

"Experimental and theoretical study of nanofiltration of weak electrolytes: $SO_4^{2-}/HSO_4^-/H^+$ system"

ATTENTION¡¡

Pages 44 to 54 of the thesis are available at the editor's web

https://www.sciencedirect.com/science/article/pii/S0376738817314448

CHAPTER 5

Publication 2

"Application of nanofiltration for acidic waters containing rare earth elements: Influence of transition elements, acidity and membrane stability"

ATTENTION¡¡
Pages 56 to 76 of the thesis are available at the editor's web
https://www.sciencedirect.com/science/article/abs/pii/S0011916417314029

CHAPTER 6

Publication 3

"*Evaluation of NF membranes as treatment technology of acid mine drainage: metals and sulfate removal***"**

ATTENTION¡¡
Pages 78 to 90 of the thesis are available at the editor's web
https://www.sciencedirect.com/science/article/abs/pii/S0011916417316703

CHAPTER 7

Publication 4

"*Integration of nanofiltration membranes in recovery options of rare earth elements from acidic mine waters***"**

ATTENTION¡¡
Pages 92 to 104 of the thesis are available at the editor's web
https://www.sciencedirect.com/science/article/pii/S0959652618335005

CHAPTER 8

Publication 5

"Recovery of sulphuric acid and added value metals (Zn, Cu and rare earths) from acidic mine waters using nanofiltration membranes"

ATTENTION¡¡
Pages 106 to 118 of the thesis are available at the editor's web
https://www.sciencedirect.com/science/article/pii/S1383586618326108

CHAPTER 9

Publication 6

"Increasing sustainability on the metallurgical industry by integration of membrane nanofiltration processes: Acid recovery"

ATTENTION¡¡
Pages 120 to 132 of the thesis are available at the editor's web
https://www.sciencedirect.com/science/article/pii/S138358661834557X

CHAPTER 10

Publication 7

"Comparison of acid-resistant ceramic and polymeric nanofiltration membranes for acid mine waters treatment"

ATTENTION¡¡
Pages 134 to 151 of the thesis are available at the editor's web
https://www.sciencedirect.com/science/article/pii/S1385894719321965

CHAPTER 11

Results

11. Results

11.1. Describing the transport of species across nanofiltration membranes

11.1.1. Solution-Electro-Diffusion Model coupled with reactive transport for a weak electrolyte

A general (quasi)analytical solution obtained for the transport of weak electrolytes of arbitrary valence type with the basis of Solution-Electro-Diffusion model taking into account equilibrium reactions.

The ion fluxes were described according to SEDM. It was assumed that there is no coupling between solute and solvent inside the membrane (i.e. no convective flux). The model uses "virtual" concentrations, defined as those that are in thermodynamic equilibrium with an infinitely small volume inside the membrane. The use of "virtual" concentrations satisfies the chemical equilibriums reactions inside the membrane with the bulk complexation constant. Moreover, the partitioning coefficients (ratio between real and virtual concentrations) are included in the permeances. Then, ion transport was described by **Eq. 1**:

$$j_i = -P_i \cdot c_i \cdot \left(\frac{dln\, c_i}{dx} + z_i \cdot \frac{d\varphi}{dx}\right) \quad (1)$$

where j_i is the flux of component i through the membrane, P_i is the membrane permeance to species i, c_i and z_i stand for its virtual concentration and its charge, respectively, φ is the dimensionless virtual electrostatic potential and x is the dimensionless position across the membrane.

The transport of ions is:

- Subjected to zero-current condition (**Eq. 2**).

$$\sum_i z_i \cdot j_i = 0 \quad (2)$$

- Subjected to the electro-neutrality condition in the virtual solution (**Eq. 3**):

$$\sum_i z_i \cdot c_i = 0 \tag{3}$$

- Virtual ion concentrations are subjected to chemical equilibrium condition at a given constant temperature and ionic strength (IS) ($\alpha = 10^{pK_a}$, according to (**Eq. 4**):

$$c_3 = \alpha \cdot c_1 \cdot c_2 \tag{4}$$

After some derivations, a (quasi)analytical solution is obtained, that can be solved in quadratures (**Eq. 5**):

$$J_v = \frac{\int_{c_{1p}}^{c_{1f}} F(c_1) dc_1}{c_{1p} \cdot \left(1 + \frac{z_1}{c_{1p} \cdot \alpha \cdot (z_1 + z_2) + z_2}\right)} \tag{5}$$

Where J_v is the solvent flux across the membrane, c_{1f}, c_{1p} are the concentrations of species "1" in the feed and permeate, respectively, and

$$F(c_1) \equiv z_2 \cdot z_3 \cdot \frac{P_1 \cdot (z_2 + c_1 \cdot \alpha \cdot z_3) \cdot (P_2 + P_3 \cdot \alpha \cdot c_1) - P_2 \cdot P_3 \cdot z_1 \cdot \alpha \cdot c_1}{z_2 \cdot (P_2 \cdot z_2 - P_1 \cdot z_1) + c_1 \cdot \alpha \cdot z_3 \cdot (P_3 \cdot z_3 - P_1 \cdot z_1)} \cdot \frac{z_2 + c \cdot \alpha \cdot z_3 - z_1}{(z_2 + c_1 \cdot \alpha \cdot z_3)} \tag{6}$$

The objective of the mathematical model is to characterise the transport of species through the membrane permeances to species. This parameter depends upon the membrane and ion properties, as well as the interaction between them. Membrane permeances englobe the diffusion coefficient of species inside the membrane and the partitioning coefficients, defined as the ratio between the real and virtual concentrations. Possible changes in the association constant are also included. Permeances are assumed to be constant over the whole length of the active layer, although the diffusion coefficient depends on concentration.

The model was implemented with Matlab® to reach the minimum deviations between the measured and predicted rejections by varying the membrane permeances. The rejection was defined according to **Eq. 7**:

$$R = 1 - \frac{C_p}{C_f} \tag{7}$$

where C_p and C_f represent the total concentration of an element regardless of its speciation in the permeate and feed streams, respectively.

11.1.2. Solution-Electro-Diffusion Model coupled with reactive transport for acidic liquid wastes

The transport of species (both charged and non-charged) was carried out with the bases of SEDM by taking into account the reactive transport to include the chemical equilibrium between the different species in solution. As in the previous case, a convective flux was not considered, and virtual concentrations were used. The mathematical model assumes the transport of species is a combination of diffusion and electromigration (for charged species). As initial approach, concentration polarisation was not considered to reduce the mathematical complexity of the system. **Equation 8** describes the species flux across the membrane.

$$j_i = -P_i \cdot \left(\frac{dc_i}{dx} + c_i \cdot \frac{d(\ln \gamma_i)}{dx} + z_i \cdot c_i \cdot \frac{d\varphi}{dx} \right) \quad (8)$$

where γ_i is the activity coefficient of species i.

The activity coefficients were calculated according to the Davies Equation, which is applicable for IS lower than 0.5 mol/L (**Eq.9**):

$$\log \gamma_i = -a^* \cdot z_i^2 \cdot \left(\frac{\sqrt{IS}}{1+\sqrt{IS}} - 0{,}3 \cdot IS \right) \quad (9)$$

where A is the Debye Hückel parameter with a value of 0.5042.

The transport of ions must satisfy the electroneutrality condition (**Eq. 10**):

$$\sum_{i=1}^{n} (z_i \cdot c_i) = 0 \quad (10)$$

Species in solution must satisfy the condition of chemical equilibrium reactions between them. For that reason, the flux of one species would not be constant along the membrane. Then, species flux equations **(Eq. 1)** are solved for each element that makes up the species. For example, for the transport of H_2SO_4 across the membrane, the equation referred to SO4 is a sum of the flux of SO_4^{2-} and HSO_4^-.

Mass balance equations were solved using Matlab®, where the membrane permeances to species were varied to minimise the deviations between the rejection obtained experimentally and the one from the model.

Predicting the performance of nanofiltration membranes

From the obtained membrane permeances, a mathematical model was developed to predict the behaviour of a NF system, where the permeate is collected. Under this situation, the composition of the feed solution would vary. Then, in order to predict the behaviour of the system, different mass balances are applied: (i) in the membrane itself (red box in **Fig. 6**), (ii) in the membrane test cell (green box in **Fig. 6**) and (iii) the tank (orange box in **Fig. 6**).

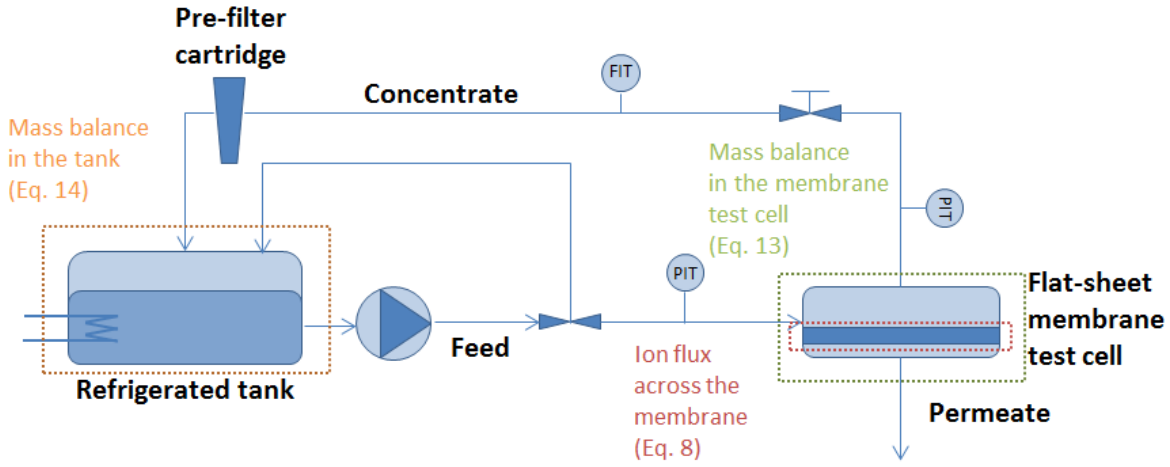

Figure 6. *Scheme of the experimental NF set-up. Dotted boxes represent the points where mass balances were solved to predict the behaviour of the system.*

The obtained membrane permeances to species are dependent on solution composition and can be fitted to the following expression (**Eq. 11**):

$$P_i = a_o + a_1 \cdot C^{a_2} \qquad (11)$$

where a_0, a_1 and a_2 are fitting parameters and X is the concentration of the electrolyte.

The flux of water across the membrane can be described according to **Eq. 12**:

$$J_v = k_w \cdot (\Delta P - \Delta\pi) \qquad (12)$$

where k_w is the hydraulic permeability of the membrane, ΔP and $\Delta\pi$ are the differences of pressure and osmotic pressure across the membrane. Osmotic pressure is calculated according to the van't Hoff equation.

In the membrane test cell, the concentration and flow of the retentate stream can be obtained by applying global and component mass balances (**Eqs. 13.a** and **13.b**):

$$Q_f = Q_r + Q_p \qquad (13.a)$$

$$c_f \cdot Q_f = c_r \cdot Q_r + c_p \cdot Q_p \quad (13.b)$$

where Q and c are the flow and concentration, respectively. Subscripts f, r and p refer to the feed, retentate and permeate, respectively.

Finally, an unsteady state mass balance is solved in the feed tank to determine how the volume of the solution varied and how the different compounds get concentrated along with the time (**Eqs. 7.a** and **7.b**).

$$\frac{dV}{dt} = Q_r - Q_f \quad (14.a)$$

$$\frac{d(c_{f,i} \cdot V)}{dt} = Q_r \cdot c_{r,i} - Q_f \cdot c_{f,i} \quad (14.b)$$

where V is the tank volume and t is the running time of the experiment.

Moreover, saturation indexes (SI) of the potentially expected mineral phases were evaluated by **Eq. 15**:

$$SI = \log\left(\frac{IAP}{K_{so}}\right) \quad (15)$$

Where K_{so} is the solubility constant and IAP is the ionic activity product of a given potential mineral involved in a scaling event.

11.2. Key findings in evaluating the potential integration of nanofiltration in acidic liquid wastes

Several polymeric NF membranes of different active layer composition were studied: NF270 (semi-aromatic poly(piperazineamide), Dow Chemical), Desal DL (semi-aromatic poly(piperazineamide), GE Osmonics),HydraCoRe 70pHT (sulphonated polyethersulphone, Hydranautics) and MPF-34 (proprietary, Koch). MPF-34 is an acid-resistant membrane with a proprietary active layer, so one of the objectives was to characterise the membrane. Moreover, a ceramic TiO_2 membrane was tested treating ALWs. This membrane was also characterised to determine its IEP.

The rejection value of a given species i can be explained by a combination of i) the physicochemical properties of the species i, ii) the solution composition, which affects the speciation of i, and iii) the membrane properties, which determine the interactions between the species with the polymer

matrix (e.g. sorption or solution of the ions into the polymer matrix) and with the free functional groups (e.g. adsorption and complexation of counter-ions to the fixed charge sites of the polymer membrane matrix, which diminishes the effective fixed charge). Moreover, the following phenomena: i) Donnan exclusion; ii) Dielectric exclusion and iii) solutes complexation can provide information about the membrane selectivity.

11.2.1. Membrane characterisation: identification of key properties for the treatment of acidic solutions

NF270, Desal DL and HydraCoRe 70pHT were not characterised since these membranes are widely studied and their properties are reported in the literature.

A ceramic membrane made of TiO_2 was analysed by Scanning Electron Microscopy (SEM). The active layer revealed an agglomerate of TiO_2 particles, which was associated with particle sintering during the thermal treatment. Moreover, it was possible to measure the thickness of the active layer (21.1±4.6 μm). No visible pores were observed. In addition, the rejection of 0.01 M Na_2SO_4 from pH 1 to 11 at 6 and 13 bar was studied to estimate the IEP of the TiO_2 ceramic membrane. Na_2SO_4 rejection showed an S-shaped curve, with values around 15% (at 6 bar of TMP) and 20% (at 13 bar of TMP) at pH<3. Rejections started to increase with an inflexion point around pH 5.4±0.5 until reach values of 72±3% at 6 bar and 85±2% 13 bar at pH>6. This behaviour was related to the presence of titania active layer surface groups (R–TiOH), and their protonation (R–$TiOH_2^+$) at acidic pH and deprotonation (R–TiO^-) at basic pH.

MPF-34 is a proprietary polymeric membrane. In this Thesis, it was analysed by SEM, FTIR-ATR and XPS. SEM analysis allowed to see the three differentiated layers. The thickness of the active layer was found to be 1.06±0.03 μm. The ATR-FTIR spectrum showed a superposition of the intermediate and active layer because of the higher radiation penetration depth than the thickness of the active layer. The spectrum revealed that the intermediate layer was made of a polyethersulphone or polysulphone. Contrarily, XPS allowed to analyse only the active layer. It revealed that the membrane was mainly composed by C (69.5%), N (16.8%), O (10.8%) and a minor presence of S (2.1%) and Cl (0.8%). The high ratio of N/C and the low amount of S suggested as a preliminary hypothesis the presence of amide groups in the active layers.

NF270, Desal DL and MPF-34 are polyamide-based membranes which present a positively charged surface at the typical acid pH of ALWs due to the protonation of free carboxylic and amine groups, respectively, to R-COOH and $R_2NH_2^+$according to:

$$R - NH_2^+ \leftrightarrow R - NH + H^+ \quad (16)$$

$$R - COOH \leftrightarrow R - COO^- + H^+ \quad (17)$$

Contrarily, HydraCoRe 70pHT presents a permanent negative surface charge due to the presence of sulphonic groups (R–SO_3H), which are expected to be ionised (R–SO_3^-) at this pH:

$$R - SO_3H \leftrightarrow R - SO_3^- + H^+ \quad (18)$$

Finally, the R-TiOH groups are responsible for the membrane charge, as follows:

$$R - TiOH_2^+ \leftrightarrow R - TiOH + H^+ \quad (19)$$

$$R - TiOH \leftrightarrow R - TiO^- + H^+ \quad (20)$$

11.2.2. Influence of acid concentration on membrane properties

Firstly, the rejection of H_2SO_4 at pH 1 to 3 was studied with the polymeric NF270 membrane by using single synthetic solutions of H_2SO_4. The rejection of total sulphate (SO_4^{2-}/ HSO_4^-, i.e. regardless its speciation) reached values around 75% at pH 3, and decreased to values of 35% as pH was lowered to 1 due to the higher amount of HSO_4^-. These values follow the trend with the sulphate rejections at neutral pH (>99%). At pH<3, NF270 presents an overall positive surface charge on its surface, whose value increases when pH is lowered. The low sulphuric acid rejection at higher pH was related to the acid dissociation (pK_a=1.92), whose presence as HSO_4^- instead of as SO_4^{2-} favoured the acid transport across the membrane due to dielectric exclusion phenomenon. Then, the decrease of rejection with decrease of pH was due to: a) changes in the speciation, which resulted in a higher HSO_4^- fraction at pH<pK_a (1.92); and b) changes in the membrane properties due to the higher protonation of amine groups. **Figure 7** shows the evolution of H_2SO_4 rejection from pH 1 to 3 and how the amounts of HSO_4^- and SO_4^{2-} varied with pH.

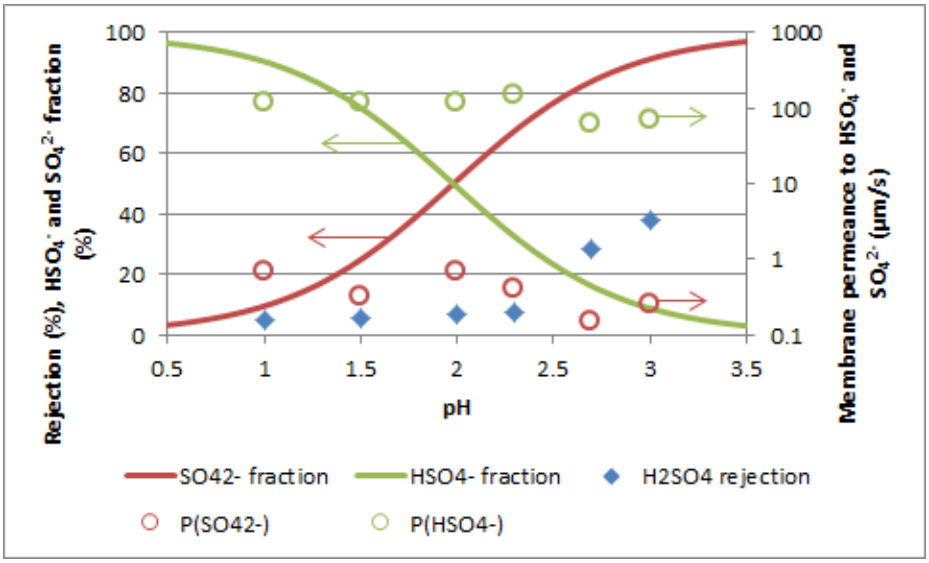

Figure 7. *Comparison of H_2SO_4 rejection from pH 1 to 3 at a trans-membrane flux of 8 µm/s for NF270. The fractions of* HSO_4^- and SO_4^{2-}, as well as their membrane permeances, are also collected.

The performance of different polymeric NF membranes for treating AMDs, which mimicked an effluent from the Iberian Pyrite Belt (Huelva, SW Spain) instead of single synthetic solutions of H_2SO_4 was also evaluated. The impact of feed solution composition onto the performance of the membrane was studied by changing the pH, Al(III) and Fe(III) concentrations.

For this kind of solution, sulphate was mainly as HSO_4^- and SO_4^{2-}, but there is a low content present as $CaSO_4$, $CaHSO_4^+$, $ZnSO_4$, $Zn(SO_4)_2^{2-}$, $CuSO_4$, $REESO_4^+$, and $REE(SO_4)_2^-$. When the pH was lowered from 1.5 to 1.0, the fraction of HSO_4^- increased, while the ones related to SO_4^{2-}, $AlSO_4^+$, and $Al(SO_4)_2^-$ decreased. Despite the complexes of metals with sulphate, the total content of metals was mainly present as its free-form ion (i.e. Al was mainly as Al^{3+}). These changes in speciation had a noticeable impact on membrane performance.

Concerning the effect of pH, it was found that NF270 and Desal DL membranes showed a decrease in sulphate rejection from 80% (at pH 2.5 and 1.5) to 45% and 55% (at pH 1.0), respectively. MPF-34, with an amide-based active layer, showed sulphate rejections below 52% for the MPF-34 and decreased to values of 47% when pH was 1.0. As explained above, this decrease was related to changes in the membrane properties (higher positive membrane charge at low pH and H_2SO_4 dissociation). Contrarily, due to its negative charge, HydraCoRe 70pHT exhibited different behaviour. This membrane has higher sulphate rejections at pH 1.5 (around 85%), and the decrease in pH to 1.0 led to sulphate rejections of 75%, despite the membrane negative charge. On the other side, sulphate rejection was lower than 20% for the TiO_2 membrane. By decreasing the pH to 1.0, the TiO_2 membrane showed sulphate rejections between 2-12%. These changes in sulphate rejection

supported the importance of dielectric exclusion in NF membranes. As explained, as the HSO_4^- fraction increased, total sulphate rejection decreased due to the lower dielectric exclusion on HSO_4^- than SO_4^{2-}.

By evaluating the behaviour of metals, the rejections (Al, REEs, Ca and Zn) for the NF270 increased from values around 75% at pH 2.5 up to values higher than 99%, while for Desal DL these values were higher than 98% at pH 1.5 and 1.0. The MPF-34, instead, exhibited rejections around 80% at both pHs. HydraCoRe 70pHT exhibited lower metal rejections (around 90%), and these decreased at pH 1.0, obtaining rejections for double and triple charged metal ions around 85% and 75%, respectively. Contrarily, the TiO_2 membrane achieved even lower metal rejections (below 30%) and decreased to 21-31% for Al and REEs and 2-12% for double-charged metals. For polyamide membranes (NF270, Desal DL and MPF-34), the high metal rejections in comparison with those of sulphate are due to Donnan and dielectric exclusion phenomena. However, the negative charge of HydraCoRe 70pHT should favour the passage of metallic cations, but the dielectric exclusion hinders their transport due to their charge. For the ceramic membrane, the lower rejections suggested that there is certain coupling between ions and water (i.e. convective flow) since rejections barely varied with the permeate flux. Moreover, metal rejections followed the trend R(Al(III))>R(REEs)>R(M(II)), which was explained by Donnan exclusion (positively charged membrane) with a little contribution of dielectric exclusion because of its relatively high pore size (1nm).

Finally, the high rejections of metals for polyamide membranes favoured the transport of H^+ across the membrane (rejections of H^+ <10%, <40% and <10% for NF270, Desal DL and MPF-34, respectively) to ensure electroneutrality in the permeate. Contrarily, HydraCoRe 70pHT exhibited higher H+ rejections (70% and 60% at pH 1.5 and 1.0, respectively). The TiO_2 membrane achieved rejections below 10% and even negatives at both pHs.

Figure 8 compares the rejections at TMP 10 bar at pH 1.5 and 1.0 for total sulphate; H^+; Al(III); double-charged metals (M(III)) including the mean values for Ca, Cu and Zn; and REEs, which comprises La, Pr, Nd, Sm, Dy, Yb.

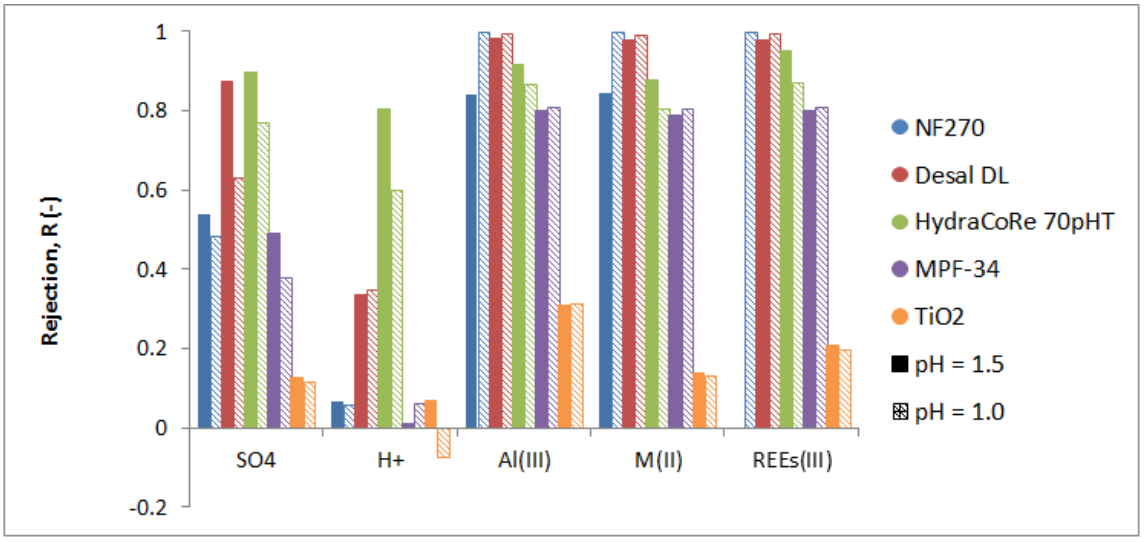

Figure 8. *Comparison of SO_4, H^+, Al(III), double-charged metals M(II) (mean of Ca, Cu and Zn) and REEs (La, Pr, Nd, Sm, Dy, Yb) rejections at TMP of 10 bar. Filled and unfilled bars represent pH 1.5 and 1.0, respectively.*

11.2.3. Influence of solution composition: the role of major solution components, Al(III), Fe(II))

The performance of NF membranes regarding minor components is strongly affected by the concentration and chemical speciation of dominant electrolytes. The influence of Al(III) concentration from 600 to 2200 mg/L on the membrane performance for Desal DL and HydraCoRe 70pHT at pH 1.0 was studied. For the MPF-34 and TiO2 ceramic membrane, the highest Al(III) concentration evaluated was 1800 mg/L. The increase in Al(III) concentration shifted the equilibrium towards the formation of SO_4^{2-}, $AlSO_4^+$, and $Al(SO_4)_2^-$, decreasing the concentration of HSO_4^-. This change in solution speciation can affect the performance of NF membranes. On one side, for the positively charged membranes (i.e. Desal DL and MPF-34) it is expected that the membrane rejected $AlSO_4^+$ and favoured the passage of $Al(SO_4)_2^-$, while the transport of SO_4^{2-} is expected to be impeded due to dielectric exclusion. As a result, the membrane would reject these ions as follows $R(SO_4^{2-})>R(AlSO4^+)>R(HSO_4^-)\approx R(Al(SO_4)_2^-)$. This change in speciation led to an increase in sulphate rejections from 60% to 80% for Desal DL, while sulphate rejections were 42-47% for the MPF-34 up to 1800 mg/L Al(III). On the other side, for a negatively charged membrane (i.e. HydraCoRe 70pHT), the expected rejection sequence is $R(SO_4^{2-})>R(HSO_4^-)\approx R(Al(SO_4)_2^-)>R(AlSO4^+)$. This change in speciation led to an increase of sulphate rejections up to 84%. This was related to the high effect of dielectric exclusion on SO_4^{2-} despite the presence of $AlSO4^+$, which is expected to be transported across the membrane because of Donnan exclusion. For the TiO_2 ceramic membranes, higher sulphate rejections (13-19%) were also observed.

In terms of metal rejections, Desal DL exhibited metal rejections higher than 98%, whereas metal rejections did not change for the MPF-34. These rejections were related to the Donnan and dielectric exclusion. Moreover, HydraCoRe 70pHT did not show variations in metal rejections. The increase in sulphate rejection and the dielectric exclusion limited the transport metals. Contrarily, the TiO_2 membrane exhibited an increase in metal rejections (11-20% for REES and 13-19% for double-charged metals).

Nevertheless, the addition of Al(III) favoured the transport of H^+ across the membrane. For all the membranes, lower rejections were obtained, for the Desal DL were below 20%, MPF-34 allowed to obtain rejections from -2 to 9%, for the HydraCoRe 70pHT slightly decreased from 60 to 57%, and for the ceramic TiO_2 membrane slightly decreased.

These results are compared in **Figure 9.** It shows the rejections at TMP 10 bar at 600 and 1800 mg/L Al(III) for total sulphate; H^+; Al(III); double-charged metals (M(III)) including the mean values for Ca, Cu and Zn; and REEs, which comprises La, Pr, Nd, Sm, Dy, Yb.

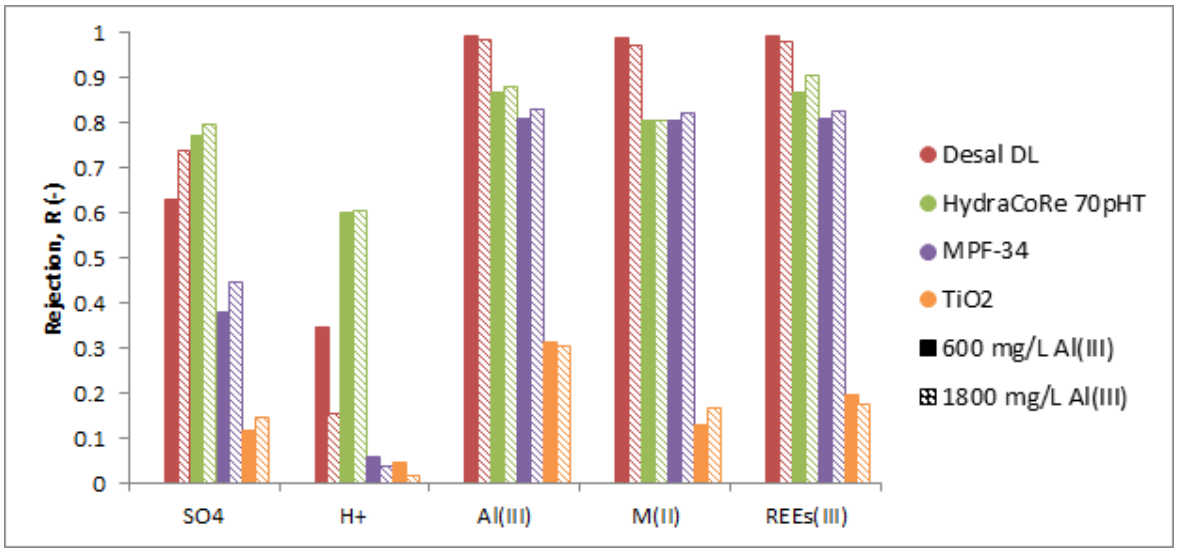

Figure 9. *Comparison of SO_4, H^+, Al(III), double-charged metals M(II) (mean of Ca, Cu and Zn) and REEs (La, Pr, Nd, Sm, Dy, Yb) rejections at TMP of 10 bar. Filled and unfilled bars represent 600 and 1800 mg/L Al(III), respectively.*

The influence of Fe(III) was studied at different concentrations. The addition of Fe(III) implied an increase of the fractions of $FeSO_4^+$ and $FeHSO_4^{2+}$ and therefore a decrease of the fraction of HSO_4^-. For the experiments with NF270, Desal DL and HydraCoRe 70pHT Fe(III) was added as $FeCl_3$, while for MPF-34 and the TiO_2 ceramic membrane was added as $Fe_2(SO_4)_3$.

At 500 mg/L Fe(III), NF270 and Desal DL exhibited higher sulphate rejections (60% and 68%, respectively). The presence of Cl^- in the solution made that sulphate rejection increased in comparison with the solution without $FeCl_3$ since it has a smaller size and higher diffusivity than HSO_4^-. Instead, chloride rejections were much lower (18% for NF270 and 23% for Desal DL). This behaviour contrasts with the one of HydraCoRe 70pHT, which showed higher rejections than the other two membranes (76% for sulphate and 40% for Cl^-). Instead, the addition of 500 mg/L Fe(III) (as sulphate) implied higher sulphate rejections (16-20%) for the TiO_2 membrane, but the variation was little for the MPF-34 (31-40%) due to the lower amount of HSO_4^-.

NF270 and Desal DL exhibited high metal (>98 %) rejections at 500 mg/L Fe(III) due to Donnan and dielectric exclusion. Metal rejections barely varied for the MPF-34. This behaviour contrast with the one of HydraCoRe 70pHT, which showed lower rejections for metals (80% for triple and 60% for double-charged metals). However, changes in the metals rejections were noticed for the ceramic membrane: Al(III) (35-46%), Fe(III) (26-37%), REEs (19-33%) and double-charged metals (12-21%). The addition of Fe(III), and the high metal rejections promoted the transport of H^+ across the membranes, achieving lower rejections, and in some cases with even negative rejections. For the NF270, H^+ rejections below 10% were obtained, while for Desal DL and MPF-34 were <36% and -5%, respectively. The TiO_2 ceramic membrane also achieved negative H^+ rejections. Contrarily, HydraCoRe 70pHT exhibited H^+ rejections around 50%.

A further increase in Fe(III) concentration to 2125 mg/L implied an increase in sulphate rejections increased up to 78%, 75% and 82% for NF270, Desal DL and HydraCoRe 70pHT, respectively. For the MPF-34, sulphate rejections increased to 50%, while for the TiO_2 membrane ranged between 25-30%. This was related to the lower presence of HSO_4^- in solution.

In terms of metal rejections, these values did not vary for NF270, Desal DL, MPF-34 and HydraCoRe 70pHT. However, metal rejections improved 10% for the ceramic membrane. The high metal rejections due to dielectric exclusion favoured more the transport of H^+ across the membrane. For example, rejections were around -20%, -10%, -5% and -5% for the NF270, TiO_2, MPF-34 and Desal DL, respectively. HydraCoRe 70pHT achieved instead positive rejections of H^+ (around 30%)

The influence of Fe(III) concentration for the NF membranes is compared in **Figure 10.** It shows the rejections at TMP 10 bar at 500 and 2125 mg/L Fe(III) for total sulphate; H^+; Al(III); Fe(III); double-charged metals (M(III)) including the mean values for Ca, Cu and Zn; and REEs, which comprises La, Pr, Nd, Sm, Dy, Yb.

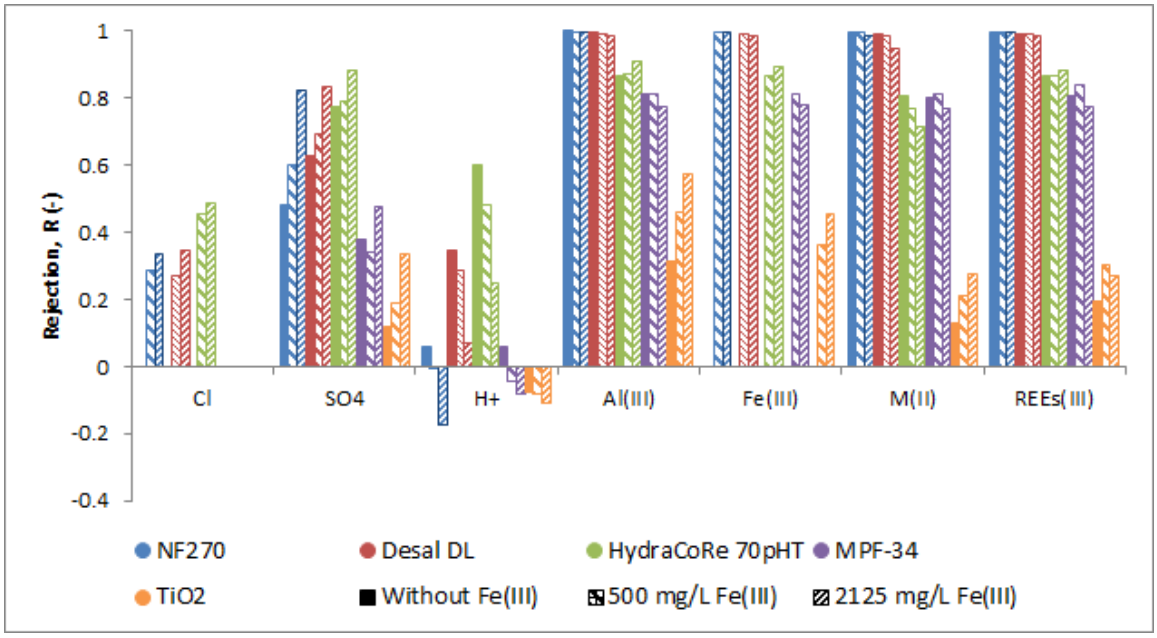

Figure 10. *Comparison of SO_4, H^+, Al(III), double-charged metals M(II) (mean of Ca, Cu and Zn) and REEs (La, Pr, Nd, Sm, Dy, Yb) rejections at TMP of 10 bar. The bars represent the cases without Fe(III), 500 and 2125 mg/L Fe(III), respectively.*

To sum up, NF270 and Desal DL allowed to recovery and purification of acids as permeate. Under different conditions, metal rejections were above 95%, while the transport of H^+ was favoured, achieving in some cases negative rejections (i.e. the permeate is more acidic than the feed stream). The other polyamide-based membrane, the MPF-34, yielded to lower metal rejections (around 80%), while allowing the transport of H^+, with low rejections (<10%). On the other side, the HydraCoRe 70pHT, characterised by a negative charge, rejected the metals more than 70% but also exhibiting high H^+ rejections. These characteristics limited the applicability of this membrane for treating AMDs. Finally, the low rejections of the ceramic membranes make them unsuitable for the treatment of acidic waters. Efforts must be towards the development of narrow pores in TiO_2 ceramic membranes to reduce the convective flux across them so that they can exhibit higher rejections. As result, the polyamide membranes NF270 are preferred for treating AMDs.

NF270 and Desal DL were studied with the same solutions to determine under a batch configuration. In this case, the permeate stream was removed from the system to study the capacity of H_2SO_4 recovery and how the metals concentrate in solution within a permeate recovery range up to 30%. Without Fe(III) and at pH 1.0, both membrane rejected metals (>98%) and yielded a permeate rich in sulphuric acid with a low amount of metallic impurities: 6 g/L with <5 mg/L of metals for NF270 and 5 g/L with <5 mg/L of metals for Desal DL. The addition of Fe(III) up to 500 mg/L, limited the transport of acid for both membranes: 4.5 g/L with <7 mg/L of metals for NF270 and 3.6 g/L with <4 mg/L of metals for Desal DL. A further increase in Fe(III) concentration (2125 mg/L) increased the presence of

impurities in the permeate, mainly Fe(III). Again, NF270 yielded a richer stream in sulphuric acid (4.2 g/L and <80 mg/L of metals) than Desal DL (3.5 g/L and <35 mg/L of metals).

As can be seen, polyamide polymeric membranes (NF270 and Desal DL) offer good characteristics, in terms of metal rejections and acid passage. However, stability tests for their application in acid waters must be performed. NF270 was immersed one month in 1 M H_2SO_4 and then was tested. While a virgin membrane exhibited metal rejections higher than 98% and sulphate rejections around 40%, the aged membrane showed lower metal (70-80%) and sulphate (around 30%) rejections.

Although the treatment of AMD involves previously the oxidation of Fe(II) to Fe(III) for its subsequent precipitation with lime, the possibility of applying NF to solutions containing Fe(II) as dominant Fe form was evaluated in SW configuration. NF270 was able to reject the metallic cations in solution by >90% at pH 2.8 and >95% at pH 2.0. The higher positive membrane charge at pH 2.0 led to higher metal rejections, which followed the trend R(Fe(II))≈R(Zn(II))≈R(Cu(II))>R(Na(I))>R(H^+), in agreement with dielectric exclusion. Contrary, HydraCoRe 70pHT exhibited lower metal rejections. At pH 2.8, these values were around 75% and decreased to 65% along with the trans-membrane flux due to concentration polarisation. However, at pH 2.0, these rejections were around 70%, and no concentration polarization was observed. Finally, a full-scale vessel was simulated with the bench-scale NF module by recirculating and filtering the concentrate stream sequentially in 6 steps at pH 2.8 and TMP of 10 bar. As the solution became more concentrated, metal rejections decreased along with the six steps (from 90% to 84% for NF270 and from 66 to 61% for HydraCoRe 70pHT). Moreover, a concentration factor of 2 and 1.5 was achieved with NF270 and HydraCoRe 70pHT, respectively. These values were similar for the metals, which indicated that a post-treatment might be needed for their separation and recovery.

The application of NF for the treatment of acidic waters from a metallurgical industry was evaluated with the NF270. This stream was characterised by the presence of different acids (H_2SO_4, HCl and H_3AsO_4) and metallic impurities (Fe, Cu, Zn). The membrane exhibited high metal rejections (>80%) and moderate sulphate, proton and arsenic rejections (<50%), with negative chloride rejections. The low sulphate rejections are explained for the reasons mentioned above: the presence of HSO_4^-, which is less affected by dielectric exclusion and by the positively charged membrane surface. Moreover, arsenic rejections can also be explained with the speciation diagrams. At the evaluated acidic pHs (from 0.7 to 0.2), As(V) was found as a non-charged species (H_3AsO_4) and, at a lower extent (below 15%), as a single charged anion ($H_2AsO_4^-$). Its presence as a non-charged species made its rejections always below 50%. The presence of weak electrolytes in solution as fully protonated non-charged species (e.g. H_3AsO_4) makes them not affected by the membrane charge, and its transport is driven by a concentration gradient.

11.2.4. Membrane stability

NF270 was characterised before and after its exposure to acid (1 M H_2SO_4 for one month) by different techniques, such as contact angle, Atomic Force Microscopy (AFM), Attenuated Total Reflectance Fourier Transform Infrared (ATR-FTIR) spectroscopy and X-ray Photoelectron Spectroscopy (XPS).

After ageing the membrane, its hydraulic permeability increased from 3.4±0.3 µm/s up to 4.0±0.3 µm/s. Moreover, the contact angle of the virgin NF270 has a value 23-32^{o} and rose to 23.2-53^{o} after immersion. AFM revealed the appearance of scattered areas with changes in the active layer after immersion and an increase in the roughness from 3.4±0.2 nm to 1.9±0.2 nm. To identify changes in the active layer functional groups, the membrane was analysed by FTIR-ATR and XPS. The ATR-FTIR spectrum of the aged membrane exhibited peaks related to the presence of HSO_4^- due to the appearance of three new bands (1468 cm^{-1} stretching band S=O; 1100 cm^{-1} OH stretching and 894.1 cm^{-1} S–O stretching). Moreover, the presence of sulphate (6.2%) onto the membrane was observed in the XPS spectrum. Furthermore, when the peaks of XPS spectra for O(1s) and N(1s) were deconvoluted, an increase in the percentage of carboxylic and amine groups was noticed, whereas those related to amide groups decreased. This indicated that the membrane suffered partial hydrolysis (**Eq. 21**). This increase in the membrane-free volume makes dielectric exclusion weaker, which explained the previous lower rejections obtained with the aged membrane.

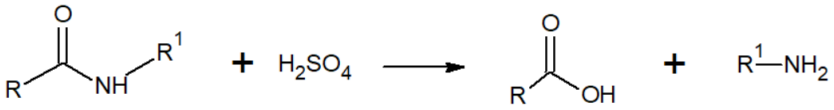

(21)

11.2.5. Determination of membrane permeances to species: an approach to describe the transport in acidic liquid wastes

Different algorithms were applied to determine the membrane permeances to the species permeating through it, depending on the experimental set-ups evaluated (SW and FS modules).

In order to provide a better insight into the influence of solution speciation on the membrane performance, a mathematical model to describe the behaviour of weak electrolytes was developed, since its dissociation has a huge impact on the membrane performance as shown in section 4.1.2. This approach, also based on the SEDM, considers a system of three ions that are interrelated among them by a chemical equilibrium reaction. As the first approach, concentration polarisation was not considered. This model was applied to determine the membrane permeances to species of a weak electrolyte (H^+/ SO_4^{2-}/HSO_4^-). The obtained NF270 membrane permeance values were in agreement

with the dielectric exclusion phenomenon, obtaining values for SO_4^{2-} (<1 µm/s) lower than those for HSO_4^- (>60 µm/s).

However, AMDs contains a considerable amount of different metals, which are complexed with sulphate ions. In this case, a different approach has been applied. The mathematical model contained the basis of the SEDM coupled with reactive transport, but it was solved firstly for the main components (i.e. H^+, Al, Fe, SO_4 and Cl) in solution, and then for the traces from the definition of the electrostatic potential. This approach allowed to simplify the resolution time of the set of equations, also providing a proper fitting of the data. Three membranes (NF270, Desal DL and HydraCoRe 70pHt) were characterised in terms of determining their membrane permeances to species at different conditions of pH, Al(III) and Fe(III) concentration.

Under the tested conditions, for all the evaluated membranes, the permeances to species were found to be dependent on the solution composition. Generally, the fastest ions were H^+ and HSO_4^-, except in the case where Cl^- was present, as calculated permeances for Cl^- were higher in comparison with those of sulphate based anions (SO_4^{2-} / HSO_4^-). The obtained values for permeances were in agreement with Donnan and dielectric exclusion. For example, they followed the trend Fe^{3+}<$FeHSO_4^{2+}$<$FeSO_4^+$<$Fe(SO_4)_2^-$ in agreement with a positively charged membrane (i.e. NF270 and Desal DL), whereas for a negatively charged membrane the sequence was Fe^{3+}<$FeHSO_4^{2+}$<$Fe(SO_4)_2^-$ <$FeSO_4^+$. In addition, membrane permeances to non-charged species (e.g. $ZnSO_4$(aq) and $CaSO_4$(aq)) were determined. It was expected that their transport was not impeded nor favoured by the membrane electric fields. Actually, non-charged species were expected to be better transported than the corresponding free metal ions (e.g. Zn^{2+} and Ca^{2+}). The obtained values of NF270 and Desal DL membrane permeances to non-charged species were higher than the corresponding ones for free metal ions, but in the case of HydraCoRe 70pHT, values for both species were quite similar. For the positively charged membranes (e.g. NF270 and Desal DL) it is expected that the transport of non-charged species is favoured instead the one of the metallic cations because of Donnan dielectric exclusion. However, for the HydraCoRe 70pHT, the transport of metallic cations is not impeded by Donnan exclusion because of the negatively charged membrane. Furthermore, the membrane permeances to species can be used as an indicator of membrane degradation as shown by the NF270 membrane, which after hydrolysis exhibited an increase of its membrane permeances (for example, membrane permeance to HSO_4^- augmented from 114 to 500 µm/s while to La^{3+} from 0.001 to 0.135 µm/s).

Membrane permeances to species were expressed as a function of the concentration of the major components in the feed (e.g. X is H^+ or Fe(III)) according to: $P_i = a_0 + a_1 \cdot X^{a_2}$.

A mathematical model was developed and validated under a batch configuration with the NF270 and Desal DL membranes, where the feed composition varied along with time. Different feed

composition scenarios were tested, one without Fe(III) and two more including Fe(III) (500 and 2125 mg/L). The membrane permeances were obtained, taking into account their dependence with feed composition. The calculated concentration values for both membranes and both streams (permeate and retentate) matched consistently the experimentally measured values for all the experiments. Some discrepancies were found for H^+ values because their values were determined with a pH glass electrode. **Figure 11** shows the rejection curves obtained with the model and during the experiment for the solution containing 2125 mg/L Fe(III) for both membranes. Usually, the recommended range for pH glass electrodes is between 2 and 12, whereas the measurements between pH 1 to 2 might have associated a high error and should be regarded as an approximation. However, acid-base titrations could not be done to measure the acidity due to the precipitation of Fe and Al as hydroxides along the titration.

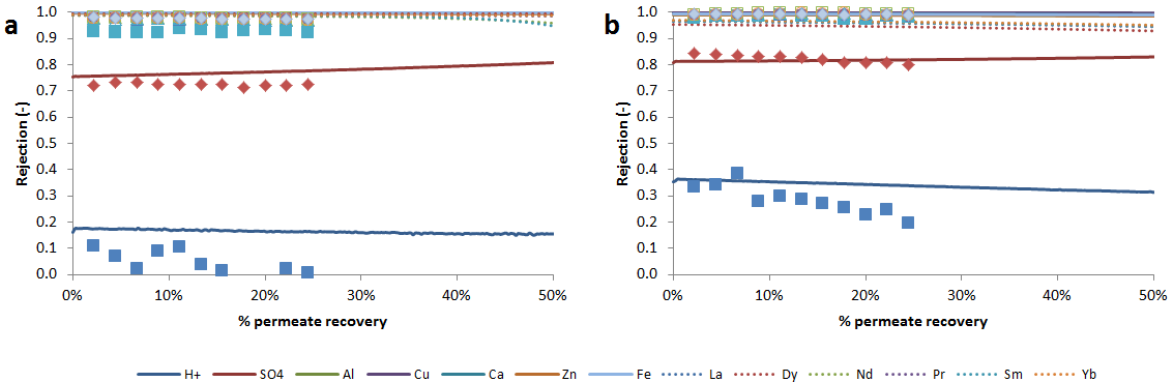

Figure 11. *Rejection of AMD at pH 1.0 containing 2125 mg/L Fe(III) at TMP 20 bar for (a) NF270 and (b) Desal DL. Lines represent the model prediction and the points the experimental data*

Moreover, the capacity of the mathematical model was evaluated by performing a parametric study to evaluate the effect of TMP (10, 20, 40 and 60 bar) and permeate recovery ratios (from 0 to 80%) on metal concentration factors and sulphuric acid recovery. A calculation related to the saturation indexes of the potential mineral phases in scaling events was incorporated. The parametric study revealed that NF270 could be a suitable membrane for acid recovery, especially working at TMP of 10 bar (**Figure 12**). Under this condition, the amount of recovered acid is maximised (H^+ rejection below 10%) keeping high metal rejections. The most likely phases to precipitate were jurbanite ($AlOHSO_4$) and gypsum ($CaSO_4 \cdot 2H_2O$).

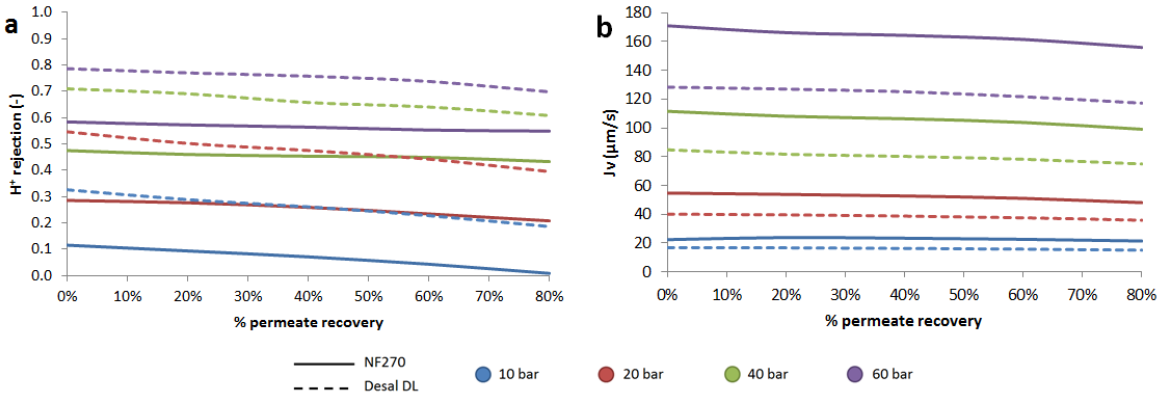

Figure 12. *Comparison of (a) H^+ and (b) Jv at for NF270 and Desal DL membranes at 10, 20, 40 and 60 bar as a function of permeate recovery ratio.*

The SEDM considering reactive transport was also applied to an effluent from a hydrometallurgy industry, containing a mixture of acids (H_2SO_4, HCl and H_3AsO_4) and metallic impurities (Fe, Cu, Zn). NF270 membrane permeances were also in agreement with Donnan and dielectric exclusion. In this case, the fastest anion in solution was Cl^-, exhibiting the highest membrane permeance values (>100 µm/s); followed by dihydrogen arsenate $H_2AsO_4^-$ (45 µm/s) and hydrogen sulphate HSO_4^- (30 µm/s). Instead, the fastest cation in solution was H^+ (>100 µm/s), whereas the metallic cations showed membrane permeances values lower than 0.5 µm/s.

The SEDFM, which considers the ion flux as a combination of diffusive and electromigration and also takes into account the concentration polarisation layer, was used to determine the membrane permeances to species. This model is applied for strong electrolytes, and no reactive transport is considered. Despite not considering reactive transport, the model fitted properly the experimental rejections obtained with the SW module. The obtained membrane permeance values represent the contribution of each species, i.e. the value determined for SO_4^{2-} consider SO_4^{2-}, $NaSO_4^-$ and HSO_4^-. The influence of speciation can also be observed in the obtained permeances. For instance, the decrease of pH from 2.8 to 2.0 led to an increase in the NF270 membrane permeance to SO_4^{2-} (from 0.17 to 0.18 µm/s) due to the shift of SO_4^{2-} toward HSO_4^-. Moreover, changes in membrane properties, such a higher positive charge due to the protonation of free amine groups, were observed. For example, the NF270 membrane permeance to Na^+ (which includes Na^+ and $NaSO_4^-$) decreased (from 1.7 to 1.2 µm/s) for the higher electrostatic repulsion between the positively charged membrane and Na^+ ions.

11.3. Key findings in evaluating the potential integration of diffusion dialysis in acidic liquid wastes

An acidic effluent from a copper smelter composed by sulphuric acid, arsenic and metals was treated with a commercial AEM (Neosepta-AFX).

The transport of the different species in solution was characterised using the diffusion dialysis coefficients and separation factors. Synthetic solutions containing only As (either As(III) or As(V) were firstly tested. Diffusion dialysis coefficients for As(III) and As(V) were $3.2 \cdot 10^{-5}$ m/h and $3.8 \cdot 10^{-5}$ m/h, respectively. The lower value for As(III) can be related to its presence as a cationic form ($H_2AsO_2^+$) in acidic media, which is expected to be fully rejected by the positively charged membrane. However, the presence of As as a non-charged species (H_3AsO_3 for As(III) or H_3AsO_4 for As(V)) can result in a noticeable passage of these species because their transport is not impeded by the membrane.

By treating the effluent from the copper smelter, the highest diffusion dialysis coefficient was for H^+, followed by sulphate (mainly as HSO_4^-) and arsenic (43% of As(III) and 57% of As(V)), while the ones for metals were one order of magnitude lower than that for H^+. The lowest separation factors were for sulphate (1.1) and As (2.7), which indicated a better affinity of the AEM for the former. Separation factors for metals ranged between 7.5 (Pb) to 22 (Fe), which indicated that the membrane was able to reject metals. Volume changes were observed in both tanks, which resulted in a predominance of drag flux (i.e. water is transported with the solvated ions) over the osmotic flux. This leads to the transport of 0.9 L of water (initial volume of 2 L) from the acid to the water side.

Regarding the operation of the DD stack at the same flow ratio of acid and water streams, arsenic speciation as a mixture of As(V) and As(III) or as As(III) did not affect the recovery of sulphuric acid. Acid recovery varied from 79.5% (195 g/L) to 63% (150 g/L) when flow rate was increased from 0.39 to 1.49 L/m^2 h. High flow rates limited the transport of the acid due to the lower residence time of both solutions. For both solutions, almost all Zn was rejected (>90%), followed by Na (>95%), which was related to the smaller radius of Na (0.358 nm) than of Zn (0.430 nm) and dielectric exclusion. However, arsenic was not repelled by the membrane due to its presence as non-charged species (H_3AsO_3 for As(III) and H_3AsO_4 for As(V)). Total arsenic passage ranged from 51% at 0.39 L/m^2 h to 31% at 1.49 L/m^2 h for the mixture of As(V) and As(III). Speciation analysis revealed that As(III) was more rejected than As(V) because of its presence as $H_2AsO_2^+$, whose transport was expected to be impeded by the membrane. For the solution containing only As(III), its passage ranged from 46% at 0.39 L/m^2 h to 30% at 1.24 L/m^2 h. It was decided to make a compromise between recovering the maximum amount of acid with the lowest amount of hazardous impurities by fixing acid flow rate at 0.86 L/m^2 h.

By keeping acid flow rate at 0.86 L/m^2 h and varying water flow rate, acid recovery increased from 65% (211 g/L) to 76% (168 g/L) when the flow rate ratio water/feed was changed from 0.7 to 1.2 for the solution containing As(III) and As(V). The increase in the water flow rate improved the driving force, but the sulphuric acid got diluted. Moreover, higher impurities were transported at high flow rates ratios. As passage increased from 34 to 44%, while the transport of Zn and Na were below 5% and 10%, respectively. For the solution containing As(III), arsenic passage ranged between 24 and 43%. Then, it was decided to take as optimum flow rate ratio value of 1.

The acid effluent from the off-gases treatment of a copper smelter was treated, maintaining a flow rate ratio of 1, working both streams at 0.86 L/m^{2}h (Table 2). From the solution containing 217.4 g/L sulphuric acid, it was possible to recover the 69±2% of the acid (146.3 g/L). The main impurity was arsenic, with a passage of 39±1% (1.3 g/L), whereas metals were effectively rejected by the membrane (total content of metals below 0.1 g/L).

Table 2. *Composition of effluent from the copper smelter, waste stream and recovered acid after the treatment with DD*

	Effluent from copper smelter (g/L)	**Waste stream (g/L)**	**Recovered acid (g/L)**	**Acid recovery / ion passage (%)**
H_2SO_4	217.47 ± 8.73	66.76 ± 8.96	146.28 ± 8.55	68.86 ± 2.34
As	3.33 ± 0.06	2.00 ± 0.27	1.26 ± 0.06	38.66 ± 1.31
Zn	0.46 ± 0.02	0.45 ± 0.07	< 0.04	
Fe	0.13 ± 0.01	0.12 ± 0.02	< 0.04	
Pb	$4.89\cdot10^{-3} \pm 4.88\cdot10^{-4}$	$4.41\cdot10^{-3} \pm 6.09\cdot10^{-4}$	$6.87\cdot10^{-4} \pm 2.33\cdot10^{-4}$	13.48 ± 1.50
Cd	0.11 ± 0.01	0.10 ± 0.01	$7.52\cdot10^{-3} \pm 3.97\cdot10^{-4}$	6.89 ± 0.26
Ni	$6.31\cdot10^{-3} \pm 1.35\cdot10^{-4}$	$6.17\cdot10^{-3} \pm 8.89\cdot10^{-4}$	$< 4\cdot10^{-4}$	
Cu	0.06 ± 0.01	$0.06\pm 7.74\cdot10^{-3}$	$3.19\cdot10^{-3} \pm 4.29\cdot10^{-5}$	5.19 ± 0.06

11.4. Integration of membrane processes in the industry

As seen, NF membranes can be used for treating AMDs. Given its properties, they can be integrated into schemes for REEs recovery (**Figure 13**). Firstly, iron should be oxidised with air to convert Fe(II) to Fe(III) and removed with CaO(s) or $CaCO_3$(s) until reaching pH values below 3.7. Then the effluent can be treated with an ion exchange resin to concentrate the valuable metals (i.e. REEs). The subsequent

regeneration with sulphuric acid can be treated in a NF stage to recover the acid as permeate, which can be recycled back to the regeneration of the resin. Besides, the REEs, which are concentrated in the NF stage, can be recovered by selective precipitation using phosphates or oxalates.

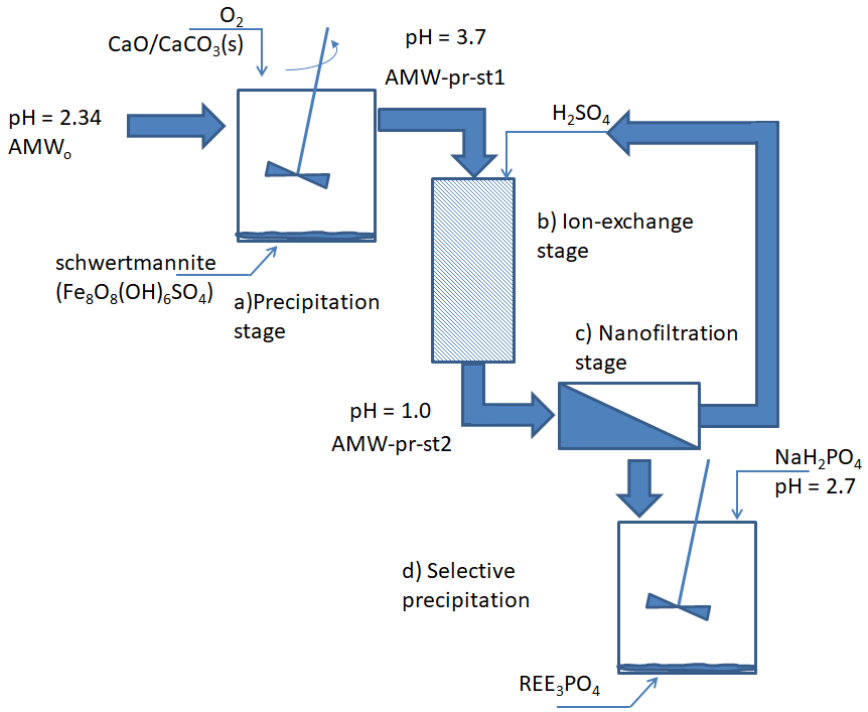

Figure 13. *Proposed treatment of an AMD including a) total oxidation of Fe(II) to Fe(III) and precipitation with $CaO/CaCO_3$; b) concentration of valuable metals with ion-exchange resins; c) recovery of H_2SO_4 and concentration of valuable metals with NF; and d) selective precipitation of REE as phosphates.*

For the case of effluents coming from the metallurgical industries, 2 scenarios can be found, depending on the acidity of the stream.

For medium acidity conditions, a proper design with different NF stages may allow to recover up to 90% of the total acids contents (**Figure 14.a**). Nevertheless, the fact that the membrane does not impede the transport of non-metallic species, such as H_3AsO_4 makes necessary one unit devoted to removing As. This unit requires the use of a reducing agent (e.g. $H_2S(g)$) to obtain As(III), and then its subsequent precipitation as $As_2S_3(s)$ (**Figure 14.b)**.

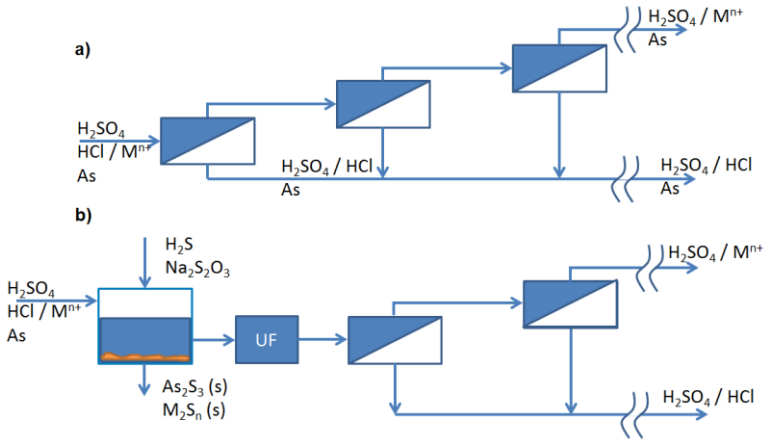

Figure 14. *Different schemes for acid recovery with NF membranes (a) without and (b) with a reducing agent for As precipitation*

The other scenario is related to high levels of acidity (220 g/L sulphuric acid). In this case, the treatment is focused on the recovery of a purified acid sulphuric by DD for its reuse (**Figure 15**). However, the concentration of arsenic in the recovered acid may limit its application. Then, a solvent extraction step using an organophosphorus extractant can be used for the removal of arsenic, after which the DD step can recover more than 69% of the acid. The residual stream exiting from the DD unit can be treated with CaO(s) and $FeSO_4$(s) to remove the metals as hydroxides and arsenic as scorodite ($FeAsO_4 \cdot 2H_2O$ (s)).

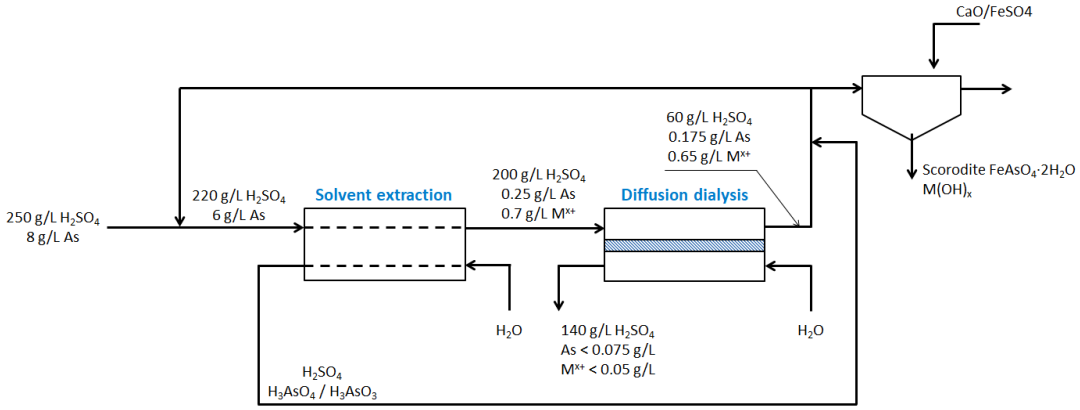

Figure 15. *Integration of solvent extraction and DD for the treatment of the acidic solution generated on the off-gases treatment of a copper smelter*

CHAPTER 12

Conclusions

12. Conclusions

Nowadays there is an increasing interest for circular schemes in the industry. The need to reduce or minimise the waste generated and to recover high-valuable components from wastes have attracted the attention of the industry and researchers. Mining, hydrometallurgical and metallurgical industries generate a huge amount of acidic liquid wastes (ALWs) characterised by the presence of valuable metals (e.g. REEs, Cu, Zn) and hazardous materials (e.g. As). Traditionally, these industrial effluents have been treated by alkali addition to neutralise the acidity and to remove metals and non-metals, and the final stream discharged in the natural bodies. However, the considerable amount of chemicals needed in this treatment have made that alternative solutions such as solvent extraction, ion exchange or membrane technologies are emerging to deal with acidic liquid effluents.

In this thesis, NF and DD have been studied for the treatment of mining, hydrometallurgical and metallurgical ALWs and resource recovery in order to provide more sustainable management of such streams. In the light of the findings of this Thesis, it can be concluded that:

a) NF membranes can be suitable for the recovery of acids and concentrate metals from acidic streams. The polyamide-based membranes (NF270 and Desal DL) showed the best results in terms of high metal rejection (>98%) and low acid rejection (<20% and <40% for NF270 and Desal DL, respectively). However, in the long term application, these membranes may suffer from hydrolysis as it was demonstrated by XPS. Then, acid-resistant membranes may be preferable. Within that group, the low rejections of ceramic membranes made them inappropriate for the treatment of acidic waters.

b) The selectivity of the membrane is highly interrelated with the solution complexation. For the simplest case with solutions containing only diluted H_2SO_4, at acid pH the equilibrium $H^+ + SO_4^{2-} \rightleftarrows HSO_4^-$ is shifted toward HSO_4^- . H_2SO_4 rejections started to decrease when HSO_4^- predominated over SO_4^{2-} at pH<pKa (=1.92), which is associated with the dielectric exclusion phenomenon. Moreover, when filtering synthetic AMDs, the complexation of metals with sulphate (e.g. $FeSO_4^+$, $FeHSO_4^+$) led to higher sulphate rejections, while the transport of H^+ was favoured. Furthermore, certain uncharged species such as fully protonated weak electrolytes (e.g. H_3AsO_4) were not rejected effectively by the membrane, since the electric fields cannot reject them.

c) The transport of species across a NF membrane was characterised in terms of membrane permeances to the species. Firstly, a model to describe the behaviour of weak electrolytes (i.e. $H^+/SO_4^{2-}/HSO_4^-$) was developed. Then, on the basis of SEDM coupled with reactive transport, a mathematical model was applied to describe the transport of species in AMD, and the influence of solution composition into the permeances was studied. The obtained

membrane permeances to species were in agreement with Donnan and dielectric exclusion. Furthermore, they were found to be dependent on solution composition. Finally, it was possible to predict the performance of a NF membrane under unsteady state conditions with the membrane permeances.

d) DD can be suitable for acid recovery and its purification from streams coming from the metallurgical industry. It was possible to recover a sulphuric acid stream free of metallic impurities. However, the presence of fully protonated weak electrolytes (i.e. H_3AsO_4 for As(V) and H_3AsO_3 for As(III)) makes the membrane not able to reject them. The presence of arsenic in the recovered acid may limit the applicability of the recovered acid in the metallurgical industry itself.

e) Analysis of the results with both membranes (NF and AEMs) have shown that transport of non-charged species as H_3AsO_3 and H_3AsO_4 is not impeded as the rejection mechanisms related to the charge (i.e. Donnan and dielectric exclusion) does not apply. Scarce data have been found for As species, and only similar results have been reported for H_3PO_4 species. Both solutes, with 126 and 142 Da, are not suffering steric hindrance. For the case of a toxic element such as As, its presence limits the application of both types of membranes when the objective is its removal from the copper metallurgical waste streams.

Finally, it has been demonstrated that NF and DD membrane technologies are suitable for the treatment of ALWs. These technologies were able to recover acids and, at the same time, to concentrate the metallic impurities in solution, which can be selectively recovered by other technologies.

ANNEX 1

Publication 8

"*From Membrane Permeances to the Prediction of Membrane Nanofiltration Performance in acidic solutions: application to the Recovery of Rare Earths Elements from Acid Mine Waters***"**

Manuscript Details

Manuscript number	SEPPUR_2019_2016_R1
Title	From Membrane Permeances to the Prediction of Membrane Nanofiltration Performance in acidic solutions: application to the Recovery of Rare Earths Elements from Acid Mine Waters
Article type	Full Length Article

Abstract

Nowadays, alternative sources for obtaining critical elements (e.g. indium, gallium, vanadium, phosphorus, rare earth elements (REEs)) are being studied due to the depletion of primary resources. In the present, the potential application of nanofiltration (NF) membranes for the recovery of REEs from acidic mine waters (AMW) as a secondary resource is being evaluated. NF membranes provide the possibility of separating and concentrating REEs from sulphuric acid solutions as a pre-treatment stage in hydrometallurgical industries. In the present study, two aromatic polyamide-based NF membranes (NF270 and Desal DL) were tested to study the sulphuric acid recovery and REE concentration from synthetic solutions mimicking AMW from the SW Spain. They all were characterised by a pH of 1.0, elevated concentration of metals Al, Cu, Ca and Zn (25-600 mg/L) and REEs (10 mg/L), and differed in their Fe concentration (0, 500 and 2125 mg/L). The sulphuric acid recovery and REEs concentration by the NF membranes for the different feed water scenarios were modelled by the Solution-Electro-Diffusion (SED) model modified to innovatively include the influence of the chemical speciation of solutes and the solution composition on membrane permeances as well as the scaling potential of the feed. Results showed that the level of Fe had effectively an influence in the permeation of other species also present in the feed water. The prediction capacity of the model applied was in general satisfactory with differences between theoretical and experimental values below 15%. The main disagreements were found for the prediction of proton concentrations. NF270 showed a higher ability in concentrating metals in the feed tank and recovering acid in the permeate than Desal DL.

Keywords	rare earth elements; acidic mine waters; NF270; Desal DL; nanofiltration
Manuscript category	Membrane filtration: Focused on fouling, theories of microfiltration, nanofiltration

Corresponding Author	Julio López
Corresponding Author's Institution	Universitat Politècnica de Catalunya
Order of Authors	Julio López, Mònica Reig, Xanel Vecino, Oriol Gibert, Jose-Luis Cortina
Suggested reviewers	Míriam Amaral, Mario Avila-Rodriguez, Jens Uwe Repke

Submission Files Included in this PDF

File Name [File Type]

SEPPUR_2019_2016_Cover letter_revised manuscript.docx [Cover Letter]

SEPPUR_2019_2016_Answer to reviewers.docx [Response to Reviewers]

SEPPUR_2019_2016_Manuscript_marked changes.docx [Revised Manuscript with Changes Marked]

SEPPUR_2019_2016_Highlights.docx [Highlights]

SEPPUR_2019_2016_Graphical abstract.docx [Graphical Abstract]

SEPPUR_2019_2016_Manuscript_clean.docx [Manuscript File]

SEPPUR_2019_2016_Figures.docx [Figure]

SEPPUR_2019_2016_Tables.docx [Table]

SEPPUR_2019_2016_declaration-of-competing-interests.docx [Conflict of Interest]

To view all the submission files, including those not included in the PDF, click on the manuscript title on your EVISE Homepage, then click 'Download zip file'.

Highlights

Acid mine drainage as a potential source for chemicals recovery

Nanofiltration membranes for acid recovery and metal concentration

Use of Solution–Electro–Diffusion model to predict the membrane performance

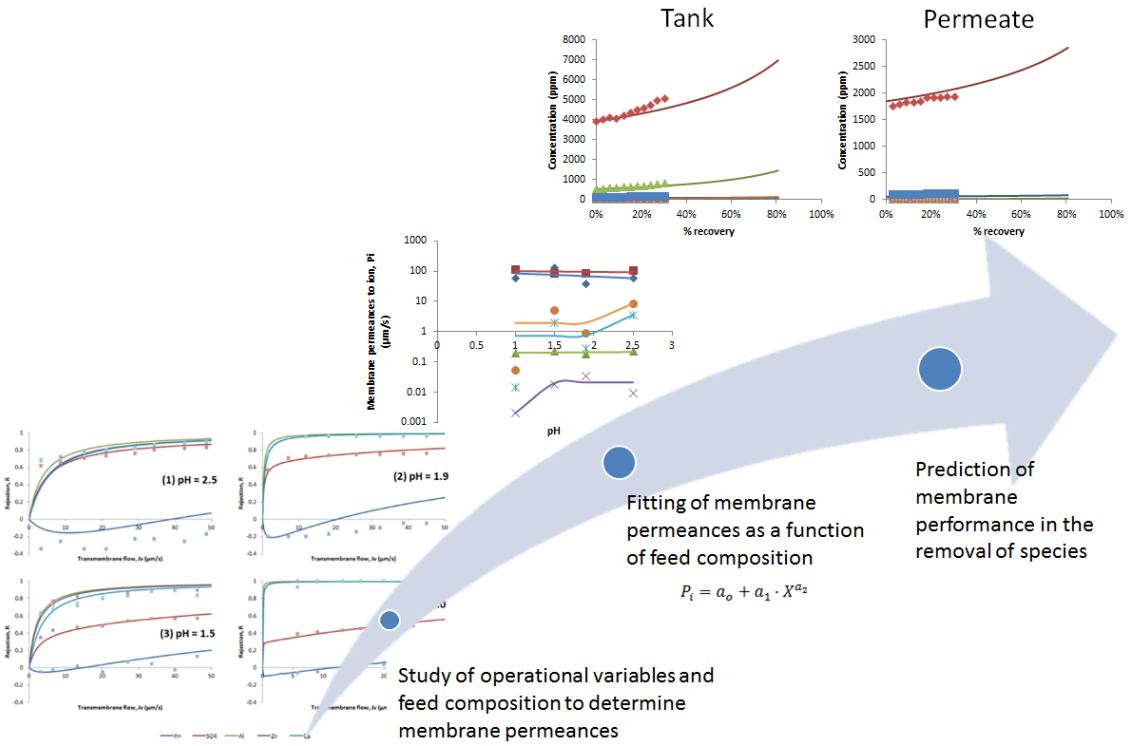
Tank
Permeate
Concentration (ppm)
% recovery
Membrane permeances to ion, Pi (μm/s)
pH
(1) pH = 2.5
(2) pH = 1.9
(3) pH = 1.5
Transmembrane flow, Jv (μm/s)
Rejection, R
Fitting of membrane permeances as a function of feed composition
$P_i = a_o + a_1 \cdot X^{a_2}$
Prediction of membrane performance in the removal of species
Study of operational variables and feed composition to determine membrane permeances

From Membrane Permeances to the Prediction of Membrane Nanofiltration Performance in acidic solutions: application to the Recovery of Rare Earths Elements from Acid Mine Waters

J. López [a*], M. Reig [a], X. Vecino [a], O. Gibert [a], J. L. Cortina [a,b]

[a] *Chemical Engineering Department and Barcelona Research Center for Multiscale Science and Engineering, UPC-BarcelonaTECH, C/ Eduard Maristany, 10-14 (Campus Diagonal-Besòs), 08930 Barcelona, Spain*

[b] *Water Technology Center CETaqua, Carretera d'Esplugues 75, 08940 Cornellà de Llobregat, Spain*

[*] julio.lopez.rodriguez@upc.edu

Abstract

Nowadays, alternative sources for obtaining critical elements (e.g. indium, gallium, vanadium, phosphorus, rare earth elements (REEs)) are being studied due to the depletion of primary resources. In the present, the potential application of nanofiltration (NF) membranes for the recovery of REEs from acidic mine waters (AMW) as a secondary resource is being evaluated. NF membranes provide the possibility of separating and concentrating REEs from sulphuric acid solutions as a pre-treatment stage in hydrometallurgical industries. In the present study, two aromatic polyamide-based NF membranes (NF270 and Desal DL) were tested to study the sulphuric acid recovery and REE concentration from synthetic solutions mimicking AMW from the SW Spain. They all were characterised by a pH of 1.0, elevated concentration of metals Al, Cu, Ca and Zn (25-600 mg/L) and REEs (10 mg/L), and differed in their Fe concentration (0, 500 and 2125 mg/L). The sulphuric acid recovery and REEs concentration by the NF membranes for the different feed water scenarios were modelled by the Solution-Electro-Diffusion (SED) model modified to innovatively include the influence of the chemical speciation of solutes and the solution composition on membrane permeances as well as the scaling potential of the feed. Results showed that the level of Fe had effectively an influence in the permeation of other species also present in the feed water. The prediction capacity of the model applied was in general satisfactory with differences between theoretical and experimental values below 15%. The main disagreements were found for the prediction of proton concentrations. NF270

showed a higher ability in concentrating metals in the feed tank and recovering acid in the permeate than Desal DL.

Keywords: rare earth elements; acidic mine waters; NF270; Desal DL; nanofiltration

1. Introduction

The European Union has identified a list of critical materials based on their high importance to its economy and the high risk associated with their supply. This list includes phosphorous, magnesium, tungsten, vanadium and rare earth elements (REEs), which comprise in turn lanthanides, scandium and yttrium to name a few [1]. Because of their chemical and physical properties, REEs are widely used in electronic, optical, magnetic and nuclear applications, among others [2,3]. Due to the scarcity of these critical elements, circular economy schemes are currently being proposed for their recovery from alternative sources and re-uses.

REEs are found in nature in sedimentary and igneous rocks as oxides and are obtained mainly from different minerals (bastnaesite, monazite and xenotime). Most of the ways to obtain each REE separately from these minerals include, first of all, acidic leaching (mainly with H_2SO_4), followed by acid neutralisation and different solvent extraction steps [4–7]. However, the exhaustion of these minerals makes it necessary to exploit other sources to acquire REEs.

On the other hand, acidic mine waters (AMWs) are a by-product of the mining industry that occurs when sulphide minerals, such as pyrite (FeS_2), are oxidised when entering in contact with water and oxygen. This process can occur naturally, but its generation can be accelerated due to human activity. The oxidation of sulphide minerals leads to sulphuric acid production, which can dissolve the surrounding soil minerals. Then, a sulphuric-based stream containing a high content of iron, aluminium, zinc and copper, and a minor presence of REEs (the so-called AMW) is released to the environment [3,8]. Although the concentration of REEs in AMW is lower than that of the transition metals mentioned above, it is around two orders of magnitude higher than the one in natural waters [9,10]. For example, AMWs from the Iberian Pyrite Belt can present concentrations from 0.3 to 11.7 mg/L of REE [10]. Therefore, AMWs can be considered as an alternative source for REEs recovery, especially in Europe, which faces a shortage of REEs primary resources. As with the leachates obtained from REE-rich minerals, the recovery of REEs from AMW is accomplished by successive acid neutralisation and solvent extractions steps.

However, because the concentration of REE in AMW is lower than in the leachates from REE-rich minerals, it may be desirable to concentrate them before the acid neutralisation and

solvent extraction steps. This can be accomplished by membrane technologies (e.g. reverse osmosis, nanofiltration (NF) or electrodialysis) [11–14]. Amongst these, NF membranes have demonstrated to offer two-fold benefits when treating AMWs: on the one hand, they can concentrate multi-charged ions (and hence REEs) in the retentate side while, on the other hand and thanks to their ability to allow permeation of mono-charged ions (e.g. H^+). They can provide a purified sulphuric stream in the permeate side, which can even be recycled and reused in leaching steps if needed [15–17].

Nevertheless, and contrarily to reverse osmosis processes, there is still a lack of mathematical models to scale and predict the behaviour of NF membranes for treating AMWs. Mathematical models such as the Solution-Electro-Diffusion (SED) can describe the transport of species across NF membranes using membrane permeances. This model is based on two assumptions: (i) the separation is achieved due to differences on species diffusivities; and (ii) membranes do not present fixed pores but have a free volume instead [18]. In general, most of the efforts have so far been centred in the description of single solutions containing strong electrolytes where the formation of chemical species between ions in solutions is not expected. However, such a scenario is only a too simple representation of real AMWs, where each element may give rise to multiple species in equilibrium with each other. A step forward has been done by a recent study on the rejection of species in acidic waters by NF considering the formation of chemical species between weak electrolytes (e.g. SO_4^{2-}/HSO_4^-) and metallic ions in solution (M^{n+}) [19]. The incorporation of the reactive transport concept of species in the SED model has led to the setup of a database of NF membrane permeances to species as a potential tool for the design of NF processes for the recovery of valuable metals (e.g. REEs) from acidic waters [20,21].

The main objective of this work was to validate the prediction capabilities of a numerical solution based on the SED model in the recovery of sulphuric acid and concentration of metals using two different commercial polyamide NF membranes: NF270 (from Dow Chemical) and Desal DL (from GE Osmonics). For this purpose, three synthetic solutions mimicking an AMW from La Poderosa Mine (Huelva, Spain), characterised by a low pH (pH of 1.0), elevated concentrations of metals (Al, Cu, Ca and Zn (25-600 mg/L)) and REEs (10 mg/L), and different Fe(III) concentration (0, 500, 2125 mg/L) were treated. Different %recovery ratios were evaluated and, under this condition, the concentration of species changes with regard to the initial feed composition. Then, the prediction capability of SED model using membrane permeances calculated in a previous study and considering chemical equilibrium among ions

was evaluated. The Hydra/Medusa and PHREEQC databases were used to determine the potential implications of scaling along the filtration treatment.

2. Experimental

2.1. Membranes and solutions

Two commercial NF membranes were tested, namely NF270 (from Dow Chemical) and Desal DL (from GE Osmonics), both with a top layer based on a semi-aromatic poly(piperazine amide). According to the manufacturers, Desal DL incorporates an additional proprietary second layer made of a material comparable to a polyamide, which impacts on membrane properties, such as surface roughness, hydrophilicity and acid-base properties. Both membranes have ionisable amine ($R–NH_2$/$R–NH_3^+$) and carboxylic ($R–COOH$/$R–COO^-$) groups, which are responsible for the membrane charge. The isoelectric points (IEPs) are 2.5 and 4.0 for NF270 and Desal DL, respectively [22]. The main properties of these membranes are collected in **Table 1**.

Table 1*. Properties of NF270 and Desal DL membranes*

	NF270	**Desal DL**
Active layer	Semi-aromatic polypiperazine-amide	
pH range	2 – 11	
Isoelectric point, IEP	2.5	4.0
Max. Operating temperature (°C)	45	90
Water permeability (L /m^2·h·bar)	10.7	8.3
Mg(II) rejection (%)	97 [a]	96 [b]
Molecular Weight Cut-Off, MWCO (Da)	300	327
Thickness (μm)	0.170	0.300
References	[22–25]	[22,25–27]

[a] [$MgSO_4$] = 500 mg/L, TMP = 0.55 MPa [24]; [b] [$MgSO_4$] = 2000 mg/L,TMP = 0.76 MPa [27]

The presence of Fe (as a mixture of Fe(II) and Fe(III)) can limit the recovery options of REEs. One of the main pre-treatment stages involves the oxidation with air of Fe(II) to Fe(III) and the

subsequent removal of Fe(III) by precipitation with a low-cost alkali reagent (e.g. CaO or $CaCO_3$). Then, two main scenarios could be found before the recovery of REEs: one with Fe(III) if is not removed or iron free solutions.

Three synthetic solutions mimicking an AMW from La Poderosa Mine at the Iberian Pyrite Belt (Huelva, Spain) were treated. All these solutions contained a sulphuric media (pH around 1.0 ± 0.1) and Al(III) (600 mg/L), Ca(II) and Zn(II) (40 mg/L each), Cu (25 mg/L) and REE such as La, Dy, Nd, Pr, Sm and Yb (10 mg/L each one), but differed in their concentration of Fe(III), which was 0, 500 and 2125 mg/L. All metals (Al, Ca, Zn and Cu) were added as metal-sulphate salts, while REEs were added as chlorides, nitrates, sulphates or oxides. As explained, the treatment of any AMW includes as a first step the oxidation of iron, so the experiments were performed with Fe(III). Iron was added to the solution as Fe(II) in the form of $FeSO_4$ and was then oxidised with an excess of H_2O_2 (the double than the stoichiometric) to convert Fe(II) into Fe(III). The following solutions and salts were used: H_2SO_4 (96 wt%, Sigma-Aldrich); $Al_2(SO_4)_3{\cdot}18\ H_2O$ (55%, Panreac); $FeSO_4{\cdot}7H_2O$ (98%, Sigma-Aldrich); $CaSO_4{\cdot}2H_2O$ (100%, Scharlau); $ZnSO_4{\cdot}7H_2O$ (100%, Panreac); $CuSO_4$ (100%, Panreac); $La_2(SO_4)_3{\cdot}9H_2O$ (99.9%, Alfa Aesar); $Pr(NO_3)_3{\cdot}6H_2O$ (100% Fluka AG); $NdCl_3{\cdot}6H_2O$ (100%, Fluka AG); $SmCl_3$ (100%, Fluka AG); Dy_2O_3 (99.9%, Fluka AG) and Yb_2O_3 (99.9% Fluka AG), H_2O_2 (30%, Sigma-Aldrich).

A speciation analysis was performed before starting the experiments with the Hydra/Medusa and PHREEQC code [28,29]. According to it, metals can be presented as a free ion (e.g. Al^{3+}, Ca^{2+}) or forming complexes with sulphate, giving negatively or positively charged ions (e.g. $AlSO_4^+$, $Al(SO_4)_2^-$, $CaHSO_4^+$) or even non-charged species (e.g. $CaSO_4$). Complexes with other anions were found at negligible concentrations. **Table 2** collects the chemical equilibrium constants for metal – sulphate complexes, which were used in mathematical modelling.

Table 2*. Chemical equilibrium constants in solution from Hydra/Medusa and PHREEQC code* [28,29]

Chemical reaction	$\log K_{T,I}$	Chemical reaction	$\log K_{T,I}$
$H^+ + SO_4^{2-} \leftrightarrow HSO_4^-$	1.98	$La^{3+} + 2\,SO_4^{2-} \leftrightarrow La(SO_4)_2^-$	5.10
$Al^{3+} + SO_4^{2-} \leftrightarrow AlSO_4^+$	3.50	$Pr^{3+} + SO_4^{2-} \leftrightarrow PrSO_4^+$	3.62
$Al^{3+} + 2\,SO_4^{2-} \leftrightarrow Al(SO_4)_2^-$	5.00	$Pr^{3+} + 2\,SO_4^{2-} \leftrightarrow Pr(SO_4)_2^-$	4.90
$Ca^{2+} + SO_4^{2-} \leftrightarrow CaSO_4$	2.30	$Nd^{3+} + SO_4^{2-} \leftrightarrow NdSO_4^+$	3.64
$Ca^{2+} + H^+ + SO_4^{2-} \leftrightarrow CaHSO_4^+$	3.07	$Nd^{3+} + 2\,SO_4^{2-} \leftrightarrow Nd(SO_4)_2^-$	5.10

190

$Cu^{2+} + SO_4^{2-} \leftrightarrow CuSO_4$	2.31	$Sm^{3+} + SO_4^{2-} \leftrightarrow SmSO_4^{+}$	3.65
$Zn^{2+} + SO_4^{2-} \leftrightarrow ZnSO_4$	2.37	$Sm^{3+} + 2\,SO_4^{2-} \leftrightarrow Sm(SO_4)_2^{-}$	5.20
$Fe^{3+} + SO_4^{2-} \leftrightarrow FeSO_4^{+}$	2.25	$Dy^{3+} + SO_4^{2-} \leftrightarrow DySO_4^{+}$	3.61
$Fe^{3+} + 2\,SO_4^{2-} \leftrightarrow Fe(SO_4)_2^{-}$	3.59	$Dy^{3+} + 2\,SO_4^{2-} \leftrightarrow Dy(SO_4)_2^{-}$	5.10
$Fe^{3+} + H^{+} + SO_4^{2-} \leftrightarrow FeHSO_4^{2+}$	4.23	$Yb^{3+} + SO_4^{2-} \leftrightarrow YbSO_4^{+}$	3.59
$La^{3+} + SO_4^{2-} \leftrightarrow LaSO_4^{+}$	3.62	$Yb^{3+} + 2\,SO_4^{2-} \leftrightarrow Yb(SO_4)_2^{-}$	5.10

Figure 1 represents the sulphate fraction for a solution mimicking the AMW at pH 1 as a function of Fe(III) concentration. Thus, it can be seen that the increase of Fe(III) concentration leads to an increase of iron-sulphate complexes (i.e. $FeHSO_4^{2+}$, $FeSO_4^{+}$ and $Fe(SO_4)^{2-}$), whereas the fraction of hydrogen–sulphate (HSO_4^{-}) and sulphate (SO_4^{2-}) decrease. The other metals, as shown in **Table 2**, also form complexes with sulphate, but their concentration in terms of sulphate fraction is lower than 1%, and therefore their profiles are not depicted in **Figure 1.**

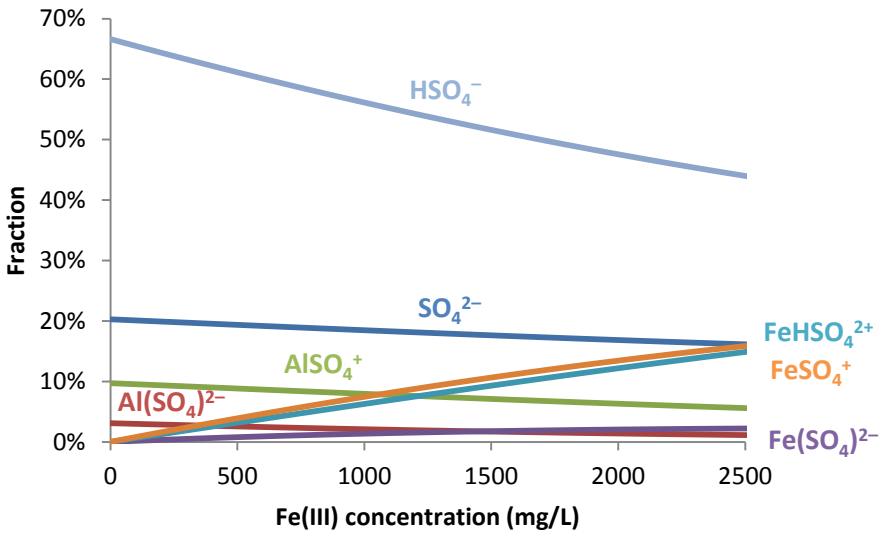

***Figure 1**. Dependence of sulphate fraction at pH = 1 with the synthetic solution mimicking the AMW on Fe(III) concentration*

2.2. Membrane cross-flow experimental set-up

Experiments were carried out with a membrane cross-flow cell (GE SEPA^{TM} CF II) using a flat-sheet membrane (0.014 m^2). A thermostated 30 L tank was used to keep the synthetic solution to be treated at a constant temperature (25 ± 2 °C). Then, the solution was pumped into the membrane cell with a high-pressure diaphragm pump (Hydra-Cell, USA) at prefixed flow rates

and pressures. The set-up was provided with a needle and a by-pass valve to vary the cross-flow velocity (cfv) and the trans-membrane pressure (ΔP). The first one was located at the retentate stream, just at the exit from the membrane test cell, whereas the other valve was placed before the entrance of the solution into the module. At the feed and concentrate lines, two manometers were placed to monitor the pressure. Just before the discharge of the retentate to the tank, a flow-meter and a pre-filter cartridge (100 µm, polypropylene) were placed. Pipes were made of stainless steel to avoid corrosion issues. A scheme of the experimental set-up is shown in **Figure 2**.

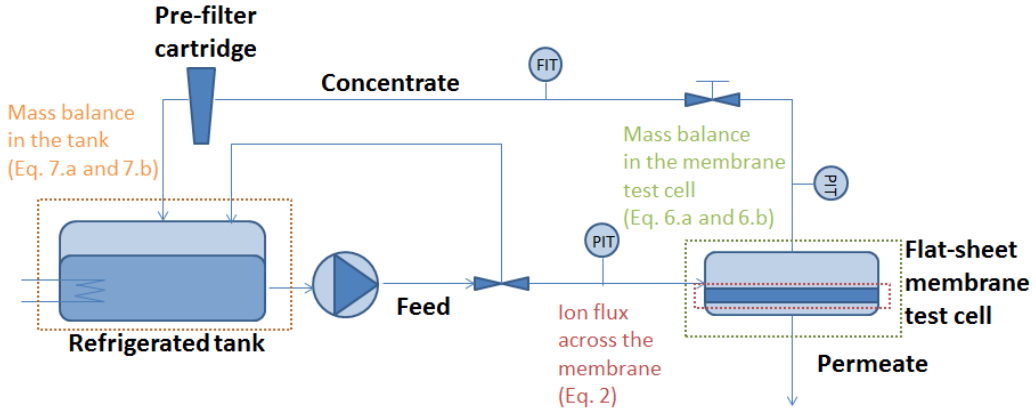

***Figure 2**. Scheme of the experimental NF set-up. Dotted boxes represent the points where mass balances were solved to predict the behaviour of the system*

Membranes were placed overnight in Milli-Q water to remove their conservation products. After that, each membrane was compacted with deionised water at 22 bar and cfv of 1 m/s for 2h. Before running an experiment, the membrane was compacted with the AMW at the same ΔP and cfv for 2 h. At this stage, both retentate and permeate were recycled back to the feed tank to keep the same conditions along the membrane compaction. Experiments were run at a pre-fixed cfv of 0.7 m/s and the ΔP was kept constant at 20 bar. In previous studies, the effect of ΔP on rejections was suited and it was observed that at 20 bar metal rejections were high (>98%), while the transport of H_2SO_4 was not impeded across the membrane [20,30,31]. Moreover, at that ΔP concentration polarization was not observed. After collecting 500 mL of permeate and onwards, samples of the solution in the feed tank and permeate were analysed and data were represented as a function of permeate recovery, defined as follows (**Eq. 1**):

$$\%\ permeate\ recovery = \frac{V_{t=0} - V_t}{V_{t=0}}\ x\ 100 \qquad (1)$$

Where $V_{t=0}$ (27 L) and V_t are the volumes of the feed tank solutions at the beginning of the experiment and at time t, respectively.

192

The concentration factor for a given species was defined as the ratio between the concentration of that species in the feed tank at time t and its initial concentration (C_t/C_0).

Experiments were finished when 30% of permeate recovery was achieved. Then the set-up was cleaned with deionised water to remove any impurity that may be left inside the cell.

2.2. Analytical methods

Samples from the feed tank and permeate were analysed during the experiments with a pH-meter and a conductivity-meter as a preliminary analysis to monitor the membrane performance. In order to determine the concentration of the solution elements, samples were analysed using Inductively Coupled Plasma Mass (7800 ICP-MS from Agilent Technologies) and Optical Emission Spectrometer (5100 ICP-OES from Agilent Technologies). Before ICP analysis, samples were previously filtered (0.2 μm) and acidified with 2% HNO_3.

With regard to the determination of the concentration of H^+ with a pH-meter, it must be highlighted that the analysable pH range with glass electrodes was, according to the manufacturer, from 2 to 12, which implied that any measurement of pH in the range of 1 to 2 might have associated a high error and should be regarded as an approximation. Acidity measurements by acid-base titration could not be done due to the precipitation of Fe and Al as hydroxides along the titration.

3. Numerical tool for prediction of the membrane performance

The equations presented in what follows were applied in the membrane itself (red box in **Fig. 2**), in the membrane test cell (green box in **Fig. 2**) and the tank (orange box in **Fig. 2**) to predict the behaviour of the experimental system.

The transport of ions across the NF membranes was described on the basis of the SED model, which was coupled with reactive transport taking into account the chemical equilibria between the different species in solution. It is acknowledged that the transport of ions through a NF membrane is a combination of diffusive forces and electromigration, while there is no coupling between ions and solvent. “Virtual” concentrations, which are in thermodynamic equilibrium with an infinitely small volume inside the membrane, were used. Thus, ion flux is described according to **Equation 2** [21,32]:

$$j_i = -P_i \cdot \left(\frac{dc_i}{dx} + c_i \cdot \frac{d(\ln \gamma_i)}{dx} + z_i \cdot c_i \cdot \frac{d\varphi}{dx} \right) \quad (2)$$

where j_i, P_i, c_i, γ_i and z_i are the flux across the membrane, the membrane permeance, the concentration, the activity coefficient and the valence charge of species i, respectively. x is the dimensionless position in the membrane and φ is the dimensionless virtual electrostatic potential in the membrane.

The transport of any species i across the membrane must satisfy: i) chemical equilibrium reactions between species, which once identified allow their flux to be solved (**Eq. 2**) for each element that composes the species (e.g. equation referred to Al is a sum of the flux of Al^{3+}, $AlSO_4^+$ and $Al(SO_4)_2^-$) and; ii) electroneutrality condition, defined as follows (**Eq. 3**):

$$\sum_{i=1}^{n}(z_i \cdot c_i) = 0 \qquad (3)$$

The membrane permeance to a given species i (P_i), which indicates the easiness of this species to be transported across the membrane is acknowledged to depend on the membrane, the species properties and the composition of the solution (e.g. concentration of H^+ or Fe(III)). Partition coefficients and possible changes in the chemical equilibrium constants are included within the membrane permeances to ions [18].

The SED model has proven to successfully describe rather complex experimental trends in NF of electrolyte mixtures containing various dominant salts and trace ions. In previous studies, the permeance of membranes NF270 and Desal DL towards the same solutes as the ones investigated in the present study (Al, Ca, Zn, Cu, REE, SO_4) were determined under a variety of pH values and Fe(III) concentrations at constant feed composition from 4 to 22 bar [20,30,31] (these values are collected in Supplementary Information). However, determined membrane permeances are not constant and depend on solution composition. In this work, since the permeate is removed from the system, it is expected that the feed solution composition changes with time. Insomuch as membrane permeances are dependent on solution composition, the values from previous studies [20,30,31] were fitted as a function of pH and concentration of Fe(III) through an expression like **Equation 4**, as proposed by Bason et al. [33] and Yaroschuck [34]:

$$P_i = a_o + a_1 \cdot X^{a_2} \qquad (4)$$

where a_0, a_1 and a_2 are fitting parameters and X is the concentration of H^+ or the one of Fe(III).

The flux of solvent across the membrane was described with the following equation (**Eq. 5**):

$$J_v = k_w \cdot (\Delta P - \Delta\pi) \quad (5)$$

where J_v is the solvent flux across the membrane, k_w is the hydraulic permeability of the membrane, ΔP and $\Delta\pi$ are the differences of pressure and osmotic pressure between feed and permeate. Osmotic pressure is calculated according to the van't Hoff equation.

In the membrane test cell, global and component mass balances were solved to determine the concentration and flow of the retentate stream (**Eqs. 6.a** and **6.b**):

$$Q_f = Q_r + Q_p \quad (6.a)$$

$$c_f \cdot Q_f = c_r \cdot Q_r + c_p \cdot Q_p \quad (6.b)$$

where Q and c are the flow and concentration, respectively. Subscripts f, r and p refer to the feed, retentate and permeate, respectively.

Finally, an unsteady state mass balance is solved in the feed tank to determine how the volume of the solution varied and how the different compounds were concentrated along with time (**Eqs. 7.a** and **7.b**).

$$\frac{dV}{dt} = Q_r - Q_f \quad (7.a)$$

$$\frac{d(c_{f,i} \cdot V)}{dt} = Q_r \cdot c_{r,i} - Q_f \cdot c_{f,i} \quad (7.b)$$

where V is the tank volume and t is the running time of the experiment.

After solving **Equations 7.a** and **7.b**, a speciation analysis must be performed to determine the composition of the different species in the feed, and then solve **Equation 2**.

The numerical code was implemented in Matlab to predict the performance of the system (**Figure 3**).

A more robust dataset of membranes permeances to species for the experiments with Fe(III) is presented. The fitting of membrane permeances was done in the range of 500-2125 mg/L Fe(III). The different experiments carried out in this work with Fe(III), 500 and 2125 mg/L, were performed in order to have one in the range of the membrane permeance fitting (500 mg/L) with interpolated values, and the other one outside this range (2125 mg/L) with extrapolated membrane permeances. Under these conditions, the prediction capabilities of the SED model were evaluate.

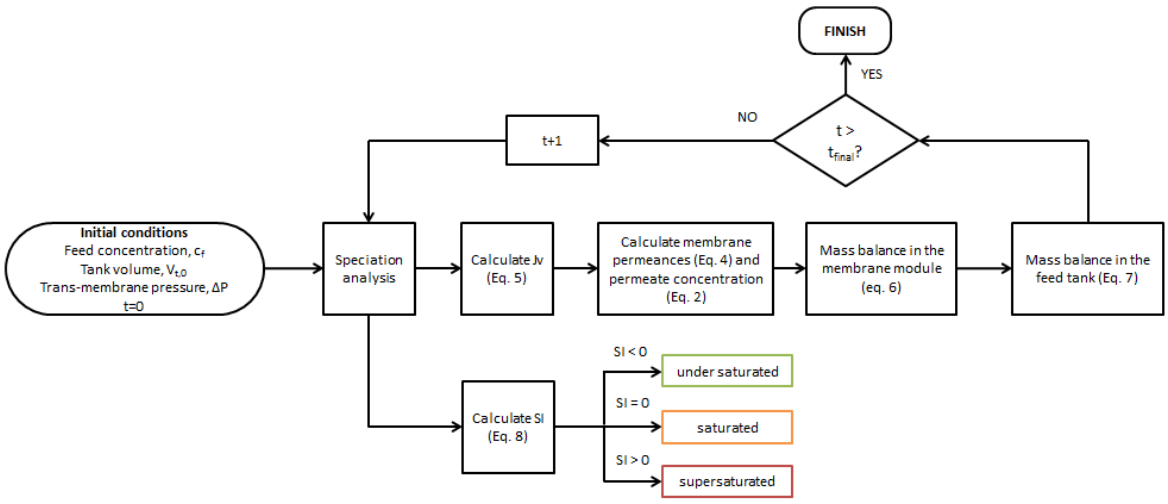

***Figure 3**. Scheme of the algorithm implemented on Matlab®*

3.1. Estimation of scaling events

Although the implemented SED model does the contemplate concentration polarisation phenomenon due to the mathematical complexity of the system, the saturation indexes (SI) of the potentially expected mineral phases were evaluated (**Eq. 8**).

$$SI = \log\left(\frac{IAP}{K_{so}}\right) \tag{8}$$

Where K_{so} is the solubility constant and IAP is the ionic activity product of a given potential mineral involved in a scaling event. For example, for the precipitation of jurbanite (i.e. $AlOHSO_4$ (s)) (**Eq. 9**):

$$AlSO_4OH(s) + H^+ \Leftrightarrow Al^{3+} + SO_4^{2-} + H_2O \tag{9.a}$$

$$SI = \log\left(\frac{IAP}{K_{so}}\right) = \log\left(\frac{[Al^{3+}][SO_4^{2-}][OH^-]}{K_{so}}\right) \tag{9.b}$$

A concentration polarisation factor up to 10 was considered in **Eq. 8** to determine if potential scaling events were expected. **Table 3** shows a summary of the main mineral phases expected to be formed in feed solutions.

***Table 3**. Solubility constants of potential minerals involved in a scaling event from Hydra/Medusa and PHREEQC code* [28,29]

Chemical reaction	$-\log K_{so}$
$AlOHSO_4(s) + H^+ \Leftrightarrow Al^{3+} + SO_4^{2-} + H_2O$	3.23
$Al(OH)_3(s) + 3H^+ \Leftrightarrow Al^{3+} + 3H_2O$	–10.3
$Al_4SO_4(OH)_{10}(s) + 10\ H^+ \Leftrightarrow 4Al^{3+} + \ SO_4^{2-} + 10H_2O$	–22.7
$CaSO_4(s) \Leftrightarrow Ca^{2+} + SO_4^{2-}$	4.6
$Fe_2(SO_4)_3(s) \Leftrightarrow 2Fe^{3+} + 3SO_4^{2-}$	–3.6
$Fe(OH)_3(s) + 3H^+ \Leftrightarrow Fe^{3+} + 3H_2O$	–4.9
$H_3OFe_3(SO_4)_2(OH)_6(s) + 5H^+ \Leftrightarrow 3Fe^{3+} + 2SO_4^{2-} + 7H_2O$	5.39
$FeOOH\ (s) + 3H^+ \Leftrightarrow Fe^{3+} + 2H_2O$	–1.0

4. Results and discussion

4.1. Concentration evolution in the feed tank and permeate with NF270 and Desal DL membranes: measured and predicted values

Three different synthetic AMWs containing different concentrations of Fe (0, 500 and 2125 mg/L) were filtered with the NF270 and Desal DL membranes. To address the influence of Fe(III) concentration on NF membranes performance, the dependence of the membrane permeances to each species (P_i) on solution composition was determined. The variation of acidity and Fe(III) affects the speciation and the membrane. Firstly, experimental data on P_i calculated in previous studies [20,30,31] and collected in **Supplementary information** were fitted to **Eq. 4** to determine their dependence on H^+ or Fe(III) concentrations. P_i in the experiments without Fe(III) was expressed as a function of H^+ concentration, while P_i in those containing Fe(III) was dependent on its concentration (pH was around 1.0 ± 0.1, and its effect on P_i was neglected). For example, **Figure 4** shows the fitting of NF270 membrane permeance values as a function of Fe(III) concentration. For Desal DL the fitting (not shown here) was as good as the one for NF270 permeances.

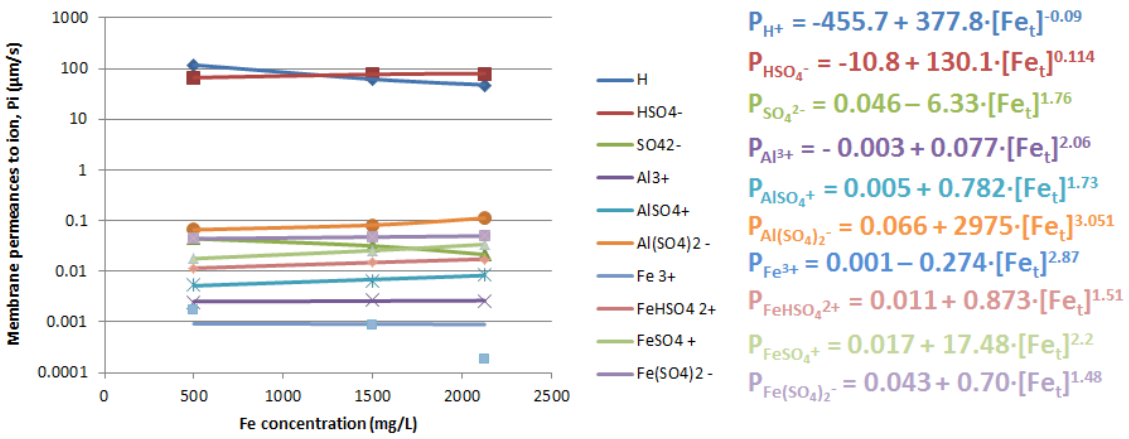

***Figure 4**. Fitting of NF270 permeance values (P_i) using Eq. 4 at different Fe concentrations. Lines represent the fitting (see equations at the right) while points are the membrane permeances calculated previously [30].*

4.1.1. Comparison of NF270 and Desal DL membranes for Fe(III) free acidic waters at pH 1.0

Figure 5 show the concentration evolution of the different components in the feed tank, and the permeate streams when filtrating a synthetic AMW without Fe(III) at pH 1.0 for the NF270 (**Figs. 5.a and 5.b**) and Desal DL (**Figs. 5.c and 5.d**) membranes.

Within the percentage of permeate recovery range studied (0-30%), both membranes rejected metals from the feed stream at percentages higher than 98% and yielded a permeate rich in sulphuric acid with a minor presence of metallic impurities. With the NF270 a permeate composed of 6 g/L of sulphuric acid and <5 mg/L of metallic impurities was obtained (see **Figure 5b**). With the Desal DL, a lower concentration of acid (around 5 g/L) was obtained, whereas the concentration of metallic impurities was also below 5 mg/L (see **Figure 5d**). This similar behaviour between these two membranes could be related to the similar composition of their active layers (both membranes are polyamide based). For both membranes, a ratio 1:1 between H^+ and S (mainly as HSO_4^-) in the permeate was observed for both membranes, which indicate that permeate is mainly composed of purified sulphuric acid. In terms of water flux across the membrane, NF270 has higher membrane permeability due to its lower polyamide layer thickness [26], exhibiting then greater permeate fluxes.

These results could be explained on the basis of the main exclusion phenomena taking place in NF membranes: the Donnan and dielectric exclusion. At pH 1.0, both NF270 and Desal DL membranes (whose IEPs are 2.5 4.0, respectively, and thus above the pH of the feed solution) are expected to be positively charged due to the partial and fully protonation of amine (R–

NH_3^+) and carboxylic groups (R–COOH), respectively. This fact originates electrostatic repulsions between the charged membrane surface and the metallic cations (e.g. Al^{3+}, Ca^{2+}, Cu^{2+}), which explains why these metallic cations are effectively rejected (Donnan exclusion) [35]. Conversely, the transport of anions (e.g. HSO_4^-) would be favoured because of the electrostatic attractions between them and the positively charged membrane surface. This phenomenon explained why both membranes permitted easy transport of sulphate (HSO_4^- /SO_4^{2-}) through them. Nevertheless, a stoichiometric number of cations must permeate to achieve electroneutrality conditions in the permeate side. Then, the H^+ was transported across the membrane because of its higher diffusivity, lower size and lower absolute charge among the cations [36].

On the other hand, the dielectric exclusion must also be considered to explain the transport of ions across the membrane. This phenomenon is caused by the interactions between the ions and bound electric charges induced in the membrane at the interface solution/membrane with different dielectric constants (i.e. polymeric matrix/bulk solution). The effect of dielectric exclusion is more pronounced than the one of Donnan exclusion because the ion-exclusion free energy is dependent on the square of the ion charge, while the Donnan exclusion is linear with it [37,38]. Dielectric exclusion explained why the transport of multivalent metallic impurities (i.e. Al^{3+}, Ca^{2+} and Cu^{2+}) was more impeded than that of H^+.

Donnan and dielectric exclusion phenomena accounted for; thus, the high selectivity of both membranes between sulphate and metal ions.

As in the previous studies [20,31], NF270 and Desal DL were able to reject the metal species effectively (e.g. >98%) while they allowed acid to permeate easily across the membrane (6 g/L and 5 g/L for NF270 and Desal DL, respectively). Moreover, as in the present case, NF270 was prone to transport better the acid than Desal DL.

In **Figure 5,** the predicted values (solid lines) were calculated by using the permeances to species from **Supplementary Information**. As can be seen, the calculated concentration values matched consistently the experimentally measured values in the feed tank for both membranes and both dominant and minor species in solution. With regard to the permeate stream, a good matching was generally obtained, although significant discrepancies were observed for H^+ and Al for the NF270 membrane. The discrepancy in acidity values could be due to the fact that their activity values (a_{H^+}) were determined with a pH glass electrode.

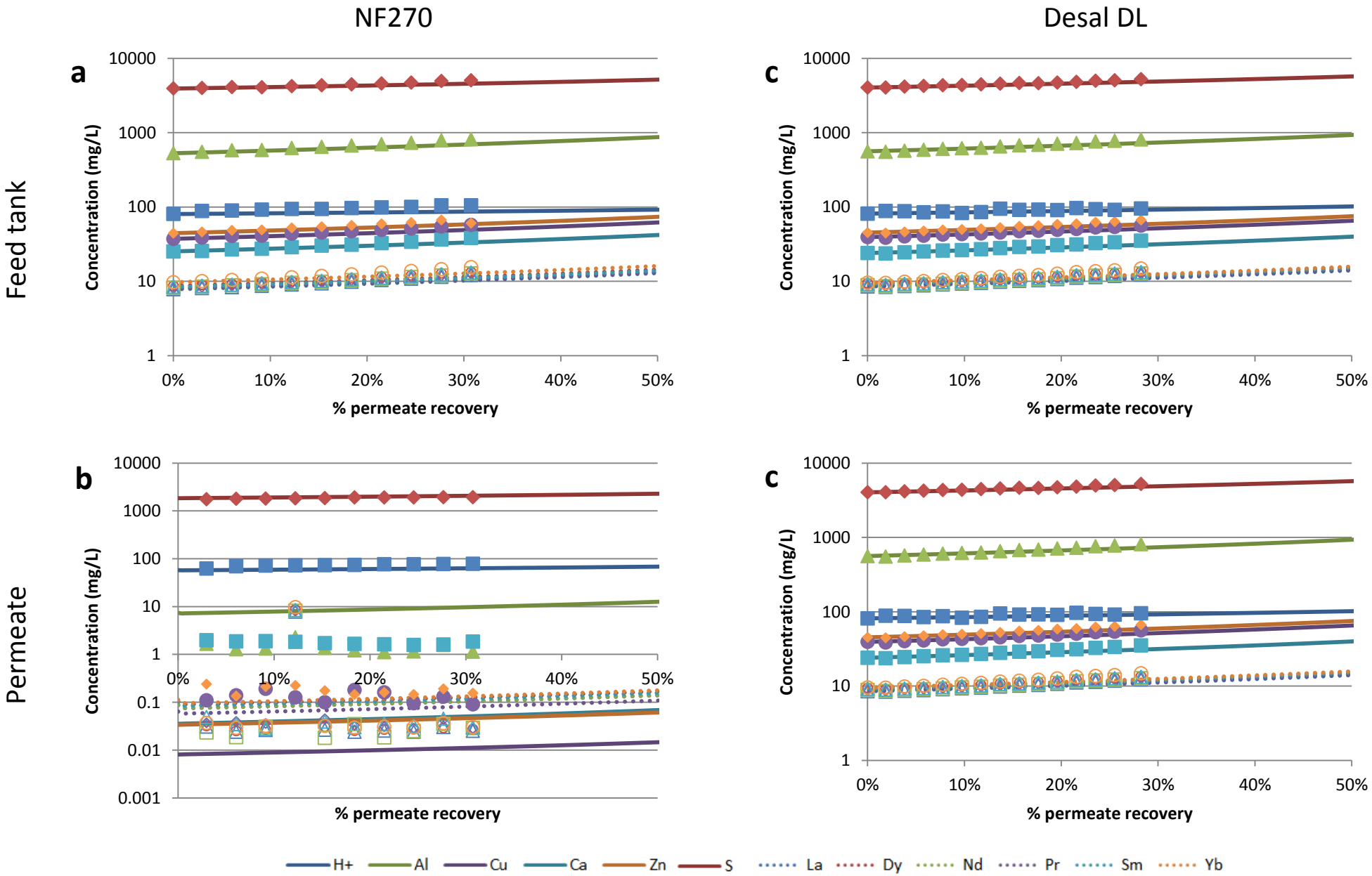

Figure 5. *Concentration evolution in (a, c) the feed tank and (b, d) the permeate for the NF270 and Desal DL with the solution without Fe(III) at pH 1.0. Points: experimental data; Lines: model prediction*

200

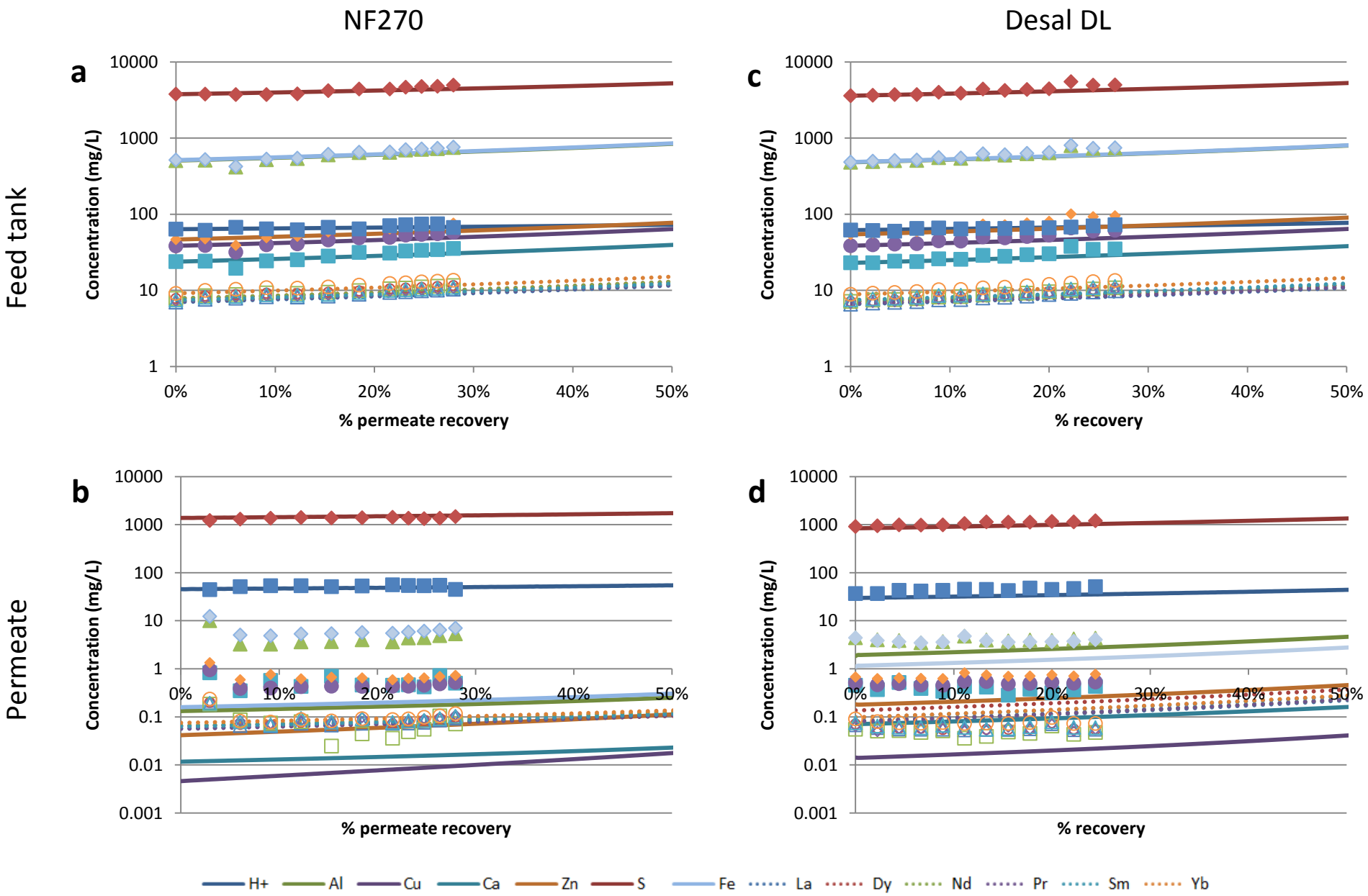

Figure 6. *Concentration evolution in (a, c) the feed tank and (b, d) the permeate for the NF270 and Desal DL with the solution with 500 mg/L Fe(III) at pH 1.0. Points: experimental data; Lines: model prediction*

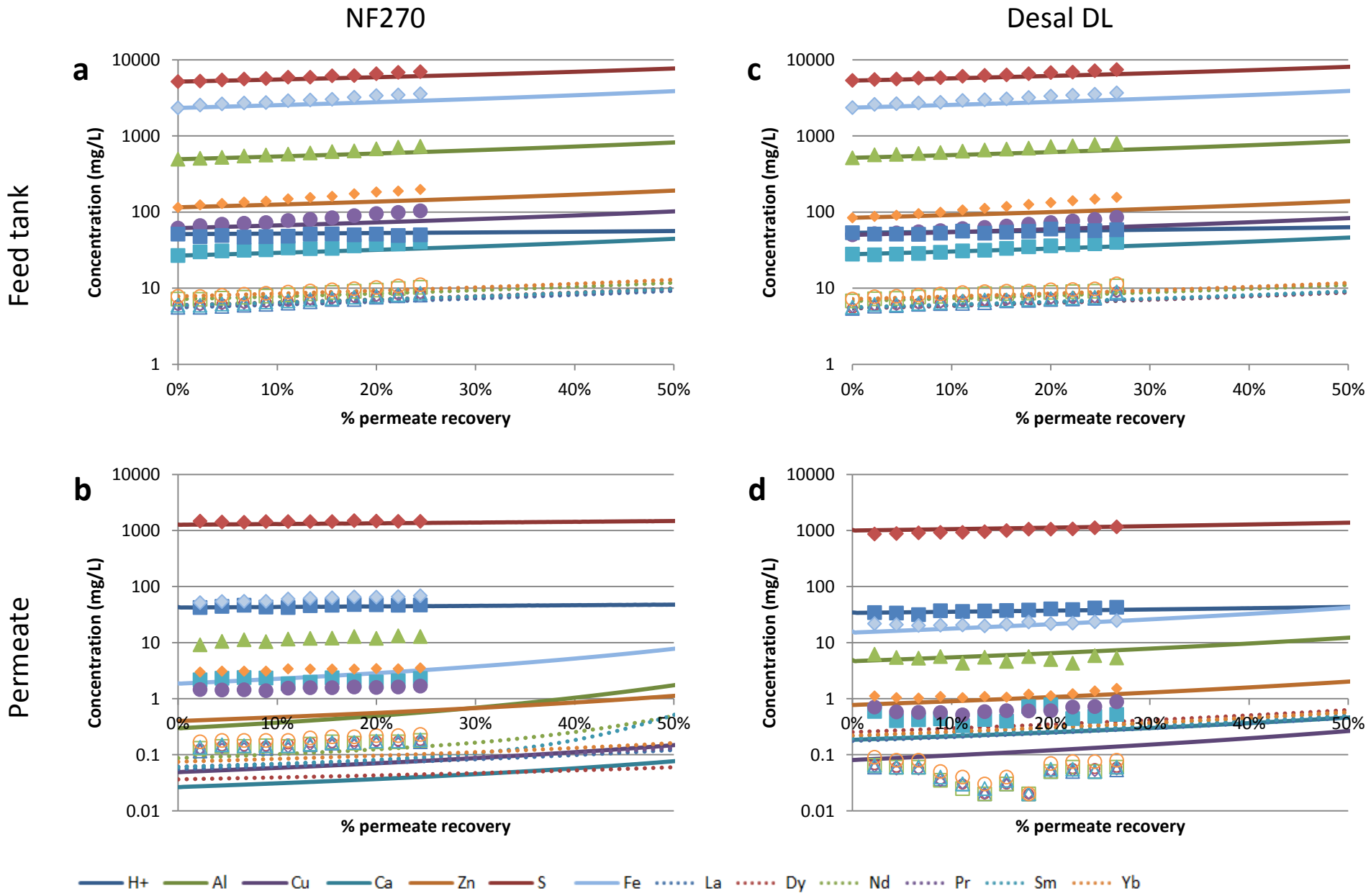

Figure 7. *Concentration evolution in (a, c) the feed tank and (b, d) the permeate for the NF270 and Desal DL with the solution with 2125 mg/L Fe(III) at pH 1.0. Points: experimental data; Lines: model prediction*

4.1.2. Comparison of NF270 and Desal DL membranes for acidic waters containing Fe(III) at pH 1.0: influence of the Fe(III) concentration

The influence of the Fe(III) concentration in the REE concentration and H_2SO_4 recovery factors was studied at two different levels 500 mg/L and 2125 mg/L. **Figure 6** shows the concentration profile evolution in the feed tank and the permeate adding 500 mg/L Fe(III) into the initial solution for NF270 (**Figs. 6.a and 6.b**) and Desal DL (**Figs. 6.c and 6.d**) membranes, respectively.

The presence of Fe(III) resulted in higher rejection percentages of sulphate across the membrane (67% for NF270 and 75% for Desal DL in front of 55 % and 69%). The reason of such increase lies on sulphate speciation. In fact, that the increase of Fe(III) concentration implied an increase of the positively-charged species $FeSO_4^+$, and $FeHSO_4^{2+}$ molar fractions, while a decrease of the negatively-charged species HSO_4^- and SO_4^{2-}(see **Figure 1**), resulting in enhanced overall transport of sulphate across the membrane due to Donnan and dielectric exclusion phenomena [37,38]. Moreover, the lower presence of HSO_4^- and SO_4^{2-} led also to a lower concentration of sulphate in the permeate (see **Figure 1**).

Fe(III) exhibited a similar behaviour than Al(III) (see **Figures 6.a and 6.c**). Both membranes effectively rejected Fe(III) (>98%), and its metallic impurities were below 7 mg/L for NF270 and 4 mg/L for Desal DL for each metal (see **Figures 6.b and 6.d**). Similarly to the previous case in the absence of Fe(III), NF270 provided a permeate stream richer in sulphuric acid than Desal DL (4.5 g/L and 3.6 g/L H_2SO_4, respectively), as it can be seen in **Figures 6.a and 6.c**. The higher concentration of HSO_4^- in solution favoured the passage of H^+ across the membrane.

The prediction capacity of the numerical code showed similar levels of accuracy than for the solution without Fe(III). The better predictions for NF270 than for Desal DL, despite their similar chemical properties from the point of view of the active layer, could be associated to the fact that the data set of membrane permeances for the former is more consolidated than that of the latter.

The membranes performance in filtrating acidic water with high Fe(III) contents (2125 mg/L) is shown in **Figure 7. Fig. 7.a and 7.c** represent the concentration profile in the feed tank while **Fig. 7.b and 7.c** show the concentration in the permeate, respectively.

The increase of Fe(III) up to 2125 mg/L led to even higher sulphate rejections (73% for NF270 and 84% for DL) (see **Figure 6 and 7**) for the same speciation reasons discussed above (see **Figure 1**). The main impurity in the permeate was Fe(III), reaching concentrations up to 68 mg/L for NF270 and 25 mg/L for Desal DL, while the other metals (i.e. Al, Ca, Cu, Zn and REEs)

remained below 10 mg/L for both membranes. Again NF270 yielded a richer stream in H_2SO_4 (4.2 g/L) than Desal DL (3.5 g/L), while both membranes achieved similar metal concentration factors. The prediction provided by the SED model described this increase of Fe(III) in the permeate up to 20-30 mg/L Fe(III) for Desal DL while predicted values for NF270 where much lower than those measured experimentally (up to 70 mg/L).

Both membranes (NF270 and Desal DL) have been studied previously in the literature for wastewaters treatments. Niewersch et al. [39] studied the selectivity of Desal DL for cations (Al, Fe, Cr, Cu) and phosphoric acid filtering sewage ash eluates. They obtained high passage of phosphorous while metals, such as Cu, were effectively rejected (>93%) at ΔP higher than 17 bar for permeate recoveries ranging from 17 to 90%. This selectivity was found to be dependent on effective pressure and composition of feed solution. Wadekar and Vidic [40] compared the performance of a TiO_2 ceramic (from Cerahelix) and a polymeric (NF270) NF membranes for treating mine drainage from a coal mine (pH 7.8). Ranging from permeate recoveries between 0 to 75% at ΔP of 35 bar, they found that NF270 was able to reject effectively (>96%) divalent and trivalent metal ions (e.g. Al(III), Ca(II) and Mg(II), among others), whereas Cl and As exhibited the lowest rejections (<10% and 20% for Cl and As, respectively). At the same time, NF270 was able to recover purified water as permeate at pH 7.8. The ceramic membrane showed metal rejections between 55 and 67%, with lower rejections of Cl and As (<20%).

It has been seen that the presence of Fe hinders the obtaining of purified H_2SO_4 in the NF permeate, making thus it necessary to remove all Fe(III) before the NF stage. This can be achieved by Fe(III) precipitation at pH ca. 4.0 with the addition of an alkali agent (e.g. caustic soda, ammonia, soda ash or hydrated lime). However, because REEs can easily precipitate with the Al-solid basaluminite ($Al_4SO_4(OH)_{10}\cdot 5H_2O$) after the NF stage at pH 4.0 [10], Fe(III) precipitation must be accomplished at pH<4.0 (e.g. 3.5-3.7). Once Fe is precipitated, it would be recommended to decrease the pH down to 1.0 using, e.g. the permeate rich in H_2SO_4 to ensure that NF membranes are positively charged and that they effectively concentrate REE in the feed tank.

4.2. Extending the limits of REEs recovery as a function of the operation parameters: prediction of metal concentration and acid recovery capacities with NF270 and Desal DL membranes

A parametric study was carried out by evaluating the effect of ΔP and permeate recovery ratios on the metal rejection (and thus concentration factors) and sulphuric acid recovery in

the permeate. Four different values of ΔP were evaluated: 10, 20, 40 and 60 bar at permeate recovery ratios (%) ranging from 0 to 80%.

Table 4 collects the concentration factor of the elements in the feed solution (i.e. metals, REEs and sulphuric acid) at the ΔP mentioned above, respectively.

Table 4*. Prediction of concentration factors in the feed tank for NF270 and Desal DL membranes at ΔP of 10, 20, 40 and 60 bar as a function of permeate recovery ratio*

Element	% of water recovery	NF270				Desal DL			
		10 bar	20 bar	40 bar	60 bar	10 bar	20 bar	40 bar	60 bar
Al	20	1.15	1.19	1.19	1.20	1.14	1.17	1.17	1.18
	40	1.36	1.47	1.47	1.47	1.32	1.40	1.41	1.43
	60	1.65	1.91	1.91	1.90	1.57	1.76	1.79	1.82
	80	2.12	2.75	2.77	2.78	1.93	2.35	2.42	2.54
Cu	20	1.15	1.19	1.19	1.20	1.14	1.17	1.17	1.18
	40	1.36	1.47	1.47	1.47	1.32	1.41	1.41	1.43
	60	1.65	1.91	1.91	1.90	1.57	1.76	1.79	1.83
	80	2.12	2.75	2.77	2.78	1.95	2.36	2.43	2.55
S	20	1.08	1.12	1.14	1.16	1.09	1.13	1.15	1.16
	40	1.18	1.28	1.34	1.37	1.20	1.30	1.35	1.39
	60	1.32	1.53	1.63	1.69	1.34	1.54	1.65	1.72
	80	1.54	1.97	2.17	2.30	1.54	1.93	2.14	2.31
Ca	20	1.15	1.19	1.19	1.20	1.14	1.17	1.17	1.18
	40	1.36	1.47	1.47	1.47	1.32	1.40	1.41	1.43
	60	1.65	1.91	1.91	1.90	1.57	1.76	1.79	1.82
	80	2.12	2.75	2.77	2.78	1.94	2.36	2.43	2.55
Zn	20	1.15	1.19	1.19	1.20	1.14	1.17	1.17	1.18
	40	1.36	1.47	1.47	1.47	1.32	1.40	1.41	1.43
	60	1.65	1.91	1.91	1.90	1.57	1.76	1.79	1.82
	80	2.12	2.75	2.76	2.77	1.93	2.35	2.43	2.55
Fe	20	1.15	1.19	1.19	1.20	1.14	1.17	1.17	1.18
	40	1.36	1.47	1.47	1.47	1.32	1.40	1.41	1.43
	60	1.65	1.91	1.91	1.90	1.57	1.76	1.79	1.82
	80	2.12	2.75	2.77	2.78	1.94	2.36	2.43	2.55
REE	20	1.15	1.19	1.19	1.20	1.13	1.17	1.17	1.18
	40	1.35	1.47	1.47	1.47	1.31	1.40	1.41	1.43
	60	1.64	1.90	1.91	1.90	1.55	1.75	1.78	1.82
	80	2.09	2.73	2.75	2.77	1.90	2.33	2.41	2.54
H^+	20	1.01	1.05	1.08	1.09	1.04	1.07	1.10	1.12
	40	1.03	1.11	1.19	1.21	1.08	1.16	1.23	1.27
	60	1.04	1.18	1.34	1.38	1.13	1.26	1.41	1.48
	80	1.04	1.29	1.57	1.68	1.18	1.40	1.68	1.82

The transport of double and triple-charged metallic cations through the studied membranes was effectively hindered by Donnan and dielectric exclusion phenomena, leading to higher concentration factors when %permeate recovery increased. As mentioned before, the transport of HSO_4^- is favoured by the membrane charge at the low working pH (1.0), which forces H^+ to be also transported to achieve electroneutrality conditions in the permeate. As a result, a permeate rich in sulphuric acid could be obtained.

Regarding the effect of ΔP on concentration factors (see **Table 4**), lower concentration factors were obtained at the lowest value of ΔP (10 bar). The only difference among operating at ΔP higher than 20 bar is the higher value of trans-membrane flux. When both membranes are compared, NF270 exhibits the highest metal rejections, leading to higher concentration factors for the different evaluated ΔP and %permeate recovery ratios than Desal DL. Rejections for H^+ were around a 20% lower for Desal DL than for NF270, which can limit the options to recover sulphuric acid in the permeate. When trans-membrane fluxes are compared, NF270 exhibited the highest ones because of its higher water permeability.

For all the conditions evaluated, once the equilibrium and speciation analysis was completed, the SI of the potential minerals involved in scaling events (collected in **Table 3**) were calculated. In the evaluated range, and also assuming concentration polarisation factors, as it is used in the software design tools of reverse osmosis applications (e.g. Wave (Dow-Chem), Hydranautics, Wind-Flow (Suez)), no saturation conditions were achieved (data not shown). However, SI values for the mineral phases of jurbanite ($AlOHSO_4$) and gypsum ($CaSO_4{\cdot}2H_2O$) were the closest to zero, indicating that their precipitation on the membrane is plausible.

Figure 8 collects the sulphate and H^+ rejections and permeate flux as a function of %permeate recovery ratios to compare the performance of both membranes. All metal rejections were higher than 99% for NF270 and higher than 98% for Desal DL, respectively. Because they barely varied, their rejection figures were excluded from the present manuscript.

NF270 can be a suitable membrane for acid recovery, especially working at ΔP of 10 bar, because the amount of recovered acid is maximized (**Figure 8**), whereas there were no significant differences in the metal concentration factors. At this pressure, H^+ rejection would be below 10%, and it could decrease to near zero values at 80% of permeate recovery. However, some amount of metals can be transported across the membrane; therefore lower concentration factors would be obtained.

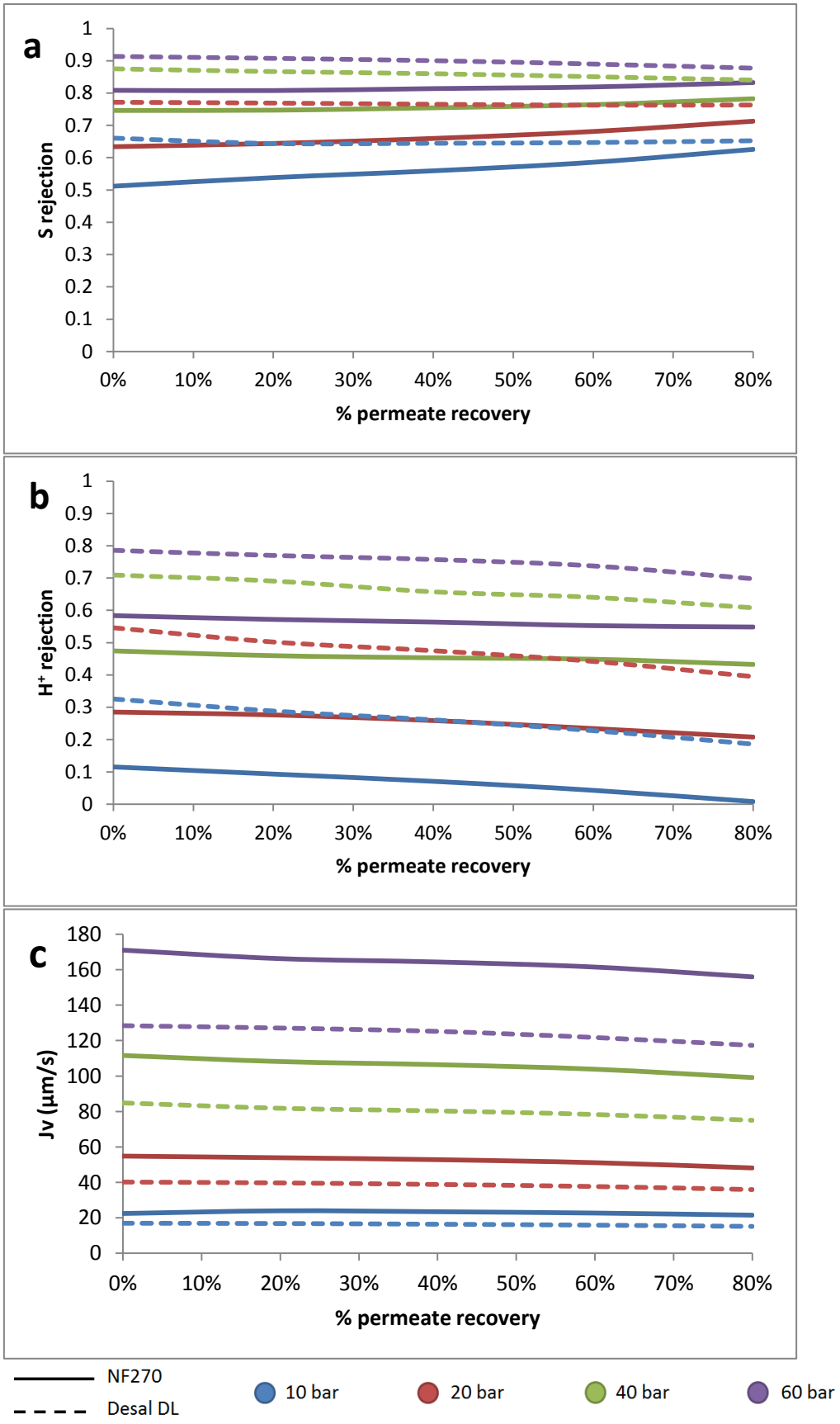

***Figure 8**. Prediction of a) S; b) H^+ rejections and; c) trans-membrane flux (J_v) for NF270 and Desal DL membranes at 10, 20, 40 and 60 bar as a function of permeate recovery ratio.*

5. Conclusions

The lack of NF prediction tools for the design and integration of NF technology in hydrometallurgical applications was addressed. The developed algorithm integrating the SED model and reactive transport has proven its applicability to determine the REE recovery factors and the sulphuric acid recovery at different % permeate recovery ratios. The recovered sulphuric can be beneficial as it can be reused on the pre-processing stages and additionally simplifies the cost of alkalis (CaO, $CaCO_3$) and reduces the presence of Ca(II) levels as interfering element on the post-processing stages of the concentrated REE. Additionally, the prediction of the acidity and total sulphate concentration are critical factors to determine the potential scaling events.

Polyamide-based NF membranes have shown their potential for treating AMWs since they allow the recovery of sulphuric acid as permeate and concentrate the metals and REEs in the feed tank solution. Both membranes (NF270 and Desal DL) exhibited a similar behaviour due to their similar active layer, but the first one is preferred since it presents higher water permeability. Results showed that the electric fields govern separation originated between the membrane and dissolved species (Donnan and dielectric exclusion). Therefore, metallic ions were effectively rejected by the membrane (>98%) whereas sulphuric acid was transported (H^+ rejections below 30%).

The effect of solution composition on membrane separation was considered within the membrane permeances, and taken into account in the model. A set of permeance functions dependent on the total, proton and sulphate concentration were developed. The mathematical model presented here can be used to predict the behaviour of any effluent in batch mode by knowing how the membrane permeances depend on solution composition.

Acknowledgements

This research was supported by the Waste2Product project (CTM2014-57302-R) and by the R2MIT project (CTM2017-85346-R) financed by the Spanish Ministry of Economy and Competitiveness (MINECO) and the Catalan Government (2017-SGR-312), Spain. MINECO supported the work of Julio López and Xanel Vecino within the scope of the grant (BES-2015-075051) and the Juan de la Cierva contract (IJCI-2016-27445), respectively. We also want to thank the contribution of Dow Chemical for the supply of the membranes; to T. Susín for his help during the modelling stage; to L. Vilaplana for her help during the experimental work and to A. Espriu-Gascón and A. Díaz for the ICP analysis.

Nomenclature

a_0, a_1, a_2	Fitting parameters in Eq. 4 (-)
c	Concentration (mol/L)
IAP	Ionic activity product
j_i	Species flux across the membrane (mol/L·µm/s)
J_v	Solvent flux across the membrane (µm/s)
$K_{T,I}$	Chemical equilibrium constant
K_{so}	Solubility constant of the mineral
k_w	Hydraulic permeability of the membrane (µm/(s·bar))
P_i	Membrane permeance (µm/s)
Q	Flow (L/min)
SI	Saturation index (-)
V	Tank volume (L)
x	Dimensionless position in the membrane (-)
X	H^+ or Fe(III) concentration in the tank in Eq. 4 (mol/L)
z	Valence charge (-)
ΔP	Trans-membrane pressure (bar)
$\Delta\pi$	Difference of osmotic pressure across the membrane (bar)
γ	Activity coefficient (-)
φ	Dimensionless virtual electrostatic potential in the membrane (-)

Subscripts

f	Feed
i	Species i
p	Permeate
r	Retentate
t	Time

Supplementary information. Membrane permeances to species

Table 1. NF270 membrane permeances to species [20,30]

	NF270						
	pH				Fe(III) concentration at pH 1.0 (mg/L)		
	1.0	1.5	1.9	2.5	500	1500	2125
H^+	58.12	133.60	37.31	57.29	117.65	63.08	46.86
HSO_4^-	114.35	84.15	81.19	106.16	66.22	76.80	79.90
SO_4^{2-}	0.20	0.23	0.18	0.22	0.04	0.03	0.02
Al^{3+}	0.02	0.02	0.04	0.01	0.01	0.01	0.01
$AlSO_4^+$	0.01	1.92	0.27	3.60	0.01	0.01	0.01
$Al(SO_4)_2^-$	0.05	5.05	0.85	8.56	0.07	0.08	0.11
Ca^{2+}	0.01	0.01	0.03	0.06	0.01	0.01	0.01
Zn^{2+}	0.01	0.14	0.08	0.01	0.01	0.07	0.07
Cu^{2+}	0.01				0.01	0.01	0.01
$CaHSO_4^+$	0.24	2.95	2.46	0.53	0.03	0.03	0.03
$CaSO_4$	0.13	9.57	1.19	13.82	0.07	0.08	0.09
$CuSO_4$	0.01				0.01	0.06	0.07
$ZnSO_4$	0.12	0.14	0.08	0.01	0.14	0.23	0.24
La^{3+}	0.01				0.01	0.01	0.01
Pr^{3+}	0.01				0.01	0.01	0.01
Nd^{3+}	0.01				0.01	0.01	0.01
Sm^{3+}	0.01				0.01	0.01	0.01
Dy^{3+}	0.01				0.01	0.01	0.01
Yb^{3+}	0.01				0.01	0.01	0.01
$LaSO_4^+$	0.10				0.09	0.06	0.10
$PrSO_4^+$	0.07				0.08	0.08	0.07
$NdSO_4^+$	0.09				0.09	0.09	0.10
$SmSO_4^+$	0.10				0.10	0.06	0.10
$DySO_4^+$	0.10				0.08	0.05	0.05
$YbSO_4^+$	0.10				0.10	0.06	0.10
$La(SO_4)_2^-$	0.16				0.11	0.03	0.10
$Pr(SO_4)_2^-$	0.18				0.15	0.15	0.11
$Nd(SO_4)_2^-$	0.17				0.12	0.12	0.10
$Sm(SO_4)_2^-$	0.16				0.08	0.03	0.09
$Dy(SO_4)_2^-$	0.16				0.13	0.03	0.03
$Yb(SO_4)_2^-$	0.16				0.10	0.03	0.10
Fe^{3+}					0.01	0.01	0.01
$FeHSO_4^{2+}$					0.01	0.02	0.02
$FeSO_4^+$					0.02	0.03	0.03
$Fe(SO_4)_2^-$					0.04	0.05	0.05

210

Table 2. Desal DL membrane permeances to species [30,31]

	Desal DL				
	pH		Fe(III) concentration at pH 1.0 (mg/L)		
	1.0	1.5	500	1500	2125
H^+	46.67	83.74	83.74	46.67	23.51
HSO_4^-	12.82	12.76	16.11	26.59	30.44
SO_4^{2-}	0.02	0.03	0.03	0.02	0.01
Al^{3+}	0.01	0.02	0.02	0.01	0.01
$AlSO_4^+$	0.32	0.08	0.08	0.32	0.47
$Al(SO_4)_2^-$	0.10	0.03	0.03	0.10	0.14
Ca^{2+}	0.01	0.01	0.01	0.01	0.02
Zn^{2+}	0.04	0.03	0.08	0.24	0.36
Cu^{2+}	0.01	0.01	0.01	0.02	0.02
$CaHSO_4^+$	0.06	0.05	0.01	0.01	0.01
$CaSO_4$	0.13	0.24	0.33	1.31	1.60
$CuSO_4$	0.23	0.28	0.03	0.15	0.27
$ZnSO_4$	0.08	0.22	0.26	1.18	1.69
La^{3+}	0.01	0.01	0.01	0.01	0.01
Pr^{3+}	0.01	0.01	0.01	0.01	0.01
Nd^{3+}	0.01	0.01	0.01	0.01	0.01
Sm^{3+}	0.01	0.01	0.01	0.01	0.01
Dy^{3+}	0.01	0.01	0.01	0.01	0.01
Yb^{3+}	0.01	0.01	0.01	0.01	0.01
$LaSO_4^+$	0.01	0.01	0.08	0.28	0.27
$PrSO_4^+$	0.01	0.01	0.08	0.27	0.28
$NdSO_4^+$	0.01	0.01	0.08	0.27	0.29
$SmSO_4^+$	0.01	0.01	0.09	0.27	0.28
$DySO_4^+$	0.02	0.01	0.13	0.27	0.29
$YbSO_4^+$	0.01	0.01	0.08	0.26	0.29
$La(SO_4)_2^-$	0.02	0.53	0.10	0.12	0.12
$Pr(SO_4)_2^-$	0.02	1.29	0.10	0.12	0.12
$Nd(SO_4)_2^-$	0.03	0.75	0.10	0.12	0.12
$Sm(SO_4)_2^-$	0.02	0.50	0.10	0.12	0.12
$Dy(SO_4)_2^-$	0.02	1.36	0.10	0.10	0.11
$Yb(SO_4)_2^-$	0.02	0.57	0.10	0.11	0.12
Fe^{3+}			0.02	0.01	0.01
$FeHSO_4^{2+}$			0.04	0.05	0.05
$FeSO_4^+$			0.05	0.20	0.29
$Fe(SO_4)_2^-$			0.05	0.05	0.05

References

[1] European Commission, Report on Critical Raw Materials and the Circular Economy PART 3/3, 2018. doi:10.1097/PPO.0b013e3181b9c5d5.

[2] S. Wu, L. Wang, L. Zhao, P. Zhang, H. El-Shall, B. Moudgil, X. Huang, L. Zhang, Recovery of rare earth elements from phosphate rock by hydrometallurgical processes – A critical review, Chem. Eng. J. 335 (2018) 774–800. doi:10.1016/j.cej.2017.10.143.

[3] S.M. MacLennan, Rare Earth Elements in sedimentary rocks: Influence of provenance and sedimentary processes., B.R. Lipin G.A. McKay "Geochemistry Mineral. Rare Earth Elem. Rev. Mineral. (1989) 169–200.

[4] F. Xie, T. An, D. Dreisinger, F. Doyle, A critical review on solvent extraction of rare earths from aqueous solutions, Miner. Eng. 56 (2014) 10–28. doi:10.1016/j.mineng.2013.10.021.

[5] R.D. Abreu, C.A. Morais, Study on Separation of Heavy Rare Earth Elements by Solvent Extraction with Organophosphorus Acids and Amine Reagents, Miner. Eng. 61 (2014) 82–87. doi:10.1016/j.mineng.2014.03.015.

[6] J. Kulczycka, Z. Kowalski, M. Smol, H. Wirth, Evaluation of the recovery of Rare Earth Elements (REE) from phosphogypsum waste - Case study of the WIZÓW Chemical Plant (Poland), J. Clean. Prod. 113 (2016) 345–354. doi:10.1016/j.jclepro.2015.11.039.

[7] L. Wang, Y. Yu, X. Huang, Z. Long, D. Cui, Toward greener comprehensive utilization of bastnaesite: Simultaneous recovery of cerium, fluorine, and thorium from bastnaesite leach liquor using HEH(EHP), Chem. Eng. J. 215–216 (2013) 162–167. doi:10.1016/j.cej.2012.09.126.

[8] G.S. Simate, S. Ndlovu, Acid mine drainage: Challenges and opportunities, J. Environ. Chem. Eng. 2 (2014) 1785–1803. doi:10.1016/j.jece.2014.07.021.

[9] C.W. Noack, D.A. Dzombak, A.K. Karamalidis, Rare Earth Element Distributions and Trends in Natural Waters with a Focus on Groundwater, Environ. Sci. Technol. 48 (2014) 4317–4326. doi:10.1021/es4053895.

[10] C. Ayora, F. Macías, E. Torres, A. Lozano, S. Carrero, J.M. Nieto, R. Pérez-López, A. Fernández-Martínez, H. Castillo-Michel, Recovery of Rare Earth Elements and Yttrium from Passive-Remediation Systems of Acid Mine Drainage, Environ. Sci. Technol. 50 (2016) 8255–8262. doi:10.1021/acs.est.6b02084.

[11] B.C. Ricci, C.D. Ferreira, A.O. Aguiar, M.C.S. Amaral, Integration of nanofiltration and reverse osmosis for metal separation and sulfuric acid recovery from gold mining effluent, Sep. Purif. Technol. 154 (2015) 11–21. doi:10.1016/j.seppur.2015.08.040.

[12] C.-M. Zhong, Z.-L. Xu, X.-H. Fang, L. Cheng, Treatment of Acid Mine Drainage (AMD) by Ultra-Low-Pressure Reverse Osmosis and Nanofiltration, Environ. Eng. Sci. 24 (2007) 1297–1306. doi:10.1089/ees.2006.0245.

[13] M. Reig, X. Vecino, C. Valderrama, O. Gibert, J.L. Cortina, Application of selectrodialysis for the removal of As from metallurgical process waters: Recovery of Cu and Zn, Sep. Purif. Technol. 195 (2018) 404–412. doi:10.1016/j.seppur.2017.12.040.

[14] S. You, J. Lu, C.Y. Tang, X. Wang, Rejection of heavy metals in acidic wastewater by a novel thin-film inorganic forward osmosis membrane, Chem. Eng. J. 320 (2017) 532–538. doi:10.1016/j.cej.2017.03.064.

[15] T.J.K. Visser, S.J. Modise, H.M. Krieg, K. Keizer, The removal of acid sulphate pollution by nanofiltration, Desalination. 140 (2001) 79–86.

[16] M. Mullett, R. Fornarelli, D. Ralph, Nanofiltration of mine water: impact of feed pH and membrane charge on resource recovery and water discharge, Membranes (Basel). 4 (2014) 163–180. doi:10.3390/membranes4020163.

[17] B. Kose Mutlu, B. Cantoni, A. Turolla, M. Antonelli, H. Hsu-Kim, M.R. Wiesner, Application of nanofiltration for Rare Earth Elements recovery from coal fly ash leachate: Performance and cost evaluation, Chem. Eng. J. 349 (2018) 309–317. doi:10.1016/j.cej.2018.05.080.

[18] A. Yaroshchuk, X. Martínez-Lladó, L. Llenas, M. Rovira, J. de Pablo, Solution-diffusion-film model for the description of pressure-driven trans-membrane transfer of electrolyte mixtures: One dominant salt and trace ions, J. Memb. Sci. 368 (2011) 192–201. doi:10.1016/j.memsci.2010.11.037.

[19] J. López, M. Reig, A. Yaroshchuk, E. Licon, O. Gibert, J.L. Cortina, Experimental and theoretical study of nanofiltration of weak electrolytes: SO42–/HSO4–/H+system, J. Memb. Sci. 550 (2018) 389–398. doi:10.1016/j.memsci.2018.01.002.

[20] J. López, M. Reig, O. Gibert, E. Torres, C. Ayora, J.L. Cortina, Application of nanofiltration for acidic waters containing rare earth elements: Influence of transition elements, acidity and membrane stability, Desalination. 430 (2018) 33–44. doi:10.1016/j.desal.2017.12.033.

[21] C. Niewersch, A.L.B. Bloch, S. Yüce, T. Melin, M. Wessling, Nanofiltration for the recovery of phosphorus — Development of a mass transport model, Desalination. 346 (2014) 70–78. doi:10.1016/j.desal.2014.05.011.

[22] M. Kallioinen, T. Sainio, J. Lahti, A. Pihlajamäki, H. Koivikko, J. Mattila, M. Mänttäri, Effect of extended exposure to alkaline cleaning chemicals on performance of polyamide (PA) nanofiltration membranes, Sep. Purif. Technol. 158 (2016) 115–123. doi:10.1016/j.seppur.2015.12.015.

[23] C. Dow Chemical, FILMTEC NF270 Nanofiltration Elements for Commercial Systems, (n.d.).

[24] Y. Yu, C. Zhao, L. Yu, P. Li, T. Wang, Y. Xu, Removal of perfluorooctane sulfonates from water by a hybrid coagulation-nanofiltration process, Chem. Eng. J. 289 (2016) 7–16. doi:10.1016/j.cej.2015.12.048.

[25] H. Saidani, N. Ben Amar, J. Palmeri, A. Deratani, Interplay between the transport of solutes across nanofiltration membranes and the thermal properties of the thin active layer, Langmuir. 26 (2010) 2574–2583. doi:10.1021/la9028723.

[26] C.Y. Tang, Y.N. Kwon, J.O. Leckie, Effect of membrane chemistry and coating layer on physiochemical properties of thin film composite polyamide RO and NF membranes. I. FTIR and XPS characterization of polyamide and coating layer chemistry, Desalination. 242 (2009) 149–167. doi:10.1016/j.desal.2008.04.003.

[27] S.W. Technologies, DL series industrial high flow nanofiltration elements, (2017). https://www.suezwatertechnologies.com/kcpguest/documents/Fact Sheets_Cust/Americas/English/FS1248EN.pdf.

[28] I. Puigdomenech, Chemical equilibirum software Hydra/Medusa, (2001). https://sites.google.com/site/chemdiagr/home.

[29] U.S. Geological Survey, PHREEQC Version 3, (2017). https://www.usgs.gov/software/phreeqc-version-3.

[30] J. López, M. Reig, O. Gibert, J.L. Cortina, Recovery of sulphuric acid and added value metals (Zn, Cu and rare earths) from acidic mine waters using nanofiltration membranes, Sep. Purif. Technol. 212 (2019) 180–190. doi:10.1016/j.seppur.2018.11.022.

[31] J. López, M. Reig, O. Gibert, J.L. Cortina, Integration of nanofiltration membranes in recovery options of rare earth elements from acidic mine waters, J. Clean. Prod. 210

(2019) 1249–1260. doi:10.1016/j.jclepro.2018.11.096.

[32] C. Niewersch, Nanofiltration for phosphorus recycling from sewage sludge, Verlagshaus Mainz GmbH, 2013.

[33] S. Bason, Y. Kaufman, V. Freger, Analysis of Ion Transport in Nanofiltration Using Phenomenological Coefficients and Structural Characteristics, J. Phys. Chem B. 114 (2010) 3510–3517.

[34] A.E. Yaroshchuk, Rejection of single salts versus transmembrane volume flow in RO/NF: thermodynamic properties, model of constant coefficients, and its modification, J. Memb. Sci. 198 (2002) 285–297. doi:10.1016/S0376-7388(01)00668-8.

[35] A.E. Yaroshchuk, Non-steric mechanisms of nanofiltration : superposition of Donnan and dielectric exclusion, Sep. Purif. Technol. 22–23 (2001) 143–158.

[36] R.A. Robinson, R.H. Stokes, Electrolyte Solutions, Second Rev, 2002.

[37] S.H. Kim, S.-Y. Kwak, T. Suzuki, Evidence to demonstrate the flux-enhancement mechanism in morphology-controlled thin-film-composite (TFC)membrane, Environ. Sci. Technol. 39 (2005) 1764–1770.

[38] A.E. Yaroshchuk, Dielectric exclusion of ions from membranes, Adv. Colloid Interface Sci. 85 (2000) 193–230. doi:10.1016/S0001-8686(99)00021-4.

[39] C. Niewersch, K. Meier, T. Wintgens, T. Melin, Selectivity of polyamide nanofiltration membranes for cations and phosphoric acid, Desalination. 250 (2010) 1021–1024. doi:10.1016/j.desal.2009.09.097.

[40] S.S. Wadekar, R.D. Vidic, Comparison of ceramic and polymeric nanofiltration membranes for treatment of abandoned coal mine drainage, Desalination. 440 (2018) 135–145. doi:10.1016/j.desal.2018.01.008.

ANNEX 2

Publication 9

"*Integration of diffusion dialysis for sulphuric acid recovery from copper metallurgical process streams: the arsenic challenge***"**

Manuscript Details

Manuscript number	SEPPUR_2019_3785
Title	Integration of diffusion dialysis for sulphuric acid recovery from copper metallurgical process streams: the arsenic challenge
Article type	Full Length Article

Abstract

Off-gases treatments in copper metallurgical plants to remove SO2(g) generate an acid solution formed by sulphuric acid, non-metals (arsenic) and transition metals (zinc, iron, copper). In order to reduce the sludge generated due to lime addition and to enhance the circularity, the recovery of sulphuric acid by diffusion dialysis technology is proposed. A diffusion dialysis stack incorporating an Anion Exchange Membrane favours the transport of hydrogen sulphate (HSO4-), while metals are effectively rejected. In the present study, an effluent from a copper smelter containing sulphuric acid (220 g/L), arsenic (3.4 g/L) and zinc (0.5 g/L) as main components was treated with a commercial Anion Exchange Membrane (Neosepta-AFX) to evaluate the sulphuric acid recovery ratio. The effect of operational variables, such as diffusate and dialysate flow rates, flow rate ratio and arsenic speciation (As(V) or As(III)), was studied. Neosepta-AFX was able to recover 67±2 % of sulphuric acid (146±12 g/L) and to reject effectively the metals (>85%), but it contained an impurity of 1.26 g/L arsenic because of its presence as neutral species (arsenic acid, H3AsO4/arsenous acid, H3AsO3). For this reason, the integration of a solvent extraction step using Cyanex 923® is proposed to remove arsenic before being treated with DD.

Keywords	Diffusion dialysis; Neosepta-AFX; sulphuric acid; arsenic speciation; acid recovery; waste minimisation
Manuscript category	Ion exchange

Corresponding Author	Julio López
Corresponding Author's Institution	Universitat Politècnica de Catalunya
Order of Authors	Julio López, Rodrigo R. de Oliveira, Mònica Reig, Xanel Vecino, Oriol Gibert, Anna de Juan, Jose-Luis Cortina
Suggested reviewers	Andrea Cipollina, Gerardo Cifuentes, Marek Bryjak

Submission Files Included in this PDF

File Name [File Type]

Cover letter.docx [Cover Letter]

Highlights.docx [Highlights]

Graphical abstract.docx [Graphical Abstract]

Manuscript.docx [Manuscript File]

Figures.docx [Figure]

Tables.docx [Table]

To view all the submission files, including those not included in the PDF, click on the manuscript title on your EVISE Homepage, then click 'Download zip file'.

Highlights

- Generation of an acidic stream in the off-gases treatment from copper smelters
- Presence of arsenic and metals in the acidic streams
- Treatment with diffusion dialysis for acid recovery
- Limitations in acid recovery due to the presence of arsenic as neutral species

Graphical abstract

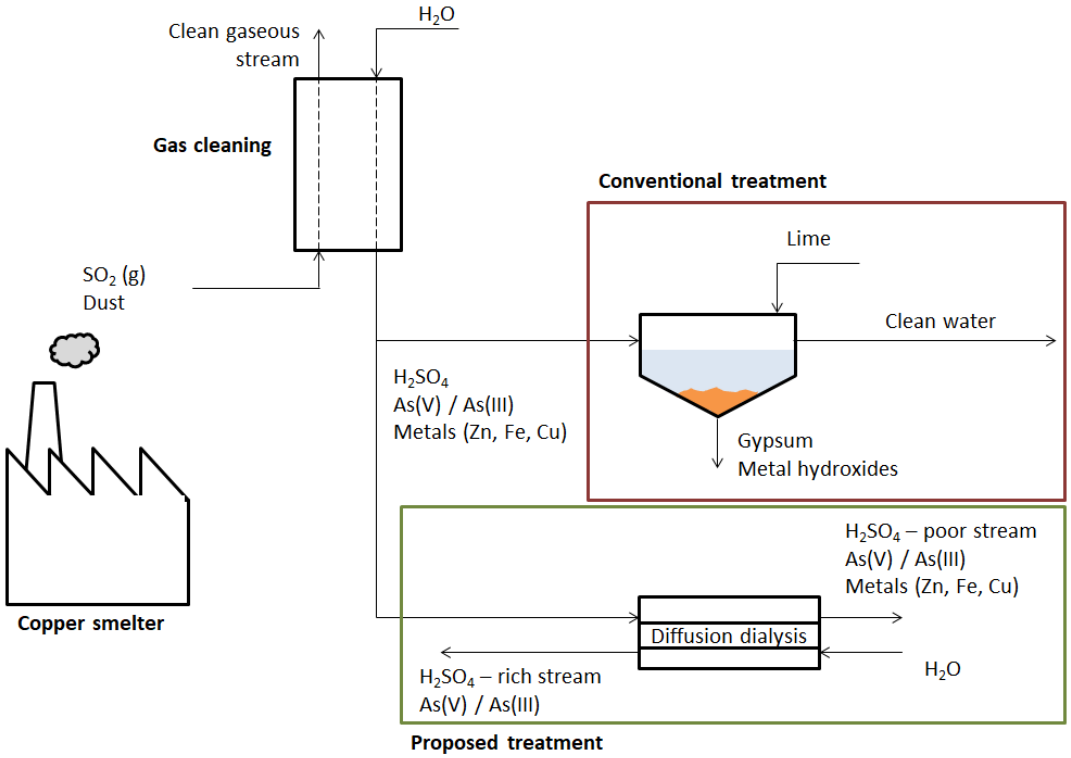

Integration of diffusion dialysis for sulphuric acid recovery from copper metallurgical process streams: the arsenic challenge

J. López [a*], R.R. de Oliveira [b], M. Reig [a], X. Vecino [a], O. Gibert [a], A. de Juan [b], J. L. Cortina [a,c]

[a] *Chemical Engineering Department and Barcelona Research Center for Multiscale Science and Engineering, UPC-BarcelonaTECH, C/ Eduard Maristany, 10-14 (Campus Diagonal-Besòs), 08930 Barcelona, Spain*

[b] *Chemometrics Group, Department of Analytical Chemistry, Universitat de Barcelona, Av. Diagonal 645, 08028 Barcelona, Spain*

[c] *Water Technology Center CETaqua, Carretera d'Esplugues 75, 08940 Cornellà de Llobregat, Spain*

Abstract

Off-gases treatments in copper metallurgical plants to remove SO_2(g) generate an acid solution formed by sulphuric acid, non-metals (arsenic) and transition metals (zinc, iron, copper). In order to reduce the sludge generated due to lime addition and to enhance the circularity, the recovery of sulphuric acid by diffusion dialysis technology is proposed. A diffusion dialysis stack incorporating an Anion Exchange Membrane favours the transport of hydrogen sulphate (HSO_4^-), while metals are effectively rejected. In the present study, an effluent from a copper smelter containing sulphuric acid (220 g/L), arsenic (3.4 g/L) and zinc (0.5 g/L) as main components was treated with a commercial Anion Exchange Membrane (Neosepta-AFX) to evaluate the sulphuric acid recovery ratio. The effect of operational variables, such as diffusate and dialysate flow rates, flow rate ratio and arsenic speciation (As(V) or As(III)), was studied. Neosepta-AFX was able to recover 67±2 % of sulphuric acid (146±12 g/L) and to reject effectively the metals (>85%), but it contained an impurity of 1.26 g/L arsenic because of its presence as neutral species (arsenic acid, H_3AsO_4/arsenous acid, H_3AsO_3). For this reason, the integration of a solvent extraction step using Cyanex 923® is proposed to remove arsenic before being treated with DD.

Keywords: Diffusion dialysis; Neosepta-AFX; sulphuric acid; arsenic speciation; acid recovery; waste minimisation

1. Introduction

There is an increasing awareness of promoting resource recovery, circular processing and conservation of the environment. Limitations on direct dumping of any hazardous waste into environmental compartments have led to stringent auditing of any by-product and waste generated during the processing stages. This includes solid, liquid and gaseous streams, containing hazardous metallic to non-metallic impurities, generated in most of the metallurgical and hydrometallurgical processing industries.

Metallurgical industries, as copper and zinc smelters, generate effluents characterised by high acidity and high metallic (e.g. Fe, Zn, Cu…) and non-metallic (e.g. As, Se, Sb…) [1]. Sulphur dioxide (SO_2), the main by-product in the sintering, roasting and smelting of sulphide minerals and concentrates, can be recovered as elemental sulphur, liquid SO_2, gypsum or sulphuric acid. Treatment of the generated off-gases includes the removal of dust by electroprecipitators and absorption of SO_2(g) in water [2]. The acid stream generated contains a mixture of acids, formed by H_2SO_4 (1 to 50%), HCl (up to 5 g/L), HF (up to 1 g/L) and arsenic as H_3AsO_4 and H_3AsO_3 (up to 10 g/L As). The presence of dust in the gases during the treatment can lead to the presence of metals, such as Cu, Zn and Fe (up to 2.5 g/L each one), Hg and Pb (<50 mg/L) in the acidic stream. Moreover, other metals as Al, Ni, Cr and Cd, can be present at much lower concentrations [3]. The liquid effluent generally requires further treatment, for instance, neutralisation with lime and iron sulphate and sedimentation for solid-liquid separation. Wastes generated, classified as hazardous, are a mixture of gypsum, calcium and iron arsenates and metal hydroxides as well other non-metallic impurities as Se, Sb and Bi Sometimes ion exchange is used to remove hazardous or valuable metal compounds (e.g. rhenium). [3].

The main challenge for copper smelters is to deal with the high impurity levels, primarily As. As a result of the constant increase in these impurities in copper ores over the years, it is expected that the slag and the off-gases produced in the processing of these ores will contain much higher impurities in the future than now[4]. The As/Cu ratio has increased by 40% in the last decade, which has led to a continuous increase in the processing and environmental costs. Additionally, the more stringent environmental regulations, particularly related to arsenic and selenium, have made the operation of mines and smelters more challenging and new solutions promoting resource recovery options and circular approaches are needed to reduce their impact [5–8]. To achieve both objectives, the recovery of H_2SO_4 free of hazardous pollutants and the safe disposal of As have been identified as the main research efforts.

Different techniques are applied to remove arsenic from waters, such as aluminium-based and ferric-based coagulation, ion exchange resins, membrane filtration, and electrochemical treatments to remove arsenic as arsine [9–16]. However, none of them

is effective when they are applied to the acid streams containing H_2SO_4 (10-25%). Alternative solutions have been applied to separate and recover the acid at a previous stage for subsequent removal and stabilisation of arsenic as a long term stable mineral form (e.g. scorodite $FeAsO_4 \cdot 2H_2O$). Different techniques such as nanofiltration [17,18], electrodialysis [19,20], diffusion dialysis (DD) [21–27], electrolytic deposition [28], ion exchange [29], solvent extraction [30,31] and membrane distillation [32] have been proposed to achieve that goal.

DD is a membrane-based process driven by a concentration gradient which uses an Anion Exchange Membrane (AEM), whose positive charge allows acid (HX) in solution to permeate while metallic ions are effectively rejected by the membrane [33]. The acid anion (X^-) is transported across the AEM with the cotransport of the fastest cation in solution; i.e., the H^+ will be transported to hold the electroneutrality condition instead of other cations in solution. This technique has been proven to be efficient for acid purification and has been applied for different acids, such as H_2SO_4, HCl or HNO_3. For example, Li et al. [21] studied the recovery of H_2SO_4 from leaching solutions (2.4 mol/L H^+, 4.2 g/L V(V), 13.8 g/L Al) with DF120 membrane. An acid recovery of 84% was achieved while metals were rejected (>90%) at feed to water flow rates ratios between 1.0 and 1.3. Wei et al. [22] evaluated the recovery of H_2SO_4 from the acid leach solution. The addition of salts containing the same anion as the acid (e.g. $FeSO_4$ and $VOSO_4$) promoted the diffusion of H^+ through the membrane (salt-effect). At flow rate ratio (diffusate/dialysate) of 1, 83% of H_2SO_4 was recovered with metal rejections higher than 93%. At higher flow rate ratio (1.6), H_2SO_4 recovery increased (87%), but also the transport of metals (90%). Jeong et al. [23] treated an industrial acidic effluent (4.5 M H_2SO_4) containing Fe(II) (52 g/l) and Ni(II) (18g/L). Metal rejections barely varied with flow rate (96 and 99% for Ni and Fe, respectively) and almost 80% of H_2SO_4 was recovered with a total metallic content of 2.0 g/L. Gueccia et al. [27] studied the recovery of HCl from pickling solutions with Fumasep membranes at different HCl (up to 105 g/L) and Fe(II) (up to 150 g/L) concentrations. They found that osmotic flux prevailed at low HCl concentrations, while at high HCl concentrations the "water ion solvation flux" predominates. Moreover, they developed a mathematical model to determine the membrane permeabilities to the acid and salt (i.e. HCl and $FeCl_2$, respectively). Typically, the studies in the literature provide information about the performance of strong electrolytes (e.g. H^+ Cl^-, H^+ NO_3^-, H^+ HSO_4^-), whereas few studies reported the behaviour of weak electrolytes as fully protonated forms (e.g. As(III) as H_3AsO_3 and As(V) as H_3AsO_4). Scarce information about the transport mechanisms and speciation in ion-exchange membranes can be found for non-charged species, as it is the case for As(III)/As(V) mixtures in the presence of a strong electrolyte such as H_2SO_4.

The main objective of this work was to study the recovery of H_2SO_4 from a stream generated during the off-gas treatment of a copper smelter by means of DD to

potentially be reused in the plant. The stream is mainly formed by 220 g/L H_2SO_4, containing as main impurities As (3.4 g/L) and Zn(II) (0.5 g/L), whereas other metal ions such as Fe, Pb, Cd, Ni, Cu and Hg are present as traces (mg/L). An AEM, Neosepta AFX was used, and the main operating variables were studied on the dialyser. Synthetic solutions formed of H_2SO_4, As(III)/As(V) and Zn(II), were also tested, where the amount of As(III) and As(V) was varied to study the effect of speciation on the membrane performance. For this purpose, a UV-Vis spectrophotometric method based on the absorption spectra of both acids and H_2SO_4 was developed. No works were found with the application of DD to treat acidic solutions with the Neosepta AFX membrane. A treatment scheme to provide a circular solution to recover a purified sulphuric stream was proposed.

2. Experimental

2.1. Experimental set-up

The schematic diagram of the experimental set-up is shown in **Figure 1**. The unit tested is the Acid Purification Lab Unit Model AP-L05 from Mech-Chem. The dialyser contains 8 sheets of one AEM in a plate and frame configuration with an active area of 7.62x15.24 cm each membrane (total area of 929 cm^2). The equipment contains two tanks with a maximum capacity of 6 L, one for the deionised water and the other one for the acidic solution. Two metering pumps are allocated at the two output streams of the membrane module, which can control the flow rates of both streams. The membranes tested were Neosepta AFX from AMSTOM, which are made of a poly-styrene-co-divinylbenzene aminated. These membranes are characterized by an area resistance between 0.7 to 1.5 $\Omega \cdot cm^2$ with an ion exchange capacity of 1.5-2.0 meq/g [33].

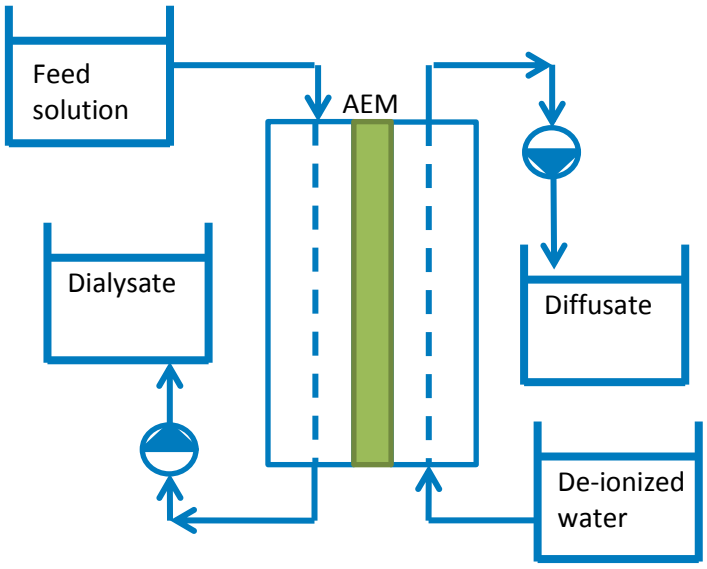

Figure 1. *Experimental set-up of the diffusion dialysis equipment*

2.2. Experimental procedure

The solution treated was generated in the off-gas cleaning of a copper smelter industry. During the gas cleaning, sulphur dioxide gets oxidised and hydrated, giving sulphuric acid stream, which is treated in a microfiltration (MF) unit to remove colloidal material. A scheme of the actual treatment unit of the acidic stream is included as supplementary information (**Figure S1**). **Table 1** shows the mean values of the composition of the effluent from a copper smelter industry at the MF exit as well as the target values to achieve in the purified acid stream. The effluent is mainly formed by H_2SO_4 (220 g/L), As (3.4 g/L) and Zn (0.5 g/L). Other metals such as Pb, Cd and Cu are presented in solution as traces.

Table 1. *Chemical composition of the acidic effluent from a hydrometallurgical industry*

	MF exit (g/L)	Target value (mg/L)		MF exit (mg/L)	Target value (mg/L)
H_2SO_4	220	Maximize	Pb(II)	5	< 1
As(III,V)	3.4	< 150	Cd(II)	100	< 1
Zn(II)	0.5	< 10	Ni(II)	6	< 0.5
Cu(II)	0.05	< 5	Hg(II)	5	<0.5
Fe(II)	0.1	< 5	Se(IV,VI)	6	<0.5

At first, experiments were carried out in a batch mode by recirculating both output streams (diffusate and dialysate) to their respective feed tanks. These tests were performed first with two synthetic solutions formed by 220 g/L H_2SO_4 and either 8 g/L As(III) or 8 g/L As(V) and afterwards with the acidic effluent from the hydrometallurgical industry. Experiments were carried out with 2 L of the acidic solution and 2 L of deionised water, and the flow rate of both streams was fixed at 1 mL/min. Samples of 3 mL were taken along the duration of the test, and the volume changes were measured in the acid tank.

For the dynamic experiments, a synthetic solution was firstly used with the major components containing 220 g/L H_2SO_4, 3.4 g/L As and 0.5 g/L Zn. The other metals were omitted in order to avoid interferences and facilitate the study of the transport of the main components. Acid and water flow rates were optimised to obtain the highest acid recovery with the lowest amount of impurities (see **Table 1**). Due to the fact that As can be present in solution either as As(III) or As(V) experiments were carried out

considering that arsenic was an equimolar mixture of As(V) and As(III). This scenario is the most likely to happen. An essential aspect of study in the separation process is the speciation of solutes present in water. **Figure 2** shows the speciation diagrams of As(III) and As(V) The speciation diagrams for the other elements in solution are collected in **Figure S2** in Supplementary information. At the working pH (around –0.5), As can be present as a neutral species (H_3AsO_3 or H_3AsO_4), but As(III) can also be present as a positively charged ion ($H_2AsO_2^+$). Taking into account that the hydrometallurgical plant has an excess of SO_2(g), this gas can be used to reduce As(V) to As(III). Then, experiments were also carried out with 3.4 g/L As(III). Finally, the acidic effluent coming from the hydrometallurgical plant was tested at the optimum conditions obtained with the synthetic solutions.

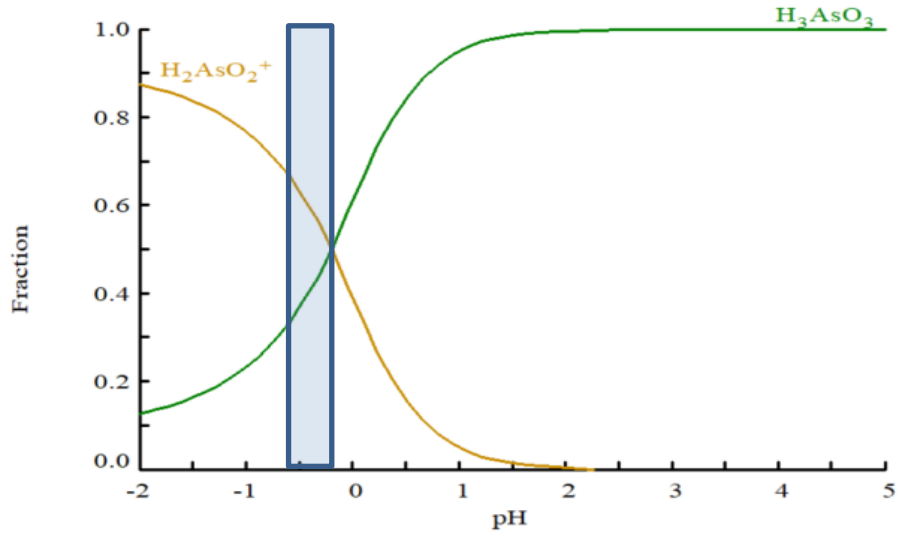

a)

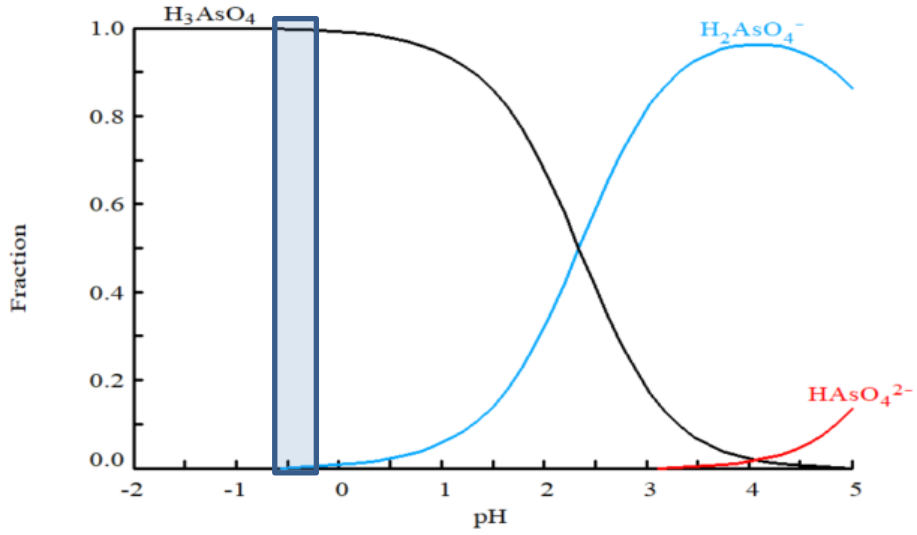

b)

***Figure 2**. Speciation diagrams of a) As(III) and b) As(V). Diagrams were built with the Hydra/Medusa code [34]. The rectangle indicates the pH range of both dialysate and*

diffusate streams along with the dialysis experiments. The initial solution had a pH value of -0.5±0.05

For simplicity, water transport was not studied in detail, and only a net evaluation was performed by monitoring the volume of both DD cell compartments. As the first approach, the separation factors and dialysis coefficients were considered for a given element without taking into account the chemical equilibrium among its species.

2.3. Chemical analysis

The acidity of the samples was outside the recommended range (2 to 12) for being measured by pH glass electrodes. The concentration of H^+ of the samples was determined by acid-base titrations using NaOH 0.5 M with an automated titrator (Excellence Titrator T5 from Metler Toledo). Samples were also analysed using Inductively Coupled Plasma Mass Spectrometry (7800 ICP-MS from Agilent Technologies) and Optical Emission Spectrometer (5100 ICP-OES from Agilent Technologies) to measure the total concentration of As and metals. Before their analysis by ICP, samples were filtered (0.2 µm) and acidified with 2% HNO_3.

2.3.1. Determination of As(III) and As(V) in the samples

The determination of As(III) concentration was based on UV-vis spectroscopy and multivariate calibration. Spectrophotometric measurements were performed with an HP 8453 UV-Vis spectrophotometer in the 190 – 290 nm spectral range. Spectra were recorded using a 1-mm pathlength quartz cuvette and Milli-Q water as blank. UV spectra of 70 synthetic samples with known concentration of As(III) (20 – 200 mg/L) were used to build the multivariate calibration model for determination of As(III) based on Partial least squares (PLS) regression. The synthetic samples contained different levels of As(V) and other major compounds, mimicking the conditions of the dynamic experiments. The UV spectra used for PLS model building were preprocessed using the 1^{st} order Savitzky-Golay derivative (2^{nd} order polynomial and 3 points window size) [35] followed by mean-centering. The related reference As(III) concentrations were also mean-centered. To build the regression model, PLS uses a set of latent variables that express the maximum covariance between the spectral information and the concentrations to be predicted [36]. The number of latent variables defining the optimal size of the PLS model was defined using cross-validation [37].

During the dynamic experiments, samples were collected from the inlet and outlet streams (i.e. diffusate and dialysate). Beforehand, samples from the initial acidic solution were 50-fold diluted, while samples collected from the dialysate and diffusate streams only 10-fold, to avoid signal saturation during the measurement of UV spectra and to be within the concentration range used to build the calibration model. UV spectra recorded in this way were used to determine the As(III) concentration of samples by

using the PLS calibration model. For every sample, the concentration of As(V) was obtained as the difference between the total As concentration, determined by ICP-OES, and the As(III) concentration, obtained as PLS prediction.

Data handling and statistical analysis were carried out in PLS_Toolbox 8.7 (Eigenvector Research, USA) running under Matlab R2019a (Mathworks, USA).

2.4. Experimental parameters

For the cycling type DD experiments, two parameters were calculated: the dialysis coefficient and the separation factor [25,26,38]. The first one is calculated according to **Eq. 1**:

$$U_i = \frac{V_1 \cdot V_2}{(V_1 + V_2) \cdot t} \cdot \ln \frac{\Delta C_{i,0}}{\Delta C_{i,t}} \quad \text{(Eq. 1)}$$

Where U_i is the diffusion coefficient of component i (m/h), V_1 and V_2 are the volumes of the diffusate and dialysate without considering volume changes (m^3), respectively, $\Delta C_{i,0}$ and $\Delta C_{i,t}$ are the total concentration differences of the selected element between dialysate and diffusate at the beginning and at time t (mol/L), respectively, S is the total effective membrane area (m^2), and t is the time (h). Only for the case of As, three different values were obtained: a global value including both As(III) and As(V), and individual values for As(III) and As(V) species.

By plotting the natural logarithm of ΔC_{it} versus time, the dialysis coefficient can be determined as described by equation 2:

$$\ln \Delta C_{i,t} = \ln \Delta C_{i,0} - U_i \cdot S \cdot \frac{V_1 + V_2}{V1 \cdot V_2} \cdot t \quad \text{(Eq. 2)}$$

The separation factor was calculated as the ratio between dialysis coefficients for H^+ and for component i.

For dynamic experiments, the acid recovery (or metal leakage) was calculated according to equation 3:

$$acid\ recovery\ (or\ metal\ leakage) = \frac{Q_{diff} \cdot c_{diff}}{Q_{diff} \cdot c_{diff} + Q_{dialy} \cdot c_{dialy}} \quad \text{(Eq. 3)}$$

Where Q_{diff} and Q_{dialy} are the flow rate of diffusate and dialysate (L/min), respectively and c_{diff} and c_{dialy} the concentrations of species i in the diffusate and dialysate (g/L), respectively.

3. Results and discussion

3.1. Calibration model for determination of As(III)

Figure 3.a shows the raw and **Figure 3.b** the preprocessed UV spectra related to the synthetic samples used to build the PLS regression model for determination of As(III) concentration. The obtained PLS model required five latent variables, as indicated by cross-validation. **Figure 3.c** shows the cross-validation (CV) prediction of As(III) *vs.* the known As(III) concentration from synthetic samples used in the model building. The root mean square error of cross-validation (RMSECV) [37] was 13.1 mg/L, and the coefficient of determination between CV As(III) prediction and reference As(III) concentration was R^2 = 0.92. The total percentage of variance captured by the regression model was 94% for the As(III) concentration. This indicates that a satisfactory calibration model was obtained for the determination of As(III) and it can be safely used afterwards to predict As(III) concentrations in the samples obtained during the dynamic experiments.

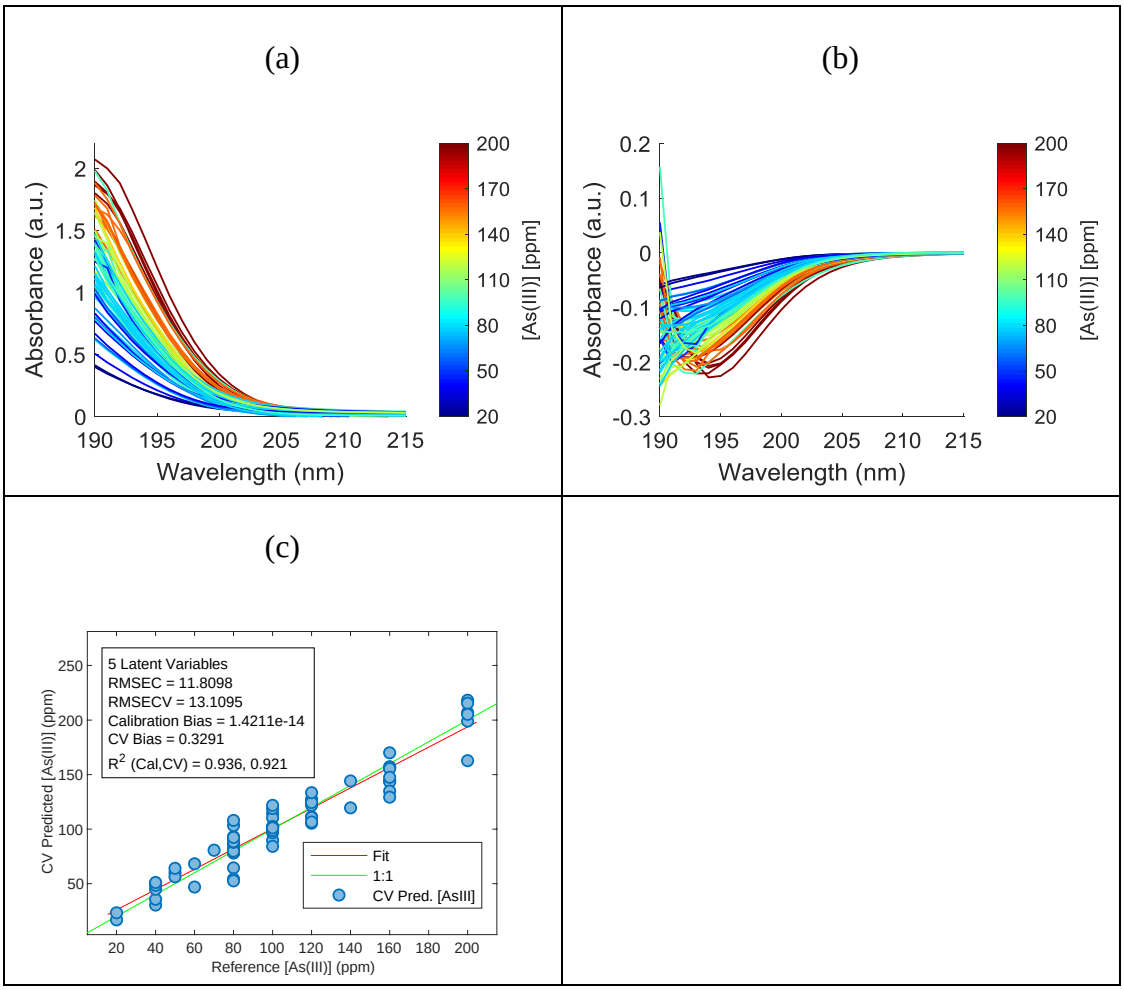

Figure 3*. (a) Raw and (b) preprocessed UV spectra related to the samples used to build the PLS calibration models. Colour scale indicates the As(III) concentration level. (c)*

Relationship between the cross-validation (CV) predictions and reference As(III) concentration in calibration samples

As mentioned in section 2.3.1, once the As(III) concentration is known, the As(V) concentration can be easily retrieved as the difference between total As, determined by ICP, concentration and As(III) concentration.

3.2. Determination of DD mass transfer parameters: dialysis coefficient and separation factor using cycling type DD experiments

Synthetic solutions containing 220 g/L H_2SO_4 and 8 g/L As (either As(III) or As(V)) were treated in a batch DD experiments for 48 h. Diffusion dialysis coefficients for As(III) and As(V) were $3.2 \cdot 10^{-5}$ m/h and $3.8 \cdot 10^{-5}$ m/h, respectively, according to **Eq. 1**. The differences in coefficient values can be related to the speciation of As(III) and As(V).

The lower value was for As(III) due to the fact that As(III) in the experimental acidic conditions is found as a cationic form ($H_2AsO_2^+$), which is expected to be rejected by the positively charged membrane. For both cases, the presence of a non-charged species (H_3AsO_3 for As(III) or H_3AsO_4 for As(V)) can result in a noticeable passage of these species because their transport is not impeded by the membrane.

A sample of the acidic effluent from the copper smelter was treated in the same configuration, and the dialysis coefficients and separation factors were calculated according to **Eq. 1** and **2**, respectively. **Table 2** collects the values of these parameters.

It can be seen that the highest dialysis coefficient is obtained for the H^+, followed by SO_4 (mainly as HSO_4^-) and As. The dialysis coefficient value for As, considering both As(III) and As(V), was in between the values calculated previously for As(III) ($H_2AsO_2^+/H_3AsO_3$) and As(V) (H_3AsO_4), suggesting that the effluent contains a mixture of both. Speciation analysis determined that 43% of the As is present as As(III) and 57% as As(V). Moreover, it can be seen that the dialysis coefficients for metals were one order of magnitude lower than the one for H^+ due to the electrostatic repulsion between the positively charged membrane and the cations. According to the speciation analysis, in most of the cases, the predominant species was the free-metal ion (M^{2+}).

The separation factors were calculated with respect to the dialysis coefficients of H^+. The lowest separation factors were for the main anions in the solution, SO_4 (1.1) and non-charged As species (2.7). The smaller value for the SO_4 suggested that the membrane has a better affinity for HSO_4^- ions than for non-charged As forms. Furthermore, the separation factors for the metals were much higher, ranging from 7.5 (Pb) to 22 (Fe). The fact that these values were larger suggests that the membrane would

be able to reject the metals for the solution, while it would allow the passage of H_2SO_4 and non-charged As species through the membrane.

***Table 2**. Dialysis coefficients (U_i, m/h) and separation factor SF (U_{H+}/U_i) of the different ions in solution. Speciation analysis was carried out using the Hydra-Medusa code [34]*

	Speciation (% in molar fraction)	**Dialysis coefficient U_i (m/h)**	**Separation factor SF (U_{H+}/U_i)**
H^+		$9.6 \cdot 10^{-5}$	-
SO_4	HSO_4^- (0.93), SO_4^{2-} (0.02), $M(SO_4)_n^{-n+2}$ (0.05)	$9.1 \cdot 10^{-5}$	1.1
Pb(II)	Pb^{2+} (0.69), $PbSO_4$ (0.25), $Pb(SO_4)_2^{2-}$(0.06)	$1.3 \cdot 10^{-5}$	7.5
Cd(II)	Cd^{2+} (0.78), $CdSO_4$ (0.15), $Cd(SO_4)_2^{2-}$ (0.07)	$7.9 \cdot 10^{-6}$	12.1
Ni(II)	Ni^{2+} (0.89), $NiSO_4$ (0.11)	$7.1 \cdot 10^{-6}$	13.5
Cu(II)	Cu^{2+} (0.88), $CuSO_4$ (0.12)	$7.0 \cdot 10^{-6}$	13.8
As(III,V)	As(III): H_3AsO_3 (0.35) / $H_2AsO_2^+$ (0.65) As(V): H_3AsO_4	$3.6 \cdot 10^{-5}$	2.7
Fe (III)	Fe^{3+} (0.05), $FeHSO_4^{2+}$ (0.95)	$4.4 \cdot 10^{-6}$	21.9
Zn(II)	Zn^{2+} (0.03), $Zn(SO_4)_4^{6-}$	$6.1 \cdot 10^{-6}$	15.7

Wang et al. [26] determined the dialysis coefficients and separation factors when treating a stone coal acid leaching (1.75 mol/L H^+, 2.1 g/L V(V), 17.5 g/L Al(III), 5.8 g/L Fe(III), 11.2 g/L F^- and 61.7 g/L HSO_4^-) with the DF-120-III. The lowest separation factor value obtained was for HSO_4^- (3.9), followed by the metals in solution (from 14.8 to 48.3). The lowest values for metals indicated that the membrane would be able to reject the metals favouring the transport of acid (mainly sulphuric) across the membrane.

Along the filtration process, water was transported mainly from the acid to the water side. Water can be transported through the membrane by a) osmotic pressure differences due to the composition of both solutions along the membrane stack, since the dialysate is deionized water and the diffusate is an acidic solution containing metals (osmotic flux), and, b) ion transport associated with the solvation of ions ("drag flux") (e.g. $H(H_2O)_n^+$, $HSO_4^-(H_2O)_m^-$). In the experiment with real effluent, volume changes were observed in both tanks and that the latter mechanism predominated over the osmotic flux, resulting in the transport of 0.9 L from the acid to the water side.

3.3. Dynamic DD experiments

3.3.1. Effect of flow rate on acid recovery and metal passage

Figure **4** and **5** show the H_2SO_4 recovery, its concentration in the diffusate and the ion passage (As, SO_4, Zn and Na) at different flow rates by keeping the ratio water to acid equal to 1 with the synthetic solution containing 3.4 g/L As (mixture of 1.7 g/L As(III) and 1.7 g/L As(V)) and 3.4 g/L As(III), respectively.

Fig. 4.a shows the H_2SO_4 recovery and its concentration in the diffusate for the solution containing As(V) and As(III). At the lowest flow rate tested (0.39 L/m^2 h), H_2SO_4 recovery was 79.5%, and its concentration in the recovered stream reached a value of 195 g/L. Higher flow rates led to a decrease in both H_2SO_4 recovery and concentration to values of 63% (150 g/L H_2SO_4 in the diffusate) at 1.49 L/m^2 h. Increasing the flow rate led to a lower residence time of both liquids inside the module, and the acid did not have enough time to permeate across the membrane, leading to lower H_2SO_4 recovery.

Ions passage is of paramount importance since the presence of metals in the recovered acid will determine whether it can be reused or not. Almost all Zn was rejected (>90%) by the membrane (**Fig. 4.b**). This rejection was due to electrostatic repulsion between the metal and the membrane. At the lowest flow rate evaluated, Zn was rejected by 92% and increased for higher flow rates up to values of 96%. Na passage was a bit higher due to the fact that a) the hydrated radio for Na (0.358 nm), which is smaller than that for Zn (0.430 nm) (hydrated radii values taken from Nightingale [39]) and because of b) dielectric exclusion. The effect of dielectric exclusion in ion-exchange membranes was first observed by Glueckauf [40], further considered by Fane et al. [41] and reviewed by Yaroshchuk et al. [42]. This mechanism is related to the differences in dielectric constants between the solution and the polymeric matrix. Dielectric exclusion is caused by the interaction between ions and the bound electric charges induced by ions at the interfaces in media of different dielectric constants (bulk solution/polymeric matrix). Initially, it was proposed that the main rejection mechanism was the Donnan exclusion caused by fixed electric charges. That conclusion was based, in fact, on the only observation that double-charged anions were rejected essentially better than single-charged ones. However, this patter is not only is characteristic of dielectric exclusion too, but it is even more pronounced because the ion-exclusion free energy is proportional to the square of ion charge (while the Donnan exclusion is linear with it). Dielectric exclusion phenomenon has found to be stronger in narrow pores [42]. These two reasons can also explain why Zn ions were more rejected than Na^+ and H^+. The transport of H^+ was mainly associated with the passage of HSO_4^- as the dominant anion in solution.

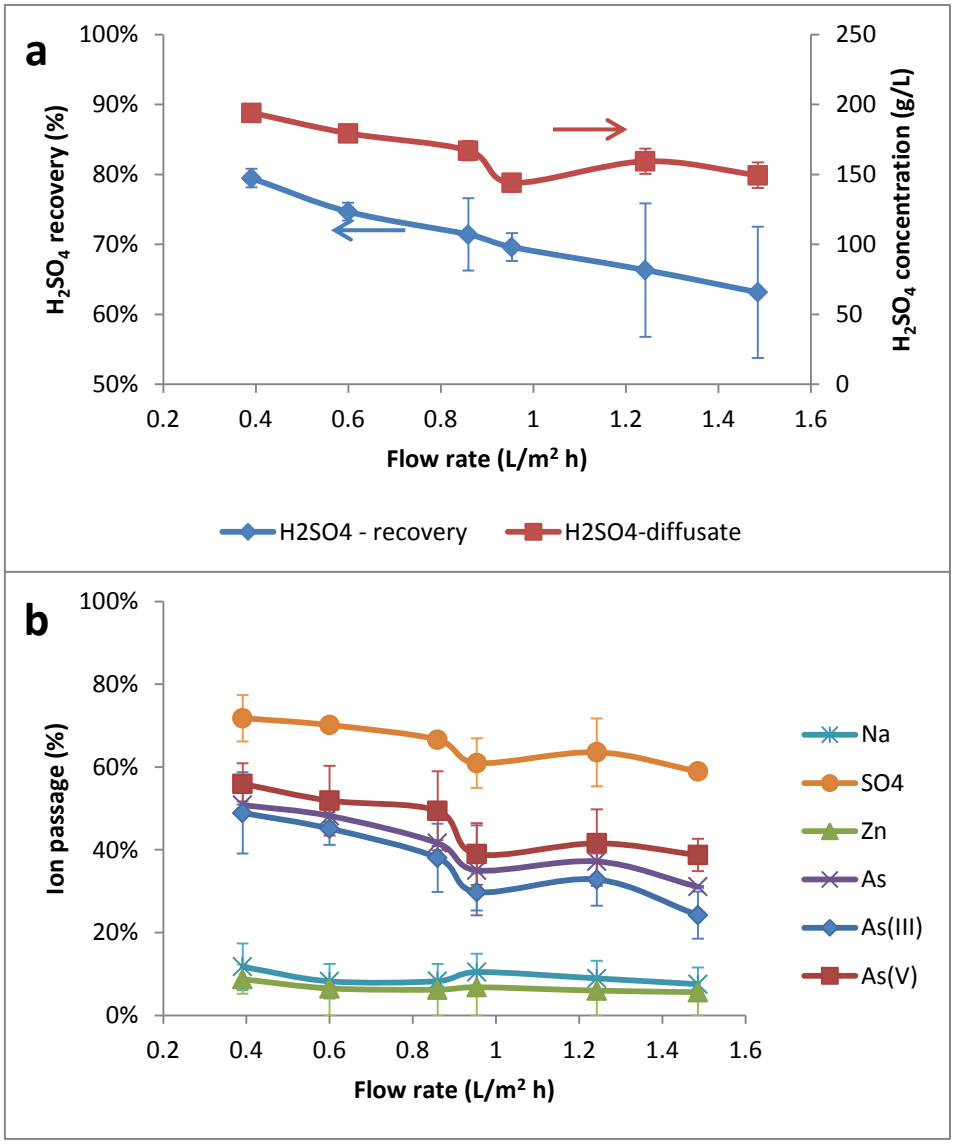

Figure 4. *Effect of flow rate on a) acid recovery and H_2SO_4 concentration in the diffusate and, b) ion passage at flow rate ratio water to feed equal to 1 with the solution containing 220 g/L H_2SO_4, 1.7 g/L As(III), 1.7 g/L As(V) and 0.5 g/L Zn*

Nevertheless, As was not effectively rejected by the membrane. As it was stressed previously, As(V) is present as a neutral species (H_3AsO_4) and As(III) is present as a mixture of a neutral and a positively charged cation (H_3AsO_3 and $H_2AsO_2^+$), and the transport of a neutral species is not expected to be impeded by the membrane charge. This suggests that their transport is governed by a combination of diffusion and size exclusion. In this study, it was observed that both species were able to permeate through the membrane, resulting in a passage of total As (As(III)+As(V)) around 51% at 0.39 L/m^2 h. This value decreased to 31% when the flow rate was increased up to 1.49 L/m^2 h. The developed method allowed the speciation of As (III) and As(V) and, as a consequence, it was possible to calculate the leakage of both forms. As expected, the

transport of As(III) was more impeded by the membrane than As(V) due to its presence as $H_2AsO_2^+$, which was expected to be rejected by the positively charged membrane. On the other hand, higher leakage of As(V) was expected on the basis of its full presence as H_3AsO_4. In fact, the leakage of As(III) varied from 49% at 0.39 L/m^2 h to 24% at 1.49 L/m^2 h, while the one of As(V) ranged from 56% at 0.39 L/m^2 h to 39% at 1.49 L/m^2 h.

Figure 5 shows the acid recovery and ion passage with the feed solution containing 220 g/L H_2SO_4, 3.4 g/L As(III) and 0.5 g/L Zn as a function of flow rate, keeping the ratio between them equal to 1. At the lowest flow rate evaluated (0.39 L/m^2 h), H_2SO_4 recovery was around 75% (178 g/L in the diffusate), and it decreased till 65% (160 g/L H_2SO_4) at a flow rate of 1.24 g/L (**Fig 5.a**). As it was previously stressed, higher flow rates led to lower time for H_2SO_4 to permeate across the membrane, leading to lower H_2SO_4 recoveries and concentrations. In comparison with the experiments carried out with a mixture of As(III) and As(V) (**Fig. 4.a**), differences in the recovery ratio and H_2SO_4 concentration in the diffusate were around 1%, and then it can be concluded that As speciation has no significant effect on acid recovery.

Fig 5.b shows the ion passage across the membrane. As in the previous case, Na and Zn were highly rejected by the membrane for the reasons above-mentioned. As(III) passage across the membrane decreased from 46% at 0.39 L/m^2 h to 30% at 1.24 L/m^2 h. In comparison to the previous case with the mixture of As(III) and As(V), total As passage was 51% at 0.39 L/m^2 h and decreased to 37% at 1.24 L/m^2 h. This can be related to the fact that As was as a mixture of a non-charged (H_3AsO_3) and a positively mono-charged ($H_2AsO_2^+$) species. This cationic species of As(III) can be rejected by the membrane due to the electrostatic repulsion produced by the positively charged membrane.

The same behaviour has been reported in the literature [21–26]. As the flow rate of both streams inside the membrane stack (acidic feed solution and water) increase, the solution components have less retention time to be transported across the membrane, which leads to lower acid recoveries and lower ion leakage. For example, Wei et al. [22] treated an acidic effluent (H_2SO_4, V(V) and Fe(III)) with a DF-120-III membrane and observed a decrease of acid recovery from 88% to 72% when flow rates increased from 0.16 to 0.3 L/m^2 h, while the metal leakage was below 8.5%. Xu et al. [25] treated a similar acidic solution containing Al(III) and Cu(II) instead of V(V) and Fe(II) with a DF-120 membrane. H_2SO_4 recovery decreased from 76% to 61% when flow rates were increased from 0.3 to 0.7 L/h. Wang et al. [26] treated an acidic solution formed by a mixture of H_2SO_4, HF and H_3PO_4 with metallic impurities (V(V), Fe(II), K(I), Al(III) and Mg) with the DF-120-III membrane. They observed the same phenomenon when flow rates increased from 2.1 to 4.8 L/m^2 h, which led to lower acid recoveries (from 74% to 68%) and lower metal leakages (<7.5%). No studies were found with the application of DD to treat acidic solutions with the Neosepta AFX membrane.

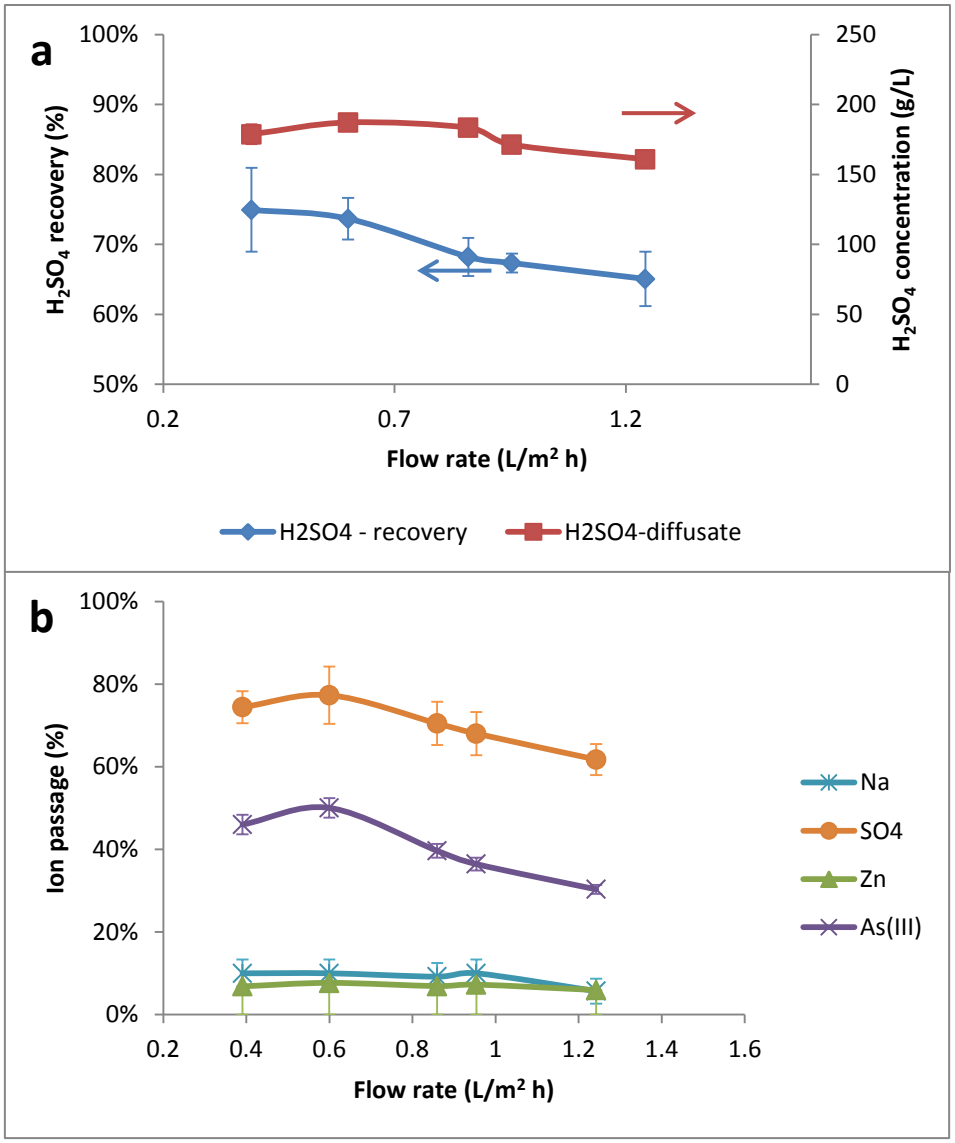

***Figure 5**. Effect of flow rate on a) acid recovery and H_2SO_4 concentration in the diffusate and, b) ion passage at flow rate ratio water to feed equal to 1 with the solution containing 220 g/L H_2SO_4, 3.4 g/L As(III) and 0.5 g/L Zn*

The goal of the application of diffusion dialysis to treat this acidic effluent was to recover the maximum amount of acid with a lower amount of hazardous impurities. The main impurity in the system (As) was rejected at a maximum of 70%. However, under the operation conditions, the H_2SO_4 concentration in the diffusate was around 150 g/L (65% of recovery). On the other side, at the lowest flow rate, H_2SO_4 concentration in the diffusate was the highest (194 g/L), but the passage of As was around 50%. Then, it was decided to take a compromise in both cases, and the acid flow rate was fixed at 0.86 L/m^2 h. Under these conditions, 68% of H_2SO_4 was recovered, with 40% of As passage.

3.3.2. Effect of flow rate ratio (water/feed) on acid recovery and metal passage

Fig. 6 and 7 show the effect of flow rate ratio (water/feed) on the performance of the diffusion dialysis at a fixed feed flow rate (0.86 L/m^2 h) at 3.4 g/L As (1.7 g/L As(V) and As(III)) and 3.4 g/L As(III), respectively.

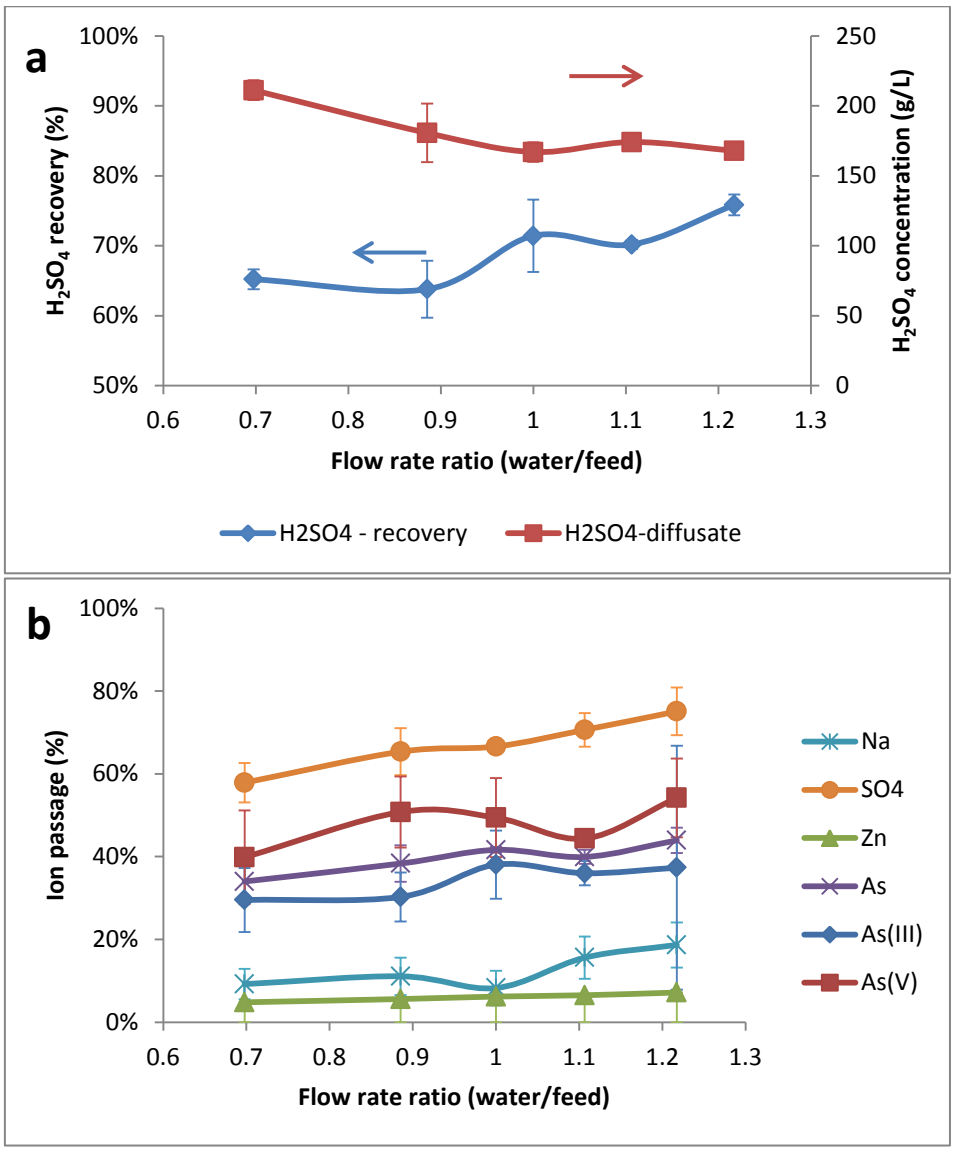

***Figure 6**. Effect of flow rate ratio on a) acid recovery and H_2SO_4 concentration in the diffusate and, b) ion passage at acid flow rate of 0.86 L/m^{2}h with the solution containing 220 g/L H_2SO_4, 1.7 g/L As(III), 1.7 g/L As(V) and 0.5 g/L Zn*

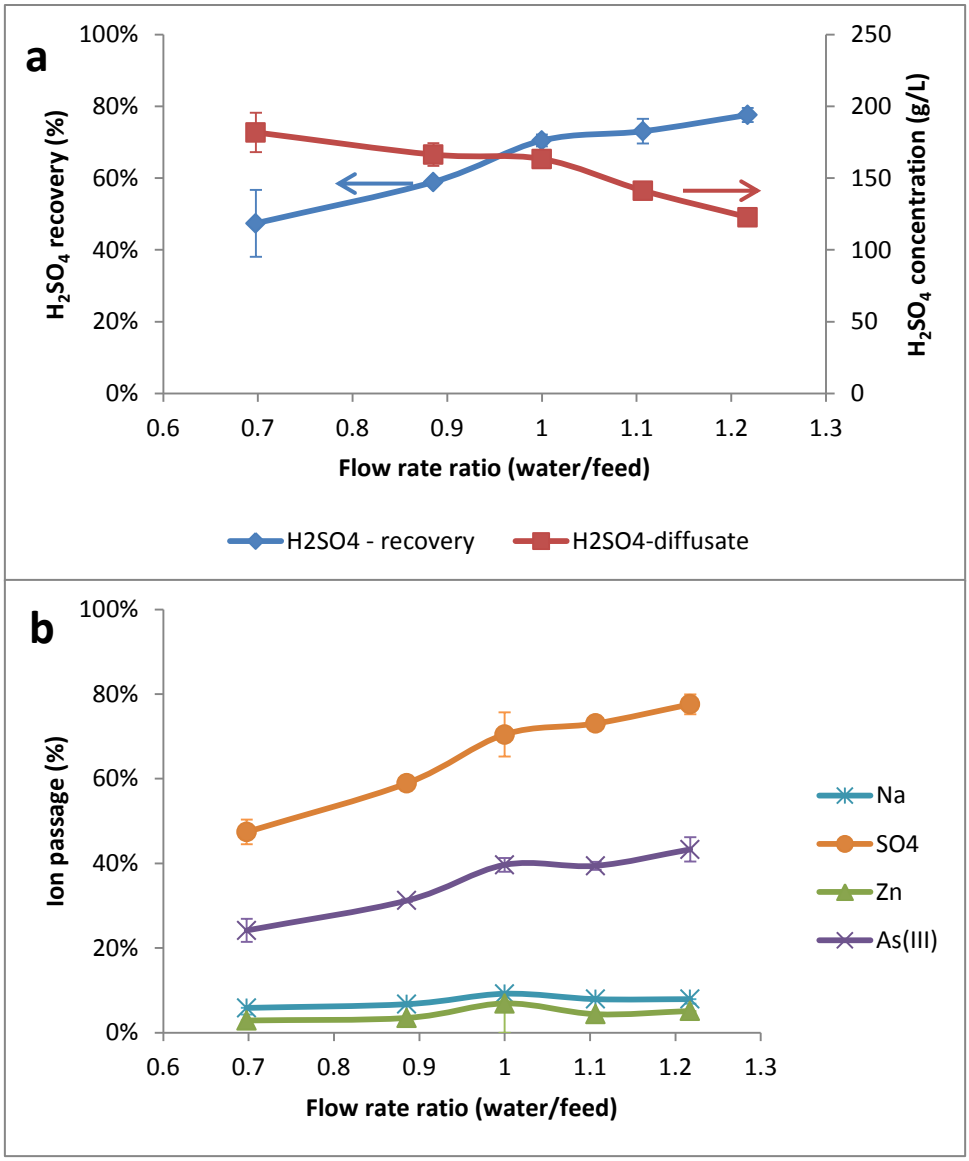

***Figure 7**. Effect of flow rate ratio on a) acid recovery and H_2SO_4 concentration in the diffusate and, b) ion passage at acid flow rate of 0.86 L/m^{2}h with the solution containing 220 g/L H_2SO_4, 3.4 g/L As(III) and 0.5 g/L Zn*

Fig. 6.a shows the obtained results for the solution containing the mixture of As(III) and As(V). H_2SO_4 concentration in the diffusate decreased from 211 g/L to 168 g/L, while acid recovery increased from 65 to 76% when the flow rate ratio was changed from 0.7 to 1.2. When the water flow rate increased, the difference in H_2SO_4 concentration between both sides became larger, leading to a higher diffusion of H_2SO_4 from the acid to the water side. Nevertheless, working at high water flow rate makes H_2SO_4 get diluted in the diffusate. Despite the increase of the H_2SO_4 recovery at high flow rates ratios, these operational conditions had increased the transport of the main impurities (As, Na and Zn) through the membrane (**Fig. 6.b**). The As passage increased from 34% to 44% when the flow rate ratio was increased from 0.7 to 1.2, while the transport of Zn

was below 5%. Na passage was slightly higher than for Zn due to the reasons mentioned above. As in the previous section, the transport of As(III) was more impeded than the As(V) due to its presence as $H_2AsO_2^+$.

Fig. 7 shows the results when the solution contained only As(III). H_2SO_4 recovery increased from 48% to 78% when the flow rate ratio was augmented from 0.7 to 1.2. These points corresponded to a H_2SO_4 concentration of 181.8 and 122.8 g/L, respectively. As in the previous section, As(III) was less transported across the membrane than As(V) due to its presence as a cation ($H_2AsO_2^+$). Moreover, the passage of As was lower than the one corresponding to the acid, ranging from 24% to 43% at flow rate ratios 0.7 and 1.2, respectively. As in the previous cases, metal passages were below 10% and 3% for Na and Zn, respectively.

This behaviour has also previously been observed [21–26]. By keeping a constant feed flow rate and by increasing the water to feed flow rate ratio, a decrease in the acid concentration and an increase in the acid recovery was observed. This behaviour was explained by a lower acid concentration in the diffusate due to the higher water flow rate, which increased the driving force and led to a higher acid transport (or recovery) across the membrane. For example, in the above mentioned studies, Wei et al. [22] by changing the water to feed flow rate ratio from 0.3 to 1.7 (at 0.45 L/h of feed flow rate) observed an increase of both H_2SO_4 recovery from 45% to 90% and metal leakage from 4% to 15%. Xu et al. [25] at 0.19 L/m^2 h of feed flow rate observed an increase of both H_2SO_4 recovery (from 66.8% to 87%) and ion leakage (from 4% to 11%) when water to feed flow rate ratio was changed from 0.8 to 1.6. Wang et al. [26] increased the water to feed flow rate ratio from 0.8 to 1.4 (at 3.2 L/m^2 h), and found that the H_2SO_4 recovery improved from 60.6% to 80.6%, while metal leakage was below 5%. These works concluded that the optimum water to feed flow rate ratio ranges from 1.0 to 1.2.

Taking into account that the goals of the application of DD are to achieve the highest concentration of H_2SO_4 in the recovered acid with the lowest amount of impurities, the optimum flow rate ratio was fixed at 1.

3.3.3. Treatment of an acidic effluent from a hydrometallurgical industry

The acid effluent from the off-gases treatment of a copper smelter, after being filtered through a MF stage (see **Figure S1**, supplementary material) for colloidal and suspended solids removal, was treated in the DD module maintaining a flow rate ratio of 1, working both streams at 0.86 L/m^{2}h. **Figure 8** shows a scheme of the DD module with the composition of the main components of the stream (H_2SO_4 and As). From a stream containing 217.4 g/L H_2SO_4, it was possible to recover the 69±2% of the acid, obtaining a stream with 146.3 g/L H_2SO_4. In addition, 39±1% of As in solution was

transported through the membrane, leading to a content of 1.3 g/L As in the recovered acid.

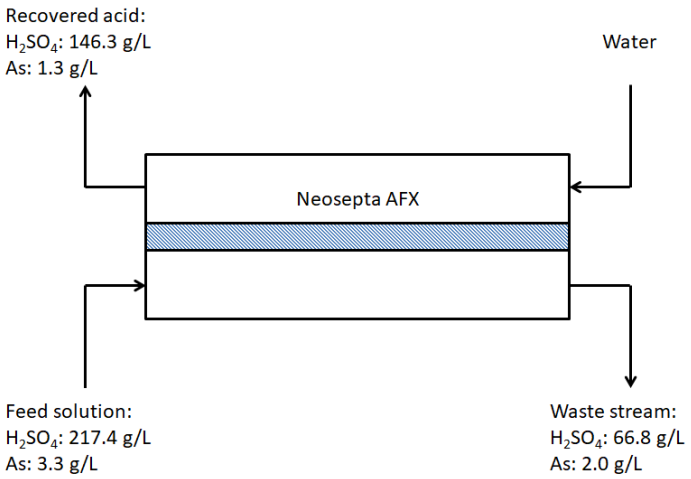

***Figure 8**. Scheme of the DD module when the MF exit was treated, working at 0.86 L/m^{2}h at a flow rate ratio of 1*

Table 3 shows a detailed description of the composition of the three streams (feed solution, waste stream and recovered acid) as well as the acid recovery, metal leakage and target values in the recovered acid. As can be seen, the metallic cations were effectively rejected. Concentrations of Zn, Fe and Ni in the recovered acid were below the detection limits. Nevertheless, target values for metals were not achieved, except for the Pb and Ni. The main impurity of the recovered acid was As.

***Table 3**. Composition of MF exit, waste stream and recovered acid after treatment with DD*

	MF exit (g/L)	Waste stream (g/L)	Recovered acid (g/L)	Acid recovery / ion passage (%)	Target value (g/L)	
H_2SO_4	217.47 ± 8.73	66.76 ± 8.96	146.28 ± 8.55	68.86 ± 2.34	Maximize	
As	3.33 ± 0.06	2.00 ± 0.27	1.26 ± 0.06	38.66 ± 1.31	< 0.150	×
Zn	0.46 ± 0.02	0.45 ± 0.07	< 0.04		< 0.010	
Fe	0.13 ± 0.01	0.12 ± 0.02	< 0.04		< $5\cdot10^{-3}$	
Pb	$4.89\cdot10^{-3}$ ± $4.88\cdot10^{-4}$	$4.41\cdot10^{-3}$ ± $6.09\cdot10^{-4}$	$6.87\cdot10^{-4}$ ± $2.33\cdot10^{-4}$	13.48 ± 1.50	< $1\cdot10^{-3}$	✓
Cd	0.11 ± 0.01	0.10 ± 0.01	$7.52\cdot10^{-3}$ ± $3.97\cdot10^{-4}$	6.89 ± 0.26	< $1\cdot10^{-3}$	✓
Ni	$6.31\cdot10^{-3}$ ± $1.35\cdot10^{-4}$	$6.17\cdot10^{-3}$ ± $8.89\cdot10^{-4}$	< $4\cdot10^{-4}$		< $5\cdot10^{-4}$	✓
Cu	0.06 ± 0.01	0.06± $7.74\cdot10^{-3}$	$3.19\cdot10^{-3}$ ± $4.29\cdot10^{-5}$	5.19 ± 0.06	< $5\cdot10^{-3}$	✓

Table 4 collects the results from different studies when treating industrial streams characterised by a high acidity (in sulphuric media) and high content of metal impurities with DD employing membranes different than the Neosepta-AFX used in this study [21–26]. As can be seen, this membrane technology allows to recover sulphuric acid with values higher than 70%, while the transport of metals across the AEMs is impeded (<10%).

***Table 4**. Comparison of sulphuric acid recovery from metal contaminated acidic wastes with diffusion dialysis technology*

Membrane	Feed composition (g/L)	Flow (L/m^2 h)	Acid recovery (%)	Ion leakage (%)	Recovered acid composition (g/L)	Ref.
Neosepta-AFX (poly-styrene-co-divinylbenzene aminated)	H_2SO_4: 217 As: 3.33 Zn: 0.46	0.86	69	As: 39 Zn: <10	H_2SO_4: 146.3 As: 1.26 Zn: <0.04	This work
DF120-III (Brominated poly(2,6-dimethyl-1,4-phenylene oxide))	H_2SO_4: 61.7 Fe: 11.2 V: 4.6	0.19	84	Fe: 5 V: 3	H_2SO_4: 51.90 Fe: 0.65 V: 0.27	Wei et al. [22]
	H^+: 1.75 mol/L V: 2.1 Al: 17.5 Fe: 5.8 Mg: 4.5 F: 11.2 P: 1.4 S: 61.7	3.2	71.1	V: 4.5 Al: 1 Fe: 2.6 Mg: 2 P: 1.7 F: 8.9 S: 30.1	H^+: 1.52 mol/L V: 0.13 Al: 0.21 Fe: 0.19 F: 0.12 P: 0.16 S: 22.4	Wang et al. [26]
DF120 (Brominated poly(2,6-dimethyl-1,4-phenylene oxide))	H^+: 2.4 mol/L V: 4.20 Al: 13.75 Fe: 6.64	Feed: 0.21 Water: 0.25	84	V: 7 Al: 7.5 Fe: 15	H^+: 2.2 mol/L	Li et al. [21]
	H^+: 4.78 mol/L Al: 20.2	$2.0 \cdot 10^{-3}$ m^3/h	85.2	Al: 4.98	H^+: 4.08 mol/L Al: 1	Xu et al. [25]
Selemion DSV (Aminated polysulfone)	H_2SO_4: 6 mol/L Fe: 52 Ni: 18	0.26	80	Fe: 1 Ni: 4	H_2SO_4: 4.4 mol/L Fe: 0.5 Ni: 0.7	Jeong et al. [23]
AEM (not specified)	H^+: 4.05 mol/L Al: 10	Feed: 1.45 Water: 0.78	78	Al: 35		Lin et al. [24]

3.4. Definition of a circular treatment train to recover H_2SO_4 from acid streams for smelter uses

The acid valorisation should be oriented towards the recovery of the main component (H_2SO_4) for its better reuse in the production processes. Then, a well-closed circuit could be created, making the process economical and eco-friendly. Actually, the treatment of such acid streams is done by the addition of lime to neutralise the acid and dispose the precipitated gypsum and metal hydroxides in a repository for hazardous waste. However, this option due to the restrictive regulations is less attractive due to the high cost associated and the need to convert As species into a long-term environmental stable form. This process also leads to the loss of sulfuric acid and various metals as impurities. The levels of As in the recovered acid will limit its application in the copper smelter plant. The concentration of both metallic and non-metallic impurities can be reduced by a chemical precipitation step using NaSH [43] or $Na_2S_2O_3$[44] to precipitate them as sulphides before being treated by DD. In the case of $S_2O_3^{2-}$, the strong acidic media leads to the formation of H_2S(g) and elemental sulphur (S(s)), which can promote the removal of arsenic as As_2S_3(s) and some of the metallic ions precipitate as MS(s). The use of such a process at industrial scale is limited by the risk associated with the in-situ generation of H_2S(g) in the precipitation reactor and the generation of metal and non-metal sulphides with high-cost management disposal.

A solvent extraction (SX) stage using an organophosphorus extractant is proposed for As(III)/As(V) removal as pretreatment. The trialkyl phosphine oxide (Cyanex923®) extractant dissolved in toluene was proposed by Wisniewski et al. [6] for both As(III) and As(V) extraction as described in **Eq. 4** and **5**:

$$H_3AsO_4(aq) + n\,S_{org} \rightleftarrows (H_3AsO_4)S_{n,org} \quad \text{(Eq. 4)}$$

$$H_3AsO_3(aq) + n\,S_{org} \rightleftarrows (H_3AsO_3)S_{n,org} \quad \text{(Eq. 5)}$$

Extraction equilibrium is achieved within 5 minutes and As extraction increased at high H_2SO_4 concentration, but some part of the acid is co-extracted as described by **Eq. 6** [8]:

$$H^+(aq) + HSO_4^-(aq) + n\,S_{org} \rightleftarrows (H^+HSO_4^-)S_{n,org} \quad \text{(Eq. 6)}$$

Where S_{org} represents tri-alkylphosphine oxide and subscript org refers to the organic phase.

H_3AsO_3/H_4AsO_4 species are stripped with water effectively [7] as described by **Eq. 7**.

$$(H^+HSO_4^-)S_{n,org} + (H_3AsO_4)S_{n,org} + (H_3AsO_3)S_{n,org} \rightleftarrows H^+HSO_4^-(aq) + H_3AsO_4(aq) + H_3AsO_3(aq) + n\,S_{org} \quad \text{(Eq. 7)}$$

The integration of the SX stage for selective removal of As(III)/As(V) before the DD stage is described in **Figure 9**. The SX stage could provide up to a 94% removal ratio for both H_3AsO_3/H_4AsO_4 using 5 extraction stages as it is described in **Figure S3** in supplementary material and the resultant purified acid from the DD, will reduce the total As concentration to values below 0.10 g/L and the total metal concentrations (Zn, Cu, Fe, Cd, Pb, Ni and Hg) below 0.05 g/L, with removal ratios above 95%. The hybrid process is operated in a feed and blended mode where the waste stream containing 67 g/L H_2SO_4 is recirculated back to the SX stage. This stream containing H_2SO_4, As and metals will be treated with CaO(s) and $FeSO_4$ to remove the metals as hydroxides and As as scorodite ($FeAsO_4 \cdot 2H_2O$).

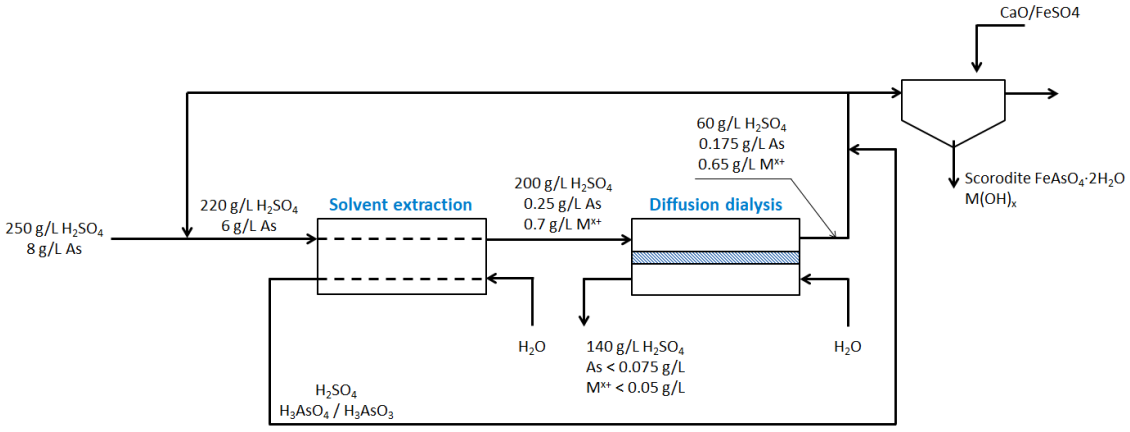

***Figure 9**. Integration of SX and DD for the treatment of the acidic solution generated on the off-gases treatment of a copper smelter*

The integration of both stages could increase the total H_2SO_4 recovery up to 70% with enough quality to be reused in the same plant. This process will reduce the cost associated with CaO(s) neutralization and the need for disposal of the sludge generated in the process containing both metal ions and arsenic. For a copper smelter producing up to 220,000 m^3/y, only from a sustainability point of view, a circular economy proposal is provided including the recovery of 31,000 ton/y H_2SO_4 and the reduction of 60,000 ton/y of a sludge contaminated with As and heavy metals.

4. Conclusions

Neosepta AFX membrane has proven to be able to recover acids from effluents of hydrometallurgical industries. H_2SO_4 recoveries varied from 50% to 80% depending on the operational variables. This membrane was able to reject the cations properly in solution (Na and Zn), but it was not efficient with As, which was related to its presence as a neutral complex in solution, H_3AsO_4 for As(V) and H_3AsO_3 for As(III). As speciation demonstrated to have an impact on its transport across the membrane, but it has little effect on the transport of the other components. The fact that As(III) can also

be presented as $H_2AsO_2^+$ led to higher rejections of As. Under the optimum operation conditions obtained with the synthetic solutions (flow rate ratio equal to 1 at 0.86 L/m^2 h), the membrane was able to recover the 70% of H_2SO_4, with an As leakage of 39%, while the metals were rejected more than 85%. Nevertheless, the transport of As across the membrane can limit its applications to be reused. In order to obtain a H_2SO_4 free of As from the DD stage, a SX pre-treatment must be done with an organophosphorus extractant to remove up to 94% of As content. The integration of this stage can provide recovery of 70% of the H_2SO_4 from the acidic solution. Such an approach provides a sustainable solution based on a circularity approach.

Acknowledgements

This research was supported by the Waste2Product project (CTM2014-57302-R) and by the R2MIT project (CTM2017-85346-R) financed by the Spanish Ministry of Economy and Competitiveness (MINECO) and the Catalan Government (2017-SGR-312), Spain. MINECO supported the work of Julio López and Xanel Vecino within the scope of the grant (BES-2015-075051) and the Juan de la Cierva contract (IJCI-2016-27445), respectively. R.R. de Oliveira and A. de Juan acknowledge the funding from Spanish government under the project CTQ2015-66254-C2-2-P. We also want to thank the contribution of B. Casas and K. Martín for their help during the experimental work and to A. Espriu-Gascón and A. Díaz for the ICP analysis.

References

[1] A. Agrawal, K.K. Sahu, An overview of the recovery of acid from spent acidic solutions from steel and electroplating industries, J. Hazard. Mater. 171 (2009) 61–75. doi:10.1016/j.jhazmat.2009.06.099.

[2] M. Canova, A. Pinasseau, B. Zerger, J. Roth, Best Available Techniques (BAT) Reference Document for Waste Treatment, 2017. http://eippcb.jrc.ec.europa.eu/reference/BREF/WT/WT_Final_Draft1017.pdf.

[3] G. Cusano, M.R. Gonzalo, F. Farrell, R. Remus, S. Roudier, L. Sancho Delgado, Best Available Techniques (BAT) Reference Document for the Non-Ferrous Metals Industries, JCR Science for Policy Report, 2016. doi:10.2791/21807.

[4] V. Montenegro, H. Sano, T. Fujisawa, Recirculation of high arsenic content copper smelting dust to smelting and converting processes, Miner. Eng. 49 (2013) 184–189. doi:10.1016/j.mineng.2010.03.020.

[5] R. Newell, Removal of Arsenic from Speiss Leach Liquor by Solvent Extraction, in: Proc. ALTA 2000 SX/IX-1, ALTA Conference Secretariat, 2000.

[6] M. Winiewski, L. Iberhan, J. Szymanowski, Extraction of Arsenic(III) and Arsenic(V) from Sulphuric Acid Solutions with Trialkylphosphine Oxides and Hydroxamic Acids, in: Solvent Extr. 21st Century. Proc. ISEC'99, Vol. 2, Society of Chemical Industry, London,

2000: pp. 1261–1266.

[7] M.B. Bogacki, M. Wisniewski, J. Szymanowski, Effect of extractant on arsenic(V) recovery from sulfuric acid solutions, J. Radioanal. Nucl. Chem. 228 (1998) 57–61. doi:10.1007/BF02387300.

[8] M. Wisniewski, Removal of arsenic from sulphuric acid solutions, J. Radioanal. Nucl. Chem. 228 (1998) 105–108. doi:10.1007/BF02387308.

[9] M. Bissen, F.H. Frimmel, Arsenic - A review. Part II: Oxidation of arsenic and its removal in water treatment, Acta Hydrochim. Hydrobiol. 31 (2003) 97–107. doi:10.1002/aheh.200300485.

[10] T.S.Y. Choong, T.G. Chuah, Y. Robiah, F.L. Gregory Koay, I. Azni, Arsenic toxicity, health hazards and removal techniques from water: an overview, Desalination. 217 (2007) 139–166. doi:10.1016/j.desal.2007.01.015.

[11] V.K. Sharma, M. Sohn, Aquatic arsenic: Toxicity, speciation, transformations, and remediation, Environ. Int. 35 (2009) 743–759. doi:10.1016/j.envint.2009.01.005.

[12] A. Criscuoli, A. Figoli, Pressure-driven and thermally-driven membrane operations for the treatment of arsenic-contaminated waters: A comparison, J. Hazard. Mater. 370 (2019) 147–155. doi:10.1016/j.jhazmat.2018.07.047.

[13] F. Beolchini, F. Pagnanelli, I. De Michelis, F. Vegliò, Treatment of concentrated arsenic(V) solutions by micellar enhanced ultrafiltration with high molecular weight cut-off membrane, J. Hazard. Mater. 148 (2007) 116–121. doi:10.1016/j.jhazmat.2007.02.031.

[14] B. Zhao, H. Zhao, S. Dockko, J. Ni, Arsenate removal from simulated groundwater with a Donnan dialyzer, J. Hazard. Mater. 215–216 (2012) 159–165. doi:10.1016/j.jhazmat.2012.02.048.

[15] D. Qu, J. Wang, D. Hou, Z. Luan, B. Fan, C. Zhao, Experimental study of arsenic removal by direct contact membrane distillation, J. Hazard. Mater. 163 (2009) 874–879. doi:10.1016/j.jhazmat.2008.07.042.

[16] M. Shih, An overview of arsenic removal by pressure-driven membrane processes, Desalination. 172 (2005) 85–97. doi:10.1016/j.desal.2004.07.031.

[17] J. López, M. Reig, O. Gibert, J.L. Cortina, Increasing sustainability on the metallurgical industry by integration of membrane nanofiltration processes: Acid recovery, Sep. Purif. Technol. 226 (2019) 267–277. doi:10.1016/j.seppur.2019.05.100.

[18] T.J.K. Visser, S.J. Modise, H.M. Krieg, K. Keizer, The removal of acid sulphate pollution by nanofiltration, Desalination. 140 (2001) 79–86.

[19] M. Boucher, N. Turcotte, V. Guillemette, G. Lantagne, A. Chapotot, G. Pourcelly, R. Sandeaux, C. Gavach, Recovery of spent acid by electrodialysis in the zinc hydrometallurgy industry : performance study of different cation-exchange membranes, Hydrometallurgy. 45 (1997) 137–160.

[20] A. Chekioua, R. Delimi, Purification of H2SO4 of Pickling Bath Contaminated by Fe(II) Ions Using Electrodialysis Process, Energy Procedia. 74 (2015) 1418–1433.

doi:10.1016/j.egypro.2015.07.789.

[21] W. Li, Y. Zhang, H. Jing, X. Zhu, Y. Wang, Separation and recovery of sulfuric acid from acidic vanadium leaching solution by diffusion dialysis, J. Environ. Chem. Eng. 4 (2016) 1399–1405. doi:10.1016/j.jece.2015.11.038.

[22] C. Wei, X. Li, Z. Deng, G. Fan, M. Li, C. Li, Recovery of H2SO4 from an acid leach solution by diffusion dialysis, J. Hazard. Mater. 176 (2010) 226–230. doi:10.1016/j.jhazmat.2009.11.017.

[23] J. Jeong, M.S. Kim, B.S. Kim, S.K. Kim, W.B. Kim, J.C. Lee, Recovery of H2SO4 from waste acid solution by a diffusion dialysis method, J. Hazard. Mater. 124 (2005) 230–235. doi:10.1016/j.jhazmat.2005.05.005.

[24] S.H. Lin, M.C. Lo, Recovery of sulfuric acid from waste aluminum surface processing solution by diffusion dialysis, J. Hazard. Mater. 60 (1998) 247–257. doi:10.1016/S0304-3894(98)00099-5.

[25] J. Xu, D. Fu, S. Lu, The recovery of sulphuric acid from the waste anodic aluminum oxidation solution by diffusion dialysis, Sep. Purif. Technol. 69 (2009) 168–173. doi:10.1016/j.seppur.2009.07.015.

[26] K. Wang, Y. Zhang, J. Huang, T. Liu, J. Wang, Recovery of sulfuric acid from a stone coal acid leaching solution by diffusion dialysis, Hydrometallurgy. 173 (2017) 9–14. doi:10.1016/j.hydromet.2017.07.005.

[27] R. Gueccia, S. Randazzo, D. Chillura Martino, A. Cipollina, G. Micale, Experimental investigation and modeling of diffusion dialysis for HCl recovery from waste pickling solution, J. Environ. Manage. 235 (2019) 202–212. doi:10.1016/j.jenvman.2019.01.028.

[28] J. Kerti, A. Mándoki, M. Széky, Method for the cyclic electrochemical processing of sulfuric acid-containing pickle waste liquors, 1976.

[29] V. Nenov, N. Dimitrova, I. Dobrevsky, Recovery of sulphuric acid from waste aqueous solutions containing arsenic by ion exchange, Hydrometallurgy. 44 (1997) 43–52. doi:10.1016/S0304-386X(96)00029-1.

[30] U. Kerney, Treatment of spent pickling acids from hot dip galvanizing, Resour. Conserv. Recycl. 10 (1994) 145–151. doi:10.1016/0921-3449(94)90047-7.

[31] F.J. Alguacil, F.A. López, The extraction of mineral acids by the phosphine oxide Cyanex 923, Hydrometallurgy. 42 (1996) 245–255. doi:10.1016/0304-386X(95)00101-L.

[32] G. Zhang, Q. Zhang, K. Zhou, Study on concentrating sulfuric acid solution by vacuum membrane distillation, J. Cent. South Univ. Technol. 6 (1999) 99–102. doi:10.1007/s11771-999-0007-5.

[33] J. Luo, C. Wu, T. Xu, Y. Wu, Diffusion dialysis-concept , principle and applications, J. Memb. Sci. 366 (2011) 1–16. doi:10.1016/j.memsci.2010.10.028.

[34] I. Puigdomenech, Chemical equilibirum software Hydra/Medusa, (2001). https://sites.google.com/site/chemdiagr/home.

[35] A. Savitzky, M.J.E. Golay, Smoothing and Differentiation of Data by Simplified Least

Squares Procedures., Anal. Chem. 36 (1964) 1627–1639. doi:10.1021/ac60214a047.

[36] H. Martens, T. Næs, Multivariate Calibration, John Wiley & Sons, New York, 1991.

[37] E.V. Thomas, A Primer on Multivariate Calibration, Anal. Chem. 66 (1994) 795A–804A.

[38] J.J. Tang, K.G. Zhou, Q.X. Zhang, Sulfuric acid recovery from rare earth sulphate solutions by diffusion dialysis, Trans. Nonferrous Met. Soc. China (English Ed. 16 (2006) 951–955. doi:10.1016/S1003-6326(06)60358-0.

[39] E.R. Nightingale, Phenomenological theory of ion solvation. Effective radii of hydrated ions, J. Phys. Chem. 63 (1959) 1381–1387. doi:10.1021/j150579a011.

[40] E. Glueckauf, A new approach to ion-exchange polymers, in: Proceeding First Int. Symp. Water Desalin, Washington DC, 1967: p. 143.

[41] A.O. Fane, A.R. Awang, M. Bolko, R. Macoun, R. Schofield, Y.R. Shen, F. Zha, Metal recovery from wastewater using membranes, 15 (2018) 5–18.

[42] A.E. Yaroshchuk, Dielectric exclusion of ions from membranes, Adv. Colloid Interface Sci. 85 (2000) 193–230. doi:10.1016/S0001-8686(99)00021-4.

[43] E. Vircikova, M. Ludovit, P. Pavol, Methods of Arsenic Waste Treatment and Dispose - Case Studies, in: L. Gaballah, J. Hager, R. Solozobal (Eds.), Rewas ’99 Glob. Symp. Recycl. Waste Treatnzent Clean Technol., 1999: pp. 65–73.

[44] F. Habashi, Mercury-Free Sulfuric Acid, in: P.W. Godbehereet (Ed.), Mater. Process. Technol. Environ. Prot. Min. Metall., Proceeding of The Metallurgical Society of CIM, Montreal, Canada, 1993: pp. 196–208.

SUPPLEMENTARY INFORMATION

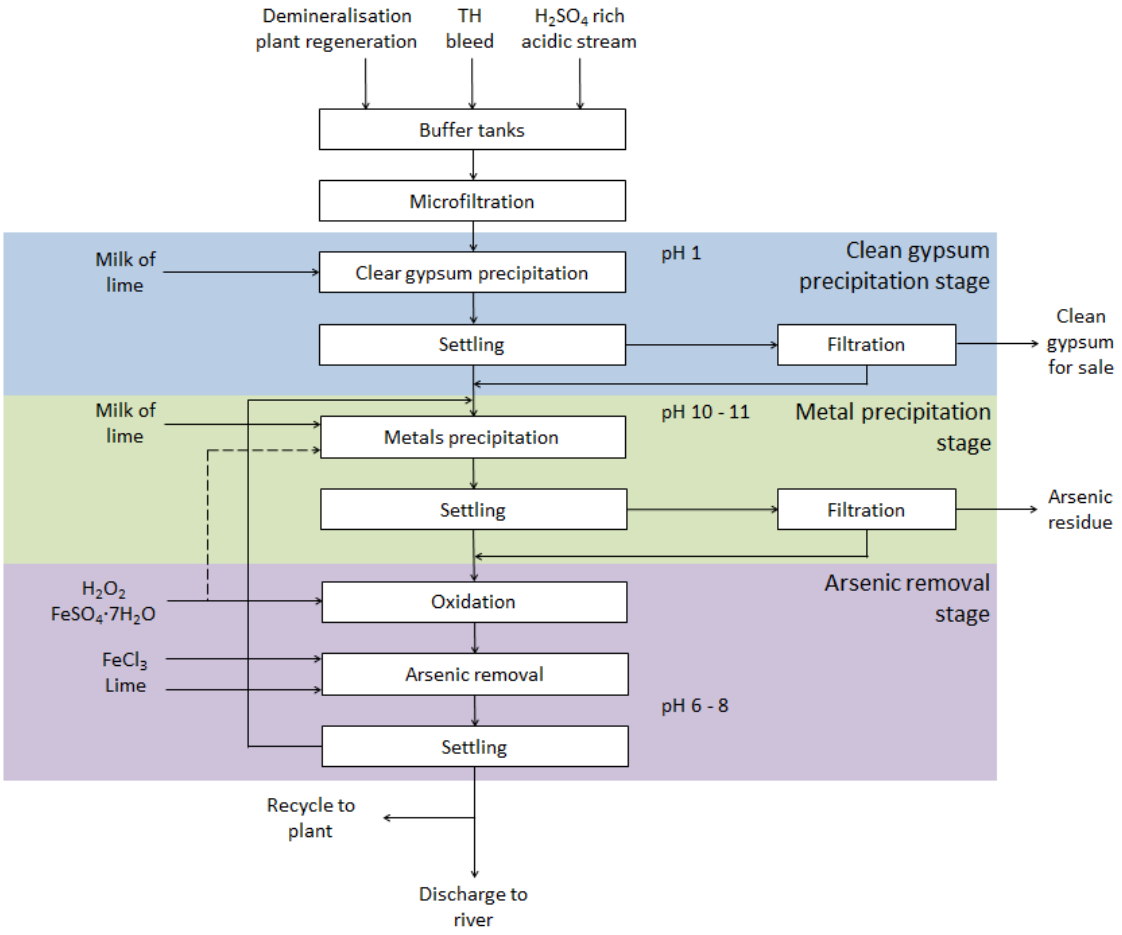

***Figure S1**. Treatment of the acidic solution in copper smelter industries [3]*

SO_4	Zn(II)
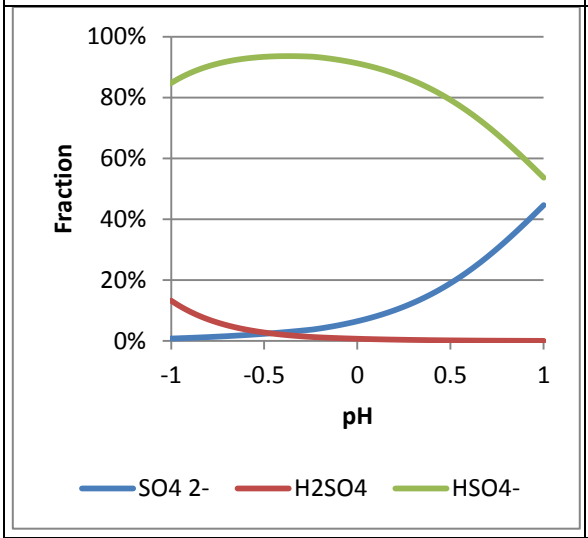	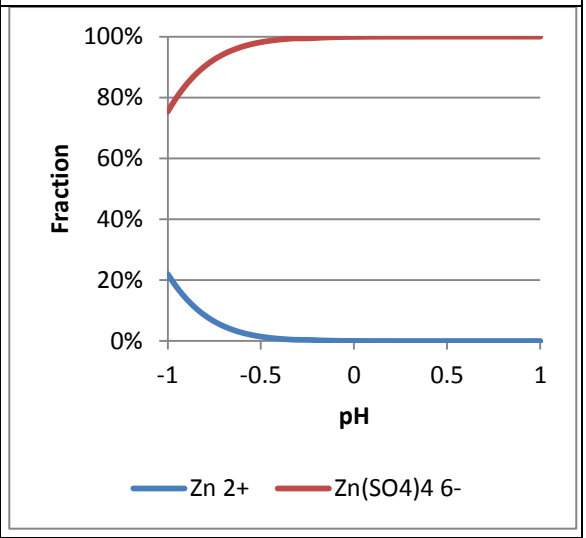
Fe(III)	Pb(II)
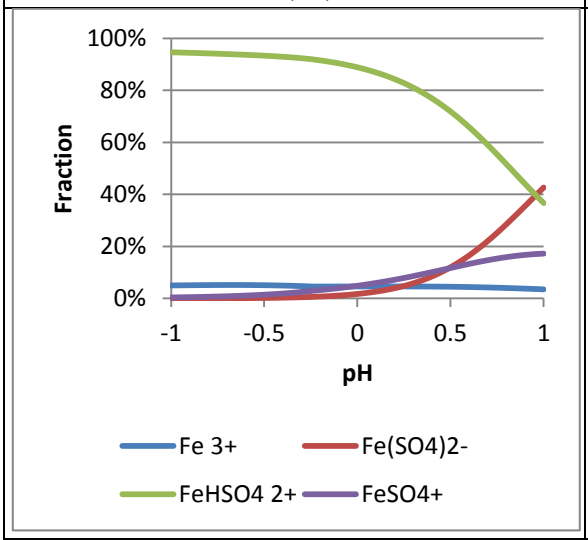	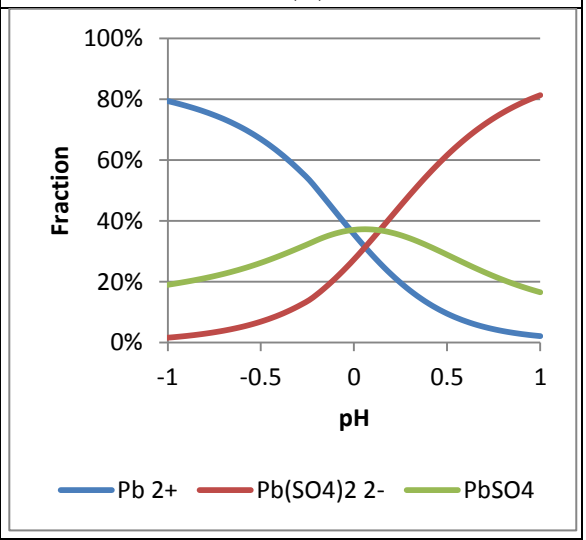
Cd(II)	Ni(II)
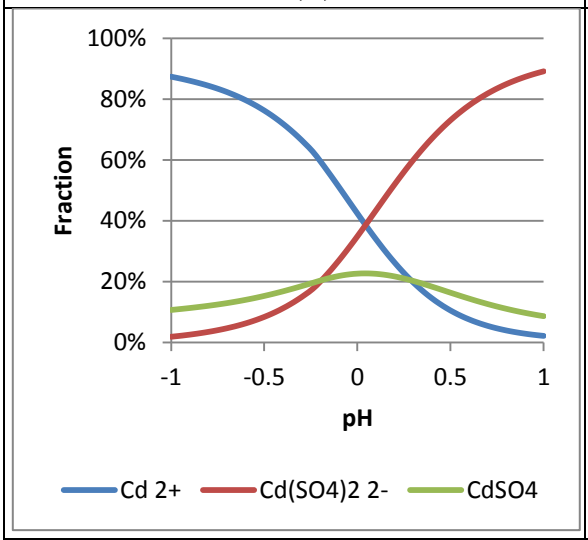	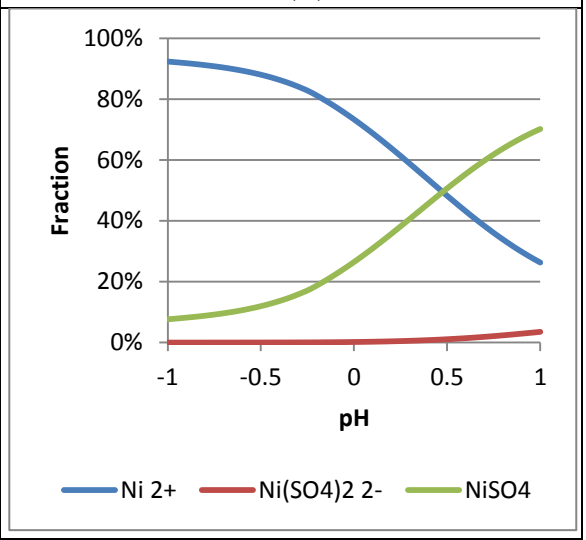
Cu(II)	

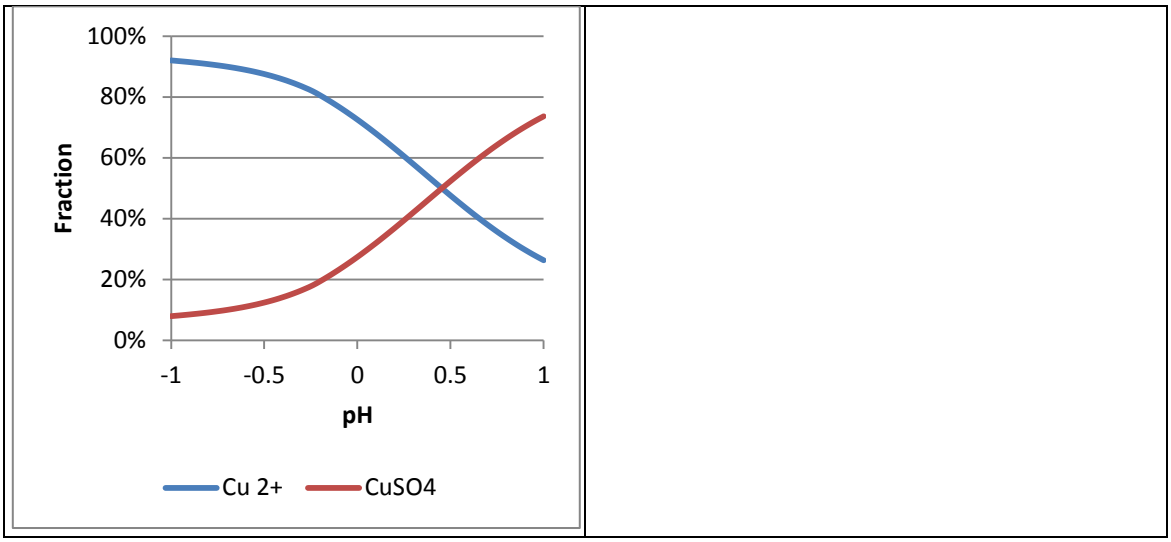

Figure S2. *Speciation diagrams for the different elements in solution. Diagrams were built with the Hydra/Medusa code* [34].

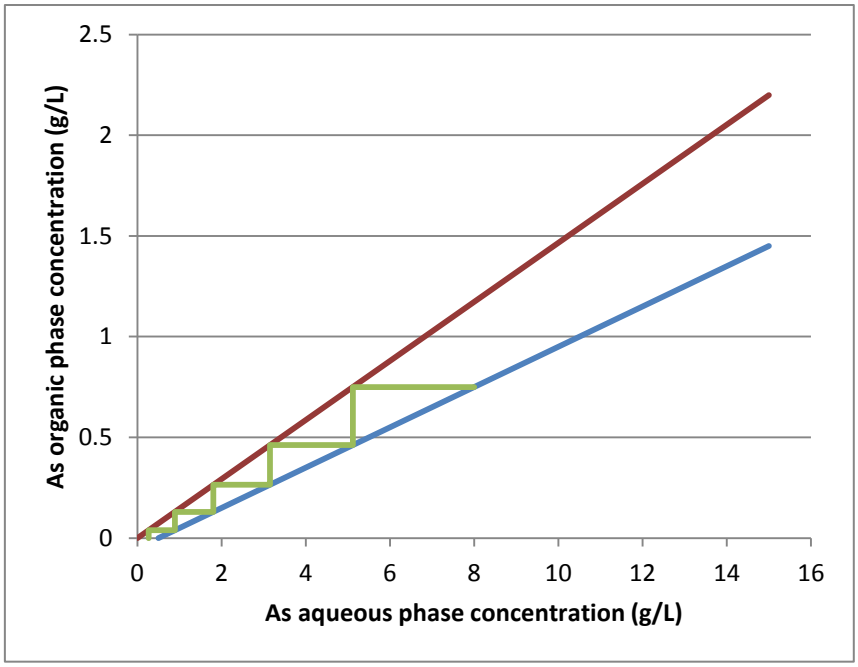

Figure S3*. As extraction isotherm with 50% Cyanex 923® in kerosene at 20ºC*